TEST PARTICLE - PLASMA INTERACTIONS

ALASDAIR L. GIBSON

1972

ProQuest LLC.
789 East Eisenhower Parkway
P.O. Box 1346
Ann Arbor, MI 48106 – 1346

C O N T E N T S

Test Particle - Plasma Interactions

Abstract

This thesis describes investigations into the properties of a two-dimensional plasma carried out by theory and computer simulation. The predictions of previous work concerning the wake generated by a suprathermal test particle in a two-dimensional plasma have been verified within the very noticeable constraints of the computer simulation model. Other work has been done, which has lent itself better to a good description by simulation. Primarily, in the electrostatic case, the slowing of a test particle in a two-dimensional collisionless plasma has been adequately quantitatively demonstrated.

In the case of two-dimensional magnetised plasma, expressions for the potential due to a test charge have been derived. It is shown that the nature of the potential distribution round the test particle, and a fortiori, the shielding properties of the plasma have been radically altered by the inclusion of the magnetic field. Whatever tractable means were available have been used to indicate the form of the potential distributions for both stationary and moving test particles.

(1) (a) Introduction

Ever since large electronic digital computers became widely available, use has been made of them by physicists to simulate the behaviour of the fully or partially ionised gases known as plasmas. There have been several reasons for this eagerness to use a new analytical tool as soon as it became available.

Firstly, a plasma is quite a difficult object on which to perform an experiment, since it often lasts in the apparatus for only a short time, can have its properties modified by the instruments intended for their measurement, and cannot easily be produced to the experimenters' desired specifications eg to given values of temperature and pressure. These objections do not apply where a computer simulation is concerned, since one can control exactly the plasma being set up, and can take any desired diagnostic measurements at any time.

The theorist as well as the experimentalist can have good motives for simulation; in this case there are two distinct situations in which it can prove useful. The first is in a problem where a linear analysis has been done and a solution has been found, but it may be felt desirable that a simulation be done to verify the results or reinforce them especially for regions of parameter space where the applicability of the linearisation is in doubt. The second case is that of non-linear phenomena, the equations describing which are not readily amenable to analytic treatment by known methods. In this instance the simulation provides an invaluable tool for research into the physics of the problem.

There are two main approaches to "simulation" of plasmas. Both involve the numerical solution of appropriate equations, but they differ in the range of physical effects which they describe. The first of these treats the plasma as a fluid, and is used for a regime where collision times are not long compared with, say, the plasma period. The phenomena which are treated occur on a much longer timescale, which may be that of the time it takes for an Alfven wave to cross the plasma, or the time in which appreciable plasma diffusion occurs.

The second approach is to consider the plasma as a large collection of charged particles each acting in the averaged field due to all the others. This latter is used to describe the "collisionless" regime where the collision time τ_c, the average time between collisions for a typical particle, is much greater than the plasma period τ_p. In this regime, events on a timescale τ_p and on a length scale of the Debye length λ_D, can be studied, as well as events on a timescale of the cyclotron period for the electrons. Since it takes of the order of a "relaxation time", which is much greater than a collision time, for a distribution function to relax to Maxwellian, it is possible to study non-Maxwellian distributions with such a model.

The results described below describe short time and length-scale phenomena of the type outlined in the previous paragraph, and were all obtained using a particle simulation code. They are all concerned with the interaction of a "test particle" with the background plasma, or with another "test particle", in the case where the plasma is two dimensional.

Chapter (1) is introductory and contains a chronological review of simple test-particle shielding theory and of plasma simulation. Chapter (2) describes the method of simulation of plasmas that is employed in this work. Chapter (3) reviews immediately previous work in detail. Chapter (4) gives results for theory and simulation in the electrostatic case which extend the results described in (3). Chapter (5) analyses the case where a constant magnetic field acts perpendicular to the two-dimensional plasma.

(1) (b) Review of Previous Work

(i) Simulation of Plasmas

The first part of this review will be concerned with the development of computer codes for plasma simulation by following the motion of each "particle" in the field due to all the others. An indication will be given of the nature and scope of work which has been done in this field. The second part of this section will be concerned with the theory which has been previously done concerning 'test particles' interacting with a plasma.

The simulation of plasmas by computer codes has been an accepted tool for research in the subject for over a decade. Some of the earliest work in this field was done by Buneman (ref 1) in 1959. As time passes it is noticeable that the number of "particles" involved in each new reported simulation increases monotonically for several years with the increasing core stores available in the computers concerned. Buneman was restricted to using 256 positive and 256 negative sheets of charge in a one-dimensional model, in which these sheets were moved according to their mutual electric fields. The mass ratio between the 'ions' and 'electrons' was 10, and the code was first employed to study the destruction of electron drifts by instabilities. Variations on the one-dimensional scheme followed such as that by Dawson (ref 2) who used a model which consisted of a large number of identically charged sheets in a uniform neutralising background. He used approximately 1000 sheets in these early calculations. Later this was extended to two species, of different masses but equal and opposite charge, where the mass ratio was taken to be less than that between the ion and electron. In order to reduce the collisional effects in a sheet model smoothing

methods were developed (3) and the emergence of codes which used finite size particles began. An indication of the size of the computations being performed by this point in time is that by Burger (4) in 1965 in which 10000 sheets of charge were used.

Once the idea of smoothing the electric field by introducing a spatial grid and assigning fractions of charge due to each particle to points of the grid had been established, one major stumbling block still remained in the way of economical codes. This was the absence of a fast method of solving Poissons equation $\nabla^2\phi = \rho$ Hockney (5) contributed greatly to the solution of this problem by developing rapid techniques to solve the equation in a grid with 2^n grid points. The gain in speed obtained now made two dimensional calculations feasible, and one of the first was reported by Hockney (3) and concerned a plasma experiment of anomalous diffusion. Other results using the same or similar techniques including the simulation of rotating discs of stars, are given in (6).

Since the original advances in two-dimensional calculation, other codes have been written at various laboratories. One such, the GALAXY code of Boris and Roberts (7) was used by several workers at Culham Laboratory for various applications, and was used in the work immediately previous to that done in this thesis (8).

With the advent of the latest generation of large, fast, computers, 70% of world production being by one firm, time and space limitations are less of a problem than formerly. This has led to the development of codes such as NOVA (9) which is used in the work described below, and is also designed to be 'portable' between computers. Portability is facilitated by the near monopolistic market giving a general uniformity among computers at different establishments.

One-dimensional plasma simulations are still very much in use, however, and they continue to give useful results. In fact for reasons of economy it can sometimes be the case that one-dimensional simulations are done instead of two-dimensional unless a description of a strictly two-dimensional phenomenon is being sought, even although a one-dimensional simulation is farther from an accurate description of a plasma than is a two-dimensional one. Occasionally, new generalisations or developments of the one-dimensional simulation plasma are published: one such is that by Hasegawa and Okuda (10), which is suitable for studying one-dimensional electromagnetokinetic disturbances propagating at an arbitrary angle to an applied magnetic field.

Some examples of successful plasma work which involved the use of computer particle simulation will now be given. Dawson (11) cites the example of research into the side-band instability due to trapped electrons in a finite amplitude plasma oscillation. It was first observed experimentally, and a crude theory which treated the trapped electrons as harmonic oscillators was developed and verified by simulation. After that, more detailed theories were carried out, but it is probable that, without the computer simulation, the original phenomenological theory would not have been published. Subsequently more complete and detailed experiments have been carried out and these exhibit much of the detail shown in the numerical simulation. This he cites as a good example of the usefulness of interplay between experiment, simulation, and theory. (References given in ref 11.)

There are many examples of simulation of actual experimental configurations using a particle code in order the better to understand or predict the behaviour in these cases. P Burger (op. cit.) used a one-dimensional code to give a satisfactory explanation of

the operation of a thermionic converter and the large amplitude oscillations which are observed. A two-dimensional particle calculation is at present being applied to an idealisation of the Levitron (12,13) configuration in the hope of simulating the behaviour of the machine under certain conditions.

In the case of non-linear phenomena, often the initial linear development of a phenomenon can be adequately dealt with by theory, but the configuration of the plasma in the subsequent non-linear regime can be best elucidated by simulation. A good example is the paper by Cook et al (14) describing computations of the non-linear growth of the ion sound instability in two dimensions. In this case in the linear growth phase theory agreed closely with simulation but the subsequent development of the two-dimensional simulation gave more insight into the physical process involved. Another example in the same vein, where a refinement of the one-dimensional code is reported for the first time is given in (15). Here the authors suppress unwanted noise by a 'quiet start' technique (described below) in their simulation, and follow the growth of plasma cyclotron instabilities from very low amplitudes.

Another example of a simulation which has given a fresh impetus to a topic is in the work of Taylor & McNamara (16) followed by that of Dawson and Okuda (17), on plasma diffusion in two dimensions in a magnetic field. Here it has been found, that contrary to previous ideas on the subject, there exist three regimes characterised by the strength of B, and the dependence of the diffusion upon B in each of these regimes is notably different. This has led to the realisation of the need for revision of the theory of a two-dimensional magnetised plasma. Work on other physical

aspects of the subject such as that in (18), (19) and (20) followed, as the subject of a magnetised two-dimensional plasma became of interest in its own right. This work has also led on to the consideration of three-dimensional plasma diffusion in a very strong magnetic field (21).

It can be seen from the above that simulation, used in an appropriate context, can be used to gain deeper insight into the physical properties of plasmas, and as such is a useful tool for the theoretical and experimental plasma physicist.

(ii) Theories of Plasma - Test Particle Interactions

Several authors in the past two decades have concerned themselves with the shielding of the charge of a test particle in a plasma, and with the forces induced on itself by the motion of such a particle in the plasma. The usual motivation for this work has been an interest in the fundamental properties of a fully ionised gas, and also the hope that results might be obtained which would advance the kinetic theory of plasmas.

The theoretical result giving an analytic expression for the potential distribution around a shielded test charge, and the value of the plasma dielectric function which are rederived in Chapter 3(a), below, has been known for some time. A derivation is given in Thompson (22), for example, and the method used derives from that of Landau (23).

An early paper which investigated screening of a charge in a plasma, was that of Bohm and Pines (24). They were concerned with trying to demonstrate the relationship between collective electron interactions and individual particle interactions. They described the gas by means of the Fourier coefficients ρ_k of the electron density at each point in space. A function q_k was then developed, which oscillates harmonically for appreciable values of k, and tends to ρ_k in the small k limit. Subsequent by the problem of separating individual and collective interactions is tackled by letting

$$\rho_k = a q_k + \eta_k$$

where q_k describes the collective interactions and η_k the individual ones,

in that it describes fluctuations associated only with the random thermal motions of the individual particles. Later the η_k are shown to be the Fourier coefficients of a density distribution in which each electron is surrounded by a comoving cloud containing a deficiency of electrons. It is then shown that the properties of this cloud are such that for a particle moving with less than the mean thermal speed the charge is screened by its comoving cloud, with a screening radius of the order of λ_D, the Debye length. This is a direct consequence of the authors' stipulation that η_k is describing phenomena where $k \gtrsim \lambda_D^{-1}$ which was decided after an earlier section in which it was concluded that collective oscillations were to be expected for $k^2 \ll \lambda_D^{-2}$

Further development reveals that a particle moving with velocity less than electron thermal cannot set up collective oscillations in the form of a wake behind it. It is then shown that if the particle is moving with velocity $V_0^2 \geq 4/3 \langle v^2 \rangle_{av}$ then it will cause the excitation of oscillations in its wake. Again, it is deduced that the particle will lose energy to these oscillations and an expression for the rate of energy loss is given, as is an expression for the energy loss due to short-range collisions. It is subsequently concluded that except for particles whose velocity is much greater than electron thermal, the charge is screened in a distance λ_D, but for the fast particles the screening is "not as good". However the fact that these latter lose energy to oscillations of the plasma is given as a mechanism for bringing them into thermal equilibrium with the rest of the assembly.

This paper demonstrates what it is possible to achieve by means of elementary techniques which seldom lose sight of the fact

that the plasma is a collection of particles. It is evident, in the main, that sound, general conclusions about shielding are obtained, but that in order to obtain more detail, a more mathematically sophisticated approach may be desired.

In contrast, Neufeld and Ritchie (25) commence by treating the plasma as a continuous medium characterised by a polarisation vector $\underline{P}_V(\underline{r},t)dV$, and start from an equation of motion for P. This equation is Fourier-analysed along with Maxwell's equations, P is eliminated and some relations are obtained between the various electromagnetic variables, among which we have

$$\epsilon_{\parallel}(k,\omega) = 1 - \omega_p^2 \int \frac{f(v)\, dv}{(\omega - \underline{k}.\underline{v})^2 + i g(\omega - \underline{k}.\underline{v})}$$

the dielectric constant for the longitudinal electric field. ω_p is the plasma frequency, g is a damping term, v is velocity, k is wave number.

The response of the plasma, described by the derived relationships, to a moving charge of velocity V is now ascertained and expressed by giving the form of the potential distribution in cylindrical co-ordinates ρ, Z, as

$$\phi(\rho,z,t) = \frac{q}{\pi V} \int_0^{\infty} K\,dK\, J_0(K\rho) \int_{-\infty}^{\infty} \frac{\exp(i\omega(z/V - t))}{k^2 \epsilon_{\parallel}}\, d\omega$$

where $k^2 = K^2 + \omega^2/V^2$. q is the test particle charge.

Now comes the approximation which ensures that much detail is lost of the form of the potential for a subthermal particle. It is assumed that $V \ll \langle v^2 \rangle^{\frac{1}{2}}$ where the right hand quantity is the root mean square plasma velocity. This leads to

$$\epsilon_{\parallel} = 1 + \omega_p^2/\varsigma^2 k^2 \qquad \text{where} \qquad \varsigma = \omega_p \lambda_D .$$

Thus essentially the authors are assuming for a slow particle what

is demonstrated later to be the form of the dielectric function for $V = 0$. They obtain

$$\phi(\underline{r},t) = q \exp(-r/\lambda_D)/r$$

$$\text{where} \quad r = (\rho^2 + (z-Vt)^2)^{\frac{1}{2}}$$

a screened coulomb potential with screening distance λ_D , the Debye length.

Other matters are now discussed, concerning such things as binary collision, which have no applicability to our present work where the plasma is taken to be 'collisionless'.

The authors consider the case of a high-velocity incident particle, where $V \gg \langle v^2 \rangle^{\frac{1}{2}}$. An expansion for ϵ_{11} is done in powers of k^2/ω^2 and the following results are obtained. The potential ahead of the particle for large distances r , falls off as $1/r^3$ approximately. This agrees with later work (29). Behind the particle, an oscillation is set up, which has the plasma frequency,, and which is not damped. This last corresponds with the result of ref (24). Subsequent calculations of stopping power are of little interest, because they use the asymptotic forms of the dielectric function, and because they involve terms arising from binary collisions.

Thus, because of approximations, the authors do not find the exact form of the potential due to the test charge, but they have produced one or two results which correspond with earlier and later work.

Chronologically, the next paper which uses the concept of 'test particles' and is of some interest, is that of Rostoker (26). This author uses Vlasov's equation and Poissons equation, suitably linearised, to find the electric field due to a 'dressed' test particle, at a point. By 'dressed' he means that the particle's field

has been modified by the presence of the plasma around it, and what it is 'dressed' with is a cloud of charge of opposite sign, which shields the particle in a way which he does not qualitatively specify. He uses the expression for the field to obtain results by a superposition method for electric field correlations and similar quantities. The case of non-zero magnetic field is also considered. This author is interested mainly in the concept of the 'dressed' test charge as an analytical tool rather than something of interest in its own right.

Another paper which uses the concept of the field due to a test particle moving with a velocity v is that by Thompson and Hubbard (27). They agree with the authors of ref (24) that for small v the particle is Debye shielded, while for large v it leaves a wake. However they go on to calculate the Fokker-Plank diffusion coefficients of the plasma by using integrals of the energy spectrum of the fluctuating microfield, the latter being given as a function of $\epsilon(k,\omega)$ and ω. In their results they claim agreement with previous workers.

The next paper that concerns itself with test charge screening in a plasma is that by Joyce and Montgomery (28). Here the plasma is given a streaming velocity in a certain direction, and the test charge is taken to be at rest at the origin. It is found that for large distances x from the test particle, in three dimensions, the potential falls off as x^{-3}, while for zero streaming a Debye screening of the form $\phi \sim q e^{-(x/\lambda_D)}/x$ is obtained. Using methods similar in conception to those of ref (26), a result is obtained for the density pair correlation function, and this is shown to fall off as an inverse power of x_{12}, the separation.

Subsequently Montgomery and Joyce, along with Sugihara, performed a more general calculation (29). Again, they start off from the expression for the effective potential of a test charge as given in (22). They then consider the dielectric function $\epsilon = D(k, -ikV_0)$ where V_0 is the velocity of the test particle. By dint of expressing it as $D = 1 + k^{-2}\Psi(\mu, \phi)$, and expressing $1/D$ as a sum of two terms, the expression for the potential is split up into two terms, such that $\phi_{effective} = \phi_1 + \phi_2$ Assuming an electrostatically stable plasma, the second term in $\phi_{eff.}$ is then expanded in inverse powers of r, the distance of the observer from the moving test particle. It is found that the first term in ϕ_2 cancels with ϕ_1 for $V_0 \neq 0$, leaving the effective potential at large r given by $\phi_{\substack{eff \\ r \to \infty}} \to \frac{-q}{2\pi^2 r^3} I_1$, q being the charge and I_1 a specified constant. This is proved without any assumptions on the distribution function except that the plasma is electrostatically stable. The results of ref (28) are recovered in a straightforward manner.

Another paper which concerns itself with shielding of slow test particles in a plasma is that by G. Cooper (30). The function $D(k, -ikV_0)$ is expressed as a small-argument limit, in $\underline{k}.\underline{v}$. This is inserted into the potential of ref (22) and an expansion carried out to second order in $|\underline{v}|/v_e$ where v is the velocity by the test particle, as previously, and v_e is the electron thermal velocity. Some manipulations are done, and the series of terms which result is such that to lowest order in $|\underline{v}|/v_e$, the potential is of the shielded Debye type again. It is shown that for large distances from the test charge, the potential falls off as r^{-3}, where r is the distance of the observer from the charge. It is shown that the shielding near the test charge is of exponential form, and as v gets

smaller, the exponential field dominates over a larger and larger range of r. This is to be expected since in the small v limit we are approaching the stationary particle case.

The paper by Laing et al (8), which forms the starting point for the work below is dealt with in more detail in a later section of this account. (Chap. 3a), calculates exact forms for the potential distribution in two dimensions.

In the summing up of the paper by Montgomery and Tappert (19), results are quoted for the form of $\epsilon(k,o)$ in a magnetic field, and these helped to provide a stimulus for the later part of the work described below.

Other work concerning itself with the slowing of test-particles in a plasma, in general considers a system which is collisional and can be described by, say, the Fokker-Planck equation, and so is not comparable with the analysis below, which is concerned with the collisionless Vlasov equation. A summary of some early work on the subject appears in ref (31).

(2) (a) Method of Plasma Simulation by Particle Model

In the computer program NOVA (9), the method used to simulate a collisionless plasma is to follow the motion of each of a large number of charged particles in two dimensions. Whenever the word particle is used here, it has the equivalent and more accurate meaning of 'rod'. This is because the simulation is a two-dimensional one, and the potential due to any charge moving in the plane of the simulation is actually that of a rod of infinite extent which passes through the position of the charge. Thus we are following the motion of each of between 10,000 and 20,000 'rods' in the field due to all the others. The approximations which are involved will be outlined as the description proceeds, and their effect will be discussed in a later section, along with the relevance of their effects to the present numerical experiments.

We follow the motion, in the present instance, only of the electrons, assuming the ions to provide a fixed, neutralising background. Ion movement can be built into the code easily, but it was not thought necessary here, especially since our investigations will be concerned with phenomena attributable to electrons. Inclusion of an equal number of ions in the calculation, though not increasing dramatically the computer time required for an average timestep, will increase the storage required for the code quite substantially. [The reason why the time required does not increase to an inconvenient degree, is that ions would be ascribed a higher mass than electrons, typically 4-10 electron masses, and so, they would have a correspondingly smaller plasma frequency ω_p. Thus, using the stability criterion quoted below (equation (10)), we see that we could afford to use a larger timestep to move the ions.]

In brief, before embarking upon a more detailed description, what is done in a NOVA simulation is as follows.

(1) Before the calculation proper gets under way the computer plasma is set up by assigning positions and velocities to all the particles. By means of a random number generator the distribution of particles in velocity space is made approximately Maxwellian and the distribution in the real space of the problem is made even down to a scale of the order of a computational grid length. Now come the three main stages in every timestep of the calculation.

(2) Knowing the positions and charges of all the particles in the computer plasma, the charge density can be calculated at all points of a superimposed computational grid.
To save time, this is in fact done to each particle immediately after a position has been assigned to that particle.

(3) Poissons equation, suitably scaled, is solved at all points of the grid. This is

$$\nabla^2\phi = \rho$$

where ϕ = potential, ρ = charge density.

(4) Using suitable equations of motion, the positions and velocities of all the simulation particles are advanced by putting the equations into difference form and solving, using a suitable timestep. The steps 2, 3, 4 are now repeated.

Now follows a more detailed description.

In order to determine a suitably averaged value for charge density at all points of the computational grid, two methods have been commonly employed in the past. These are referred to as the Nearest Grid Point (N.G.P.) and Cloud in Cell (C.I.C.) methods, and it is the

latter which is utilised in NOVA. For the sake of comparison, with a view to outlining the relative advantages of C.I.C. over N.G.P., both will be described here.

In the N.G.P. approximation, with the computational area divided into a rectangular mesh, the position of each particle being given with respect to the mesh, the charge due to any particle is ascribed to a sum of charge which is assigned to the nearest grid point of the computational grid (see Fig (1)). When this has been done for all particles, individual point particle interactions have been eliminated, and a smoothing has been effected. What has in fact been done is to say that the particle gives rise to a charge density contribution which is the same wherever it is in the rectangle whose dimensions are the same as a grid rectangle and which is centred on the nearest grid point. Another point of view is to consider that we have ascribed a finite size to the particle.

In comparison, the C.I.C. method shares the charge, in NOVA, among the four nearest grid points. There are a number of ways of doing this, but the simplest is just to draw a rectangle, centred on the particle under consideration, and of the same size as a rectangle of the space grid, and assign fractions of charge proportionately to the areas of this rectangle which intersect the four rectangles drawn with centres on the four grid points nearest (see Fig (2)). This is exactly the method used in NOVA. Intuitively one expects this method to give a more accurate approximation than the N.G.P. method of charge sharing and this is confirmed in practice. One way of looking at this approximation to the charge density due to a particle is in the sense of an even cloud of charge which can overlap all the other similar clouds of which the computer plasma is composed.

With the charge density distribution now set up, Poisson's equation is solved at all points of the computational grid. In general this will be expected to be a time-consuming part of the calculation, and in NOVA with this point in mind, the main Poisson-solving routines have been written in USERCODE in preference to FORTRAN.

The method used to solve Poisson's equation is one of Double Fourier Analysis (D.F.A.) which is very similar to that of Boris and Roberts (7). The authors of the code consider that though this method is expected to be slower than others mentioned in Hockney (6), the availability of Fourier transforms at every step is a useful diagnostic as well as being a connection with theory. It is also useful to apply simple smoothing to the fields and into the code is built a data-driven method of suppressing unwanted short-wavelength high-frequency modes, to decrease noise.

All Fourier transforms in the code use the complex periodic transform method due to Singleton (33). The boundary conditions are periodic in the simulation so that in effect we are considering an area of plasma of L_x by L_y Debye lengths which is surrounded by an infinite mesh of identical such areas. The real transforms are done two (rows or columns) at a time.

Instead of the analytical transform equation

$$\rho_{lm} = \int_0^{L_y} dy \int_0^{L_x} dx \, e^{-ik_x x - ik_y y} \rho(x,y) \qquad (2)$$

the transform routine uses

$$\rho_{lm} = \Delta x \Delta y \sum_{j=0}^{N_y-1} e^{-ik_y Y_j} \sum_{i=0}^{N_x-1} e^{-ik_x X_i} \rho_{ij} \qquad (3)$$

where L_x, L_y are the dimensions of the rectangle of the computation in

appropriate units (usually Debye lengths), N_x, N_y are the number of grid spacings, and points in the x and y directions. Δx, Δy are the grid-spacings, and $K_x = \frac{2\pi l}{L_x}$, $K_y = \frac{2\pi m}{L_y}$

The Fourier coefficients of the density having been found, the corresponding Fourier coefficients of the potential are simply obtained from the transform of Poisson's equation

$$\phi_{lm} = \left(4\pi k_{lm}^{-2}\right) \rho_{lm} \qquad (4)$$

In a continuum, we would have $k_{lm} = (k_x^2 + k_y^2)^{\frac{1}{2}}$. However, the area-weighting of force and charge, and the finite differencing of ϕ to get the electric field E, introduce errors of order $(K\Delta)^2$. The factor $\left(1 + \frac{1}{3}(k_x\Delta x)^2 + \frac{1}{3}(k_y\Delta y)^2\right)$ is therefore used to remove these errors along with the use of a six-point difference formula for calculating the electric field. Before this stage the potential is obtained by an inverse transform.

$$\phi_{ij} = \frac{1}{L_x L_y} \sum_{l=-\frac{N_x}{2}}^{\frac{N_x}{2}-1} e^{ik_x x_i} \sum_{m=-\frac{N_y}{2}}^{\frac{N_y}{2}-1} e^{ik_y y_i} \bar{\phi}_{lm} \qquad (5)$$

which is the discrete analogue of a Fourier series of infinite summation limits. $\underline{E}$ is now found by a simple difference method from $E = -\text{grad}\,\phi$, and then modified as follows

$$EX(JX,JY) = \tfrac{1}{6}\left[EX(JX,JY+1) + 4EX(JX,JY) + EX(JX,JY-1)\right]$$

where JX, JY are levels for the grid points and similarly for EY. This removes anisotropy errors of $O(k\Delta)^2$ while introducing a magnitude error which is compensated for by the factor described above.

The third main part of the calculation is the moving of the particles. The equations of motion used in the work described below are

$$m\frac{d\underline{v}}{dt} = q\left(\underline{E} + \frac{\underline{v}\times\underline{B}}{c}\right) \qquad (6)$$

$$\frac{d\underline{x}}{dt} = \underline{v} \qquad (7)$$

These are solved by a difference method

$$m\left(\frac{v^{t+\frac{1}{2}\Delta t} - v^{t-\frac{1}{2}\Delta t}}{\Delta t}\right) = q\left(E^t + \frac{v^{t+\frac{\Delta t}{2}} + v^{t-\frac{\Delta t}{2}}}{2}\frac{B}{2}\right) \qquad (8)$$

$$\frac{x^{t+\Delta t} - x^t}{\Delta t} = v^{t+\frac{\Delta t}{2}} \qquad \text{where } \Delta t \text{ is the timestep.} \qquad (9)$$

It can be seen from these that we have imposed a time-staggering of the dependent variables X and v, X being defined at all points after integral numbers of timesteps, while v is defined at half-integral times. This is a convenient manipulation as it enables us to write an explicit time-centred scheme which has by virtue of being time-centred an accuracy of $O(\Delta t)^2$. This is important since time is the only independent variable in these equations which appears explicitly and is discretised explicitly. These equations (8) and (9) are solved for $x^{t+\Delta t}$, $v^{t+\frac{\Delta t}{2}}$ at all points of the spatial grid. This is a fast method, being explicit, but it involves the stability criterion.

$$\omega_p \Delta t < 2 \qquad (10)$$

where ω_p is the plasma frequency. This is a 'Courant-Friedrichs-Lewy' condition, which has the meaning that the timestep Δt must be smaller than a time of the order of the inverse plasma frequency. This is physically reasonable, for otherwise physics on a timescale $O(\omega_p^{-1})$ would be obliterated by the computation; this would be wholly unsatisfactory. In practice the timestep, for the sake of achieving reasonable accuracy, is taken as $\frac{1}{8}\omega_p^{-1}$ or $\frac{1}{4}\omega_p^{-1}$ and the C-F-L condition is well satisfied.

Before going on to more details about the code itself and its structure, the possible sources of discrepancy between real and simulated plasmas will now be discussed, in the following section.

(2) (b) Critique of Particle Codes

Much work has been done by way of theory and numerical experiment to isolate the main causes of non-physical effects in simulated plasmas.

Most of the drawbacks which have to be allowed for in the fundamental all-particle model used in NOVA and similar codes are associated with the small number of particles which can be represented, partly due to the limitations imposed by the storage space available in the computer. If we were to include the individual forces between every pair of particles, we would only be able to deal with approximately 1000 particles. In the present instance, where averaged forces derived from the electromagnetic field equations are used, we can use many more particles, and the number we decide to use depends as much upon the time available on the machine for performing the calculation, as on space available, though it will also depend to some extent upon the phenomenon we are hoping to simulate. However, despite the approximations we make, a factor of $10^6 - 10^7$ less particles is being used in these simulations, compared with the number density we should expect in a real plasma. Thus every particle in the simulation can be thought of as a "superparticle" representing some 10^6 actual plasma particles.

One result of an insufficient number of particles is that the fluctuation about the mean, say of the density n, which is theoretically $1/5n$ will be noticeably increased - in this case by a factor 10^3 over the value which would obtain in a real plasma. This is referred to as particle noise (34).

Also, this lower particle density will lead to a decrease in collision times compared with a real plasma; this would, for example, act towards reducing the persistence of a non-Maxwellian distribution function in the plasma, which would be a drawback if such a distribution was being used, since if collision times are reduced, relaxation times will be reduced also. The ratio between the collision frequency ν and the electron plasma frequency ω_{pe} is given by [ref (32)]

$$\frac{\nu}{\omega_{pe}} = \frac{1}{N_{\lambda_D}}$$

where N_{λ_D} is the number of particles in a Debye square, in the two-dimensional case. Typically N_{λ_D} is of the order of 64, so that in the numerical experiments described below there are only about 64 plasma periods in a collision time. In most cases, our initial distribution is of Maxwellian form, so that this is not a factor to give rise to worry in that respect. Since the theory that is used below utilises the Vlasov equation, which assumes that the plasma is 'collisionless', that is, that the collision times are much longer than times of interest, we should like to be sure that our simulation will obey this condition also. Since no run, below, lasts longer than a few ($\ll 64$) plasma periods, we can see that this 'collisionless' criterion certainly will hold for the duration of any of these numerical experiments.

Both the effects described above can be reduced by increasing the number of particles in the simulation plasma, if the need arises.

Fortunately, however, such quantities as the Debye length and the electron plasma period remain the same whether a plasma of particles of charge q and mass m, density n, or a simulation of it with particles of charge sq, mass sm, and density n/s is being considered. For the electron plasma period of the real plasma is given by

$$\omega_{pe}^2 = \frac{4\pi n q^2}{m_e} = \frac{4\pi (Sq)^2 n}{S(m_e S)} = \frac{4\pi Q^2 N}{M} = \omega_{pe}^2 \qquad (2)$$

where ω_{pe}^2 is evidently the plasma period of the computer plasma, consisting of a density N of charges Q with mass M.

In Hockney (32) results are given for the measurement of certain average parameters, all expected to be approximately the same, and all estimates of relaxation time by different methods. They all agree with the value τ calculable from the expression

$$\frac{\tau}{\tau_{pe}} = \frac{N_{\lambda_D}}{2} \qquad (3)$$

where τ = relaxation time, τ_{pe} = electron plasma period, and N_{λ_D} = number of simulation particles per Debye square. This is clearly seen to be the inverse of equation (1) above and shows that when N_{λ_D} is substantially less than the number of plasma particles per Debye square in the real plasma, the relaxation time is, correspondingly, proportionately less.

Another, equally important source of error or difficulty is the non-physical interaction of the particles with the spatial or temporal grids used for computing such quantities as densities, potentials, fields and forces. This also gives rise to an increase in noise, called grid noise. It can always be reduced, but never totally eliminated by using finer grids.

Inaccuracies due to the presence of the grid can lead to numerical heating of the plasma. Let us suppose that the electric field is given at any grid point by

$$E = E_{correct} + E_{error\ field} \qquad (4)$$

The error field will be random, and will therefore tend to heat the computer plasma stochastically. However, in the case of NOVA, no serious increase has occurred in total kinetic energy during any run, so that this heating is not a worry though it is noticeable always that total kinetic energy increases monotonically. According to Hockney (32) the C.I.C. method, the one used here, only heats up at $^1/_{10}$ the rate of the N.G.P. method.

The use of N.G.P. and C.I.C. methods give rise to effective force laws between the 'superparticles' in the simulation which are notably different from those in the physical plasma.
The effective force laws are given in the diagrams shown in Figs. (3) and (4). It is evident from these diagrams that the force singularity at $r = 0$ has been completely removed. A smoothing has in fact been made which has eliminated the short range inter-particle interactions which produce effects characterised by short wavelengths: that is short range collisional effects between 'superparticles' are reduced as compared with the point-particle case, because of the nature of the superparticles under consideration. This does no harm to the calculation since one is at present interested in the more important collective long-range interactions with typical wavelengths much larger than inter-particle spacings and frequencies whose periods are much longer than particle crossing times. Also, any factor which reduces short range collisional effects is welcome since we are intending to simulate a 'collisionless' plasma.

In (34), mathematical formulations are given for the case where we consider the simulation particles with their associated charge which essentially covers an area equal to a grid cell uniformly, as particles of finite size or clouds which can pass through one another.

Various plasma parameters have been rederived for these 'finite size particles'; these are modified versions of the equivalent parameters in the real case. Instead of a charge density of $q\,\delta(x)$ being allotted to any particle in the theory, $q\,S(x)$ is used where the factor $S(x)$ is called the shape factor and gives the density of the cloud, suitably normalised, as a function of X. In the present case, for example, S(x) is as shown in Fig. (5) and has the cross-section of a rectangle centred on the particle. This leads to results such as the formula for the longitudinal dielectric function c.f. Chapter 3.

$$\epsilon(k,\omega) = 1 + S^2(k)\frac{\omega_p^2}{k^2}\int k.\frac{\partial f_0}{\partial v}\frac{dv}{(\omega - k.v)} \qquad (5)$$

where S(k) is given by the transformation

$$S(k) = \int dx\, S(x)\exp(-ik.x) \qquad (6)$$

Another result given by these authors is for the potential energy V(X) of charged clouds in the vicinity of a stationary test particle in the plasma, which they plot as a function of X. The smaller the size of the charge cloud, the larger the value of V(0), but it is noticeable primarily that the value of V(0) is finite, in contrast to the point-particle case. It is noticeable in the numerical output from the simulation below that the potential actually at the position of one of our simulated test particles is always finite, because of the fact that it is in reality a 'test cloud of charge' instead of being a 'test-particle', bearing out this result of Birdsall et al. This has to be borne in mind when simulating test-particle interactions, along with the result for the form of the

interparticle force-law reproduced in Fig. (4). Care has to be taken that the centres of two interacting charged clouds, whose interaction is to be studied, come no closer than the width of the clouds, for at closer distances the forces which act will be seriously non-physical.

The results of Birdsall et al, concerning small amplitude electron plasma oscillations, show discrepancies between point-particle plasmas and finite-size cloud plasmas only when very short wavelengths are being considered, well into the region where damping dominates.

Another fact that must always be borne in mind in discussing the results of a given simulation is that the disposition of the particles in phase space is unlikely to be exactly in thermal equilibrium. In fact, in many of the computer simulations described below the initialisation of the velocity components of the particles was almost random in the interval $[2v_{th}, -2v_{th}]$ where v_{th} is the thermal speed. Also, since the laying-down of particles was done in position space similarly - positioning every 4 particles randomly in successive grid squares, we might expect there to be more energy in certain short wavelength modes than might be obtained in a real plasma. Even if we set up the simulation plasma as close as possible to a state of thermal equilibrium, it must be remembered that fluctuations are a few orders of magnitude greater than for the corresponding real plasma because of the difference in particle density.

In order to study, for example, the linear growth phase of an instability, as a check on the basic physics of the model before going on to the non-linear phase, one would like to be able to follow modes of small amplitude, without their being obscured by

fluctuation effects. One would therefore like these fluctuations to be many orders of magnitude less than typical particle kinetic energies, in order to be able to 'prime' the required mode at a low energy and observe its growth until saturation at around 10^{-2} of the typical plasma kinetic energy. To make the system 'quiet' ie to substantially reduce noise, and ensure that it remains so for the duration of the experiment one would like to have

$$\frac{\partial \rho}{\partial x} = 0 \qquad \text{for each species and } E = 0 \text{ , or } \int q \rho \, dv = 0$$

Methods of doing this have been used with success by other workers, especially in one-dimensional simulations. Byers and Grewal (15) record one of the earliest instances of their use, in which they simulate the linear phase and saturation of an instability. They not only load phase space in a uniform way, to reduce noise, but do this also by truncating the spatial Fourier spectrum in the simulation. (A facility for doing this is built into NOVA.) In the work of Hung (35) this is done, in one dimension by having many streams of particles at different velocities. [The layout of particles on these would be ideal if in one timestep each one jumps into the position of the particle immediately in front of it on its particular orbit.] If this happens, then to a very good approximation the simulation plasma is such that the distribution function is a constant to within the accuracy of the computer, and since the particles are evenly spaced E is near to zero at all points. The only difficulty is discovering how many orbits, or streams of particles are required. If there are too few, an unwanted instability, the two-stream instability will develop. Using this method, effective potential energies of 10^{-6} or 10^{-7} of the kinetic energy of the plasma can be obtained, compared with kinetic energy for a non-'quiet' start of say 10^{-3} times the kinetic energy.

In two dimensions, similar principles can be applied. The author has written a quiet start procedure which, on the basis of an assumed Maxwellian velocity distribution generates sets of orbits closed in the computational rectangle, modulo the lengths of the sides. Unfortunately it is somewhat expensive in computer time and space to 'tune' this when say 10,000 particles are used, and no value of potential energy smaller than that of the 'random' start has been obtained. Whether this lack of success is due to poor 'tuning', or to the fact that a 'quiet' start is difficult to achieve by this method in a two-dimensional electrostatic plasma is a matter for conjecture.

Many predictions of the theory for a plasma of finite size particles have been verified by Okuda (36), who concludes that "it is certain that the finite size particle model with a spatial grid behaves like a real plasma as long as the Debye length and the particle size are not too small compared with the grid size". Since in our numerical experiments below we are dealing with the case where the Debye length is 4 times the grid size and the particle size, we can proceed in the confident expectation that a plasma will be adequately represented by the computer simulation.

(2) (c) Structure and Running of NOVA

The program NOVA is "a general purpose particle code for plasma simulation" and was originated in 1970-71 at L.RL Livermore by McNamara and Langdon (9). It is written in a modular form, and is designed to be run in a variety of modes for a variety of purposes. It is also intended to be easy to use without the user's having to appreciate any of the finer points of the calculation.

The user's main task is two-fold. He has to decide, on the basis of the problem he wishes to solve, what initial conditions to set up. Here he becomes involved with the need for scaling of the values of the physical quantities of the problem, but there are default options built into the code. In all the simulations described below the length is scaled to Debyelength units, which is one of the default options. Once this length scaling is established, other quantities are automatically scaled by one of the routines. In order to set up the initial conditions the user has to set up a module, called by the name YOUSET, for the purpose. Then the second part of preparing the code for dealing with a given problem is to decide what diagnostics are required; for these, extra routines may have to be written. Once all this has been completed, the code, in theory can be data-driven without further additions.

However, on the I.C.L. 4/70 installation, running under the MULTIJOB system, limitations of space become apparent. In its present form the code cannot be run at convenient times of day, since there are only 200K bytes available in daylight hours, and the code requires over 400. However it can be run, as it has been in almost every case below, with a non-standard supervisor which allows 500K bytes. Even so, in order to allow for the possibility, if required, of as many

particles as possible in the simulation, the code is segmented, as shown in Fig (6) in order to save as much space as possible. On the I.B.M. system 370/165, however, with 1000K bytes of store always available, no space problem as outlined above was encountered on the few occasions where this machine was used. Of the two computers mentioned above, the I.C.L. machine is at the U.K.A.E.A. Culham Laboratory, while the I.B.M. one is at A.E.R.E. Harwell.

A typical run of 100 timesteps with 16000 particles on the 4/70 took about 30 minutes. This was after some optimization. The fact that NOVA is written mainly as a large number of FORTRAN subroutines has facilitated development, but leads to slow running. The "particle pushing" in which the equation of motion is solved by a finite difference method for each particle in turn, can be expected to take up some 50% of the computation time, so it is of great importance to optimise the routines involved. At present they are written in optimised FORTRAN, with the minimum number of arithmetic operations being performed, by means of absorbing scaling factors and timestep into both the position and velocity co-ordinate values. Also the original versions have now been modified to include the statements from the two area-weighting routines called by the 'pushers'. Since these routines were called once each for every particle, a saving of 32,000 subroutine calls per time step has been effected in a typical simulation with 16,000 particles. This reduced the time taken for a typical run by some 20%. It would certainly have been preferable to have the particle-pushing routines written in USERCODE, but because of large delays in implementing properly at Culham Laboratory the author's version of the code, time was not available to do this.

Few more details will be given here of the code. It is more flexible than GALAXY (7) the previous large particle code at the Culham Laboratory which was designed to be of optimal speed on the English Electric K.D.F9, a machine of one quarter the power of the I.C.L. 4/70. So far no outstanding improvement in performance speed of NOVA over GALAXY in a similar mode has been noted.

The increased flexibility of use comes from the following sources.

(1) NOVA is in FORTRAN, while GALAXY was latterly in ALGOL and USERCODE: this makes NOVA more transportable, since not all systems have an ALGOL compiler and no other assembly language is the same as K.D.F.9 usercode, while 4/70 USERCODE is the same as I.B.M. system 360 and 370 assembler.

(2) NOVA allows for more variety in boundary conditions. The computational area is not constrained to be a square, and 'perfectly conducting walls' are available as a boundary condition to supplement the double-periodic case. It can also, with some alteration to the Poisson-solving routines, be run as a one-dimensional simulation code which, for example, is at present being done by Hung (35), with good results.

GALAXY, however, can avoid these criticisms somewhat, since it was designed more as an exercise in optimisation of a given computer's facilities than with many users in mind.

(3) (a) Immediately Previous Work: Exact Forms for Field Due

(3) (a) Immediately Previous Work: Exact Forms for Field Due
to a Test Particle in a Plasma in Two Dimensions

The subject of all the investigations reported below is that of the interaction of a test particle with a plasma. A test particle not in equilibrium with a plasma is not an object which commonly occurs in nature, but consideration of it can lead to results about electrostatic shielding in two dimensions which are of some interest. A short historical review of previous work on the subject is given in Chapter (1) (b) above.

This section of this chapter contains a detailed description of the work done by Laing et al which is reported in Ref (8). This forms the starting point for the investigations described in Chapter 4, and concerns the calculation of the exact form of the potential due to a moving charged particle in a collisionless plasma. Previous investigators eg Montgomery et al (29), had merely given asymptotic forms for the potential.

The analytic form for the potential due to a moving test-particle has been given by several authors, for example by Thompson (1964). In Ref (8) it is derived in a slightly different way.

It is supposed in this derivation that for times $t<0$, there is a uniform collisionless plasma described by an equilibrium distribution function $f_0(v)$, and that there is no electric field. At $t=0$, the test particle is introduced into the plasma, inducing a first order electric field $E_1(x,t)$ and a perturbation of the distribution function $f_1(x,v,t)$. The charge density due to the test particle is given by $\rho_T = q\,\delta(\underline{x} - \underline{u}t)$

where u = velocity of particle; q = charge on particle.

The reaction of the plasma on the test particle (see 4 below) is not included in this analysis. The equations used are the Vlasov and Poisson equations, and once these have been linearised as described above, we obtain

$$\frac{\partial f_1}{\partial t} + \underline{v} \cdot \frac{\partial f_1}{\partial \underline{x}} + \frac{e}{m} \underline{E}_1 \cdot \frac{\partial f_0}{\partial \underline{v}} = 0 \qquad (1)$$

$$\mathrm{div}\, E_1 = 4\pi e \int f_1 \, d\underline{v} + 4\pi \rho_2 \qquad (2)$$

Introducing a Fourier analysis of the $\underline{v}$-dependence, and a Laplace transformation of the time variable, we get

$$(p + i\underline{k}.\underline{v})\bar{f}_1 - i\frac{e}{m}\bar{\Phi}\,\underline{k} \cdot \frac{\partial f_0}{\partial \underline{v}} = 0 \qquad (3)$$

$$k^2 \bar{\Phi} = 4\pi e \int \bar{f}_1 \, d\underline{v} + \frac{4\pi q}{(p + i\underline{k}.\underline{u})} \qquad (4)$$

The 'barred' quantities are the Fourier-Laplace transforms of the corresponding functions of $\underline{X}$ and $\underline{t}$; the relation $E = -\nabla\Phi$ has been used. We now eliminate $\bar{f}_1$, to obtain

$$\bar{\Phi}(\underline{k}, p) = \frac{4\pi q}{(p + i\underline{k}.\underline{u})k^2 \epsilon(\underline{k}, p)} \qquad (5)$$

where

$$\epsilon(\underline{k}, p) = 1 - \frac{4\pi i e^2}{m k^2} \int dv \, \frac{\underline{k} \cdot \frac{\partial f_0}{\partial v}}{(p + i\underline{k}.\underline{v})} \qquad (6)$$

is the Fourier-Laplace transform of the plasma dielectric coefficient.

Thus if we now assume that the plasma is two-dimensional, which is done in this paper to facilitate comparison of results of analysis with those from a two-dimensional computer code, we obtain an expression for the potential

$$\underline{\phi}(x,t) = \frac{q}{\pi}\int \exp(i\underline{k}.\underline{x})\,d\underline{k}\;\frac{1}{2\pi i}\int_{\sigma-i\infty}^{\sigma+i\infty}\frac{\exp(pt)\,dp}{(p+i\underline{k}.\underline{u})k^2\epsilon(\underline{k},p)} \qquad (7)$$

where σ is such that the path of the p-integration lies to the right of all singularities of the integrand.

The solution of the inner integral here is taken to be that which ignores contributions due to the zeros of $\epsilon(\underline{k},p)$ and includes only the residue at the pole $p = -i\underline{k}.\underline{u}$. This leads to

$$\underline{\phi}(\underline{x},t) = \frac{q}{\pi}\int \frac{\exp[i\underline{k}.(\underline{x}-\underline{u}t)]\,d\underline{k}}{k^2\epsilon(\underline{k},-i\underline{k}.\underline{u})} \qquad (8)$$

This is the equilibrium state. Introduction of the relative co-ordinate $r = \underline{x} - \underline{u}t$ leads to

$$\underline{\phi}(\underline{r}) = \frac{q}{\pi}\int \frac{\exp(i\underline{k}.\underline{r})\,dk}{k^2\epsilon(\underline{k},-i\underline{k}.\underline{u})} \qquad (9)$$

Introduction of polar co-ordinates (r,θ) and (k,ϕ) for $\underline{r}$ and $\underline{k}$, with $\underline{u}$ along the polar axis, gives

$$\underline{\phi}(r,\theta) = \frac{q}{\pi}\int_0^\infty k\,dk\int_0^{2\pi}\frac{\exp[ikr\cos(\theta-\phi)]}{k^2+k_D^2 f(\cos\phi)}\,d\phi \qquad (10)$$

Here $f(\cos\phi) = 1 + \xi\cos\phi\,Z(\xi\cos\phi)$ where $\xi = \frac{u}{v_e\sqrt{2}}$ where v_e is the electron thermal speed, and Z is the plasma dispersion function ( ). $k_D = 1/\lambda_D$, where λ_D is the Debye length $\lambda_D = (kT/4\pi ne^2)^{\frac{1}{2}}$

Using the expression

$$\exp\left[i k r \cos(\theta - \phi)\right] = \sum_{n=-\infty}^{\infty} i^n J_n(kr) \exp\left[in(\theta - \phi)\right] \quad (11)$$

and the substitutions $x = kr$, $a = k_D r$, we obtain

$$\underline{\Phi}(a, \theta) = \frac{q}{\pi} \sum i^n \exp(in\theta) \int_0^{\infty} J_n(x)\,dx \int_0^{2\pi} \frac{\exp(-in\phi)\,d\phi}{x^2 + a^2 f(\cos\phi)} \quad (12)$$

This expression, suitably put entirely in terms of real quantities is used in an exact calculation of $\underline{\Phi}$, where it is expressed in the form

$$\underline{\Phi}(a, \theta) = \sum_{n=0}^{\infty} A_n(a) \cos n\theta \quad (13)$$

Each term $A_n(a)$ is separately evaluated by numerical techniques. Depending upon the value of ξ a cut off in the summation is imposed at N, which is 7 for low velocities, and as high as 16 for some values of $\xi > 1$.

The diagrams showing the result of this exact computation are reproduced here in Figs (7a), (7b) and (7c). The first of these shows a contour map of $\underline{\Phi}(a)$ for $\xi = 1$, with the test-particle at the origin of co-ordinates. The second of these shows the cross section of the potential distribution along the line of motion of the test-particle, for $\xi = 1$. The third shows part of the potential distribution for a fast test-particle which has $\xi = 2.4$.

In the case when $\xi = 1$, the test-particle is moving with a velocity of the same order as the electron thermal velocity. A great concentration of electrons has occurred downstream, immediately

behind the test particle. The authors state that this is in effect a heavily damped plasma oscillation. With increasing velocity the damping has diminished, until we observe the fully developed plasma oscillation shown in the 3rd diagram, established behind the test particle as a wake.

In the second diagram (Fig 7b), there is a comparison between the potential profile obtained by the calculation described above and that obtained from a plasma simulation using the GALAXY code (7) of Boris and Roberts. The two results agree very closely indeed.

A second section of Ref (8) deals with the series expansion for ϕ in terms of powers of u/v_e taken to third order, starting from equation (10). Using the expression for $Z(t)$ valid for $t < 1$ given in Ref (37)

$$Z(t) \cong i\pi^{1/2}(1-t^2) - 2t \qquad (14)$$

leads to an expansion of the denominator of the integrand of equation (10) as follows

$$k^2 + k_D^2 f(\cos\phi) \cong k^2 + k_D^2\left(1 + i\pi^{1/2} t(1-t^2) - 2t^2\right) \equiv D \qquad (15)$$

where $t = \xi \cos\phi$, as above.

The inverse of D is expanded to order t^3 , and $\exp(ikt\cos(\theta-\phi))$ is expanded again as in equation (11). When these are both inserted in equation (10) we obtain

$$\underline{\Phi}(r,\theta) = 2q\left(A_0 + A_1\cos\theta + A_2\cos 2\theta + A_3\cos 3\theta\right) \qquad (16)$$

$$A_0 = I_0^0 + \tfrac{1}{2}\xi^2\left(2I_0^1 - \pi I_0^2\right)$$

$$A_1 = \pi^{\frac{1}{2}}\xi\left[I_1^1 - \tfrac{3}{4}\xi^2\left(I_1^1 - 4I_1^2 + \pi I_1^3\right)\right]$$

with similar expressions involving powers of ξ for A_2 and A_3. The factors I are given by

$$I_n^m(a) = a^{2m}\int_0^\infty \frac{x\,J_n(x)\,dx}{(x^2+a^2)^{m+1}} \qquad (17)$$

For $n \neq 0$, it can be shown that $I_n^m(a)$ behaves as $1/a^2$ for large a. This is then the dominant asymptotic behaviour of $\underline{\Phi}$, except when $\xi = 0$, the stationary test-particle case, when $\underline{\Phi} = I_0^0(a) = K_0(a)$, the modified bessel function, which is the two-dimensional analogue of exponential Debye shielding. The result concerning asymptotic behaviour for $\xi \neq 0$ is the two-dimensional analogue of the result of Montgomery et al, who proved the asymptotic dependence of the test-particle potential to be $1/a^3$ given a stable distribution function, in three dimensions.

An analysis was done of a comparison between these results and those found by the "exact calculation", and resulting plots of $\underline{\Phi}_{\text{exact}}/\underline{\Phi}_{\text{expansion}}$ are reproduced in Fig (8A). This diagram shows this ratio as a function of ξ for various values of a. One can readily see from this diagram and from the other one in this paper that the expansion method gives its best results when $\xi \leq 1$. To get greater accuracy would necessitate taking more terms in the expansions, which would have been a prohibitively time-consuming process.

The third piece of analytic work which is described is an asymptotic expansion for $\underline{\Phi}$ in terms of $t = \xi \cos\phi$ when $u \gg v_e$, ie when ξ is large. Since ξ is large there will only be a small range of ϕ, centred upon $\pi/2$ and $3\pi/2$ where the approximation of large t will be invalid, and the authors assume that the effect of extending the range of validity to the whole range is negligible. From Ref (37) we take

$$t\,Z(t) = -\left(1 + \frac{1}{2t^2}\right) + i\pi^{\frac{1}{2}}\, t \exp(-t^2) \qquad (18)$$

making the denominator of equation (10)

$$D = k^2 - \frac{k_D^2}{2t^2} + i\eta\cos\phi \qquad (19)$$

where η is very small.

Now let $\alpha = \frac{k_D}{\xi\sqrt{2}} = \frac{k_D v_e}{u}$ This leads to

$$\underline{\Phi}(\underline{r}) = \lim_{\eta \to 0} \int \frac{\exp(i\underline{k}.\underline{r})\, d\underline{k}}{k^2 - (\alpha^2/\cos^2\phi) + i\eta\cos\phi} \qquad (20)$$

Expressing $\underline{k}$ as (k_x, k_y) we obtain

$$\underline{\Phi}(\underline{r}) = \lim_{\eta \to 0} \frac{q}{\pi} \int_{-\infty}^{\infty}\int \frac{k_x^2 \exp(ik_x x)\exp(ik_y y)\, dk_x\, dk_y}{(k_x^2 + k_y^2)(k_x^2 - \alpha^2 + i\eta k_x)} \qquad (21)$$

$$= \lim_{\eta \to 0} \frac{q}{\pi} \int_{-\infty}^{\infty} \frac{\exp(ik_x x)\exp(-|k_x y|)\,|k_x|\, dk_x}{k_x^2 - \alpha^2 + i\eta k_x}$$

$$\begin{cases} = 0 : x > 0 \\ = 2\pi q \exp(-\alpha|y|)\sin\alpha x : x < 0 \end{cases}$$

A diagram showing contours of this function is reproduced in Fig (8B). It can be compared with Fig (7C) which was the result of an exact calculation for $\frac{v}{v_t} = 2.4$. In the latter, some slight damping of the maxima behind the particle is evident, but in the case of the asymptotic expansion outlined above no damping is manifest because of the approximations that have been made.

In this case, of $\frac{v}{v_t} > 1$, no computer simulation was done by the authors for reasons outlined below.

The simulation program, GALAXY, Ref (7), used by the authors followed the motion of a large number of charged particles in two dimensions. Provision was made for whatever diagnostics were required; in this case the potential distribution over the plane of the calculation was of most interest. The calculation is performed in a square, of typically 16 x 16 Debye lengths; the simulation plasma consisted of about 16,000 'ions' and 'electrons'. These parameters are very close to those used in most of the square mesh calculations described below in Chapter 4. The boundary conditions are double-periodic, so that the authors were in fact following one of an infinite array of test particles moving in a plasma. It was hoped that with boundaries of length 16 Debye lengths spurious effects due to boundary periodicity would not be important within, say, 8 Debye lengths of the test particle, and so a comparison should be possible with the theory outlined above, which applies to a single test particle in an infinite medium. The fact that good agreement between theory and simulation is obtained Fig (7b) shows the assumptions about the effect of the boundary conditions to be justified. The result of another procedure for comparing theoretical and analytic results is reproduced in Fig (8c). Here, for the case of zero test particle velocity, the

potential distribution near the test particle is compared with $K_0(x)$ and with $-\log(x)$ for various values of t. $\log(x)$ is the form of the potential for an unshielded charged rod. The diagram indicates clearly that at $t=0$, no shielding has been set up, but that at later times the potential agrees well with the shielded form $K_0(x)$ for the two-dimensional case.

The reason why the authors of Ref (8) could not proceed with simulation of the case where $\xi > 1$ was due to a restriction in the code. GALAXY was written to run on a square mesh, and in order to encompass the whole of a wake in the computational area, the dimensions of the square required would have been such as to make any computation prohibitively expensive. The flexibility of NOVA in this regard makes it ideally suitable for use in a programme of investigations starting off from this unfinished work by attempting to simulate the wake of a fast particle using a rectangular array.

The main achievement of Ref (8), then, is the calculation of the exact form of the potential due to a test charge in two dimensions, which had not previously been done. Another notable feature of the paper is the excellent agreement between results of collisionless plasma theory and those from computer simulation.

In addition, the work outlined in that paper gives ideas for further research into plasma-test particle interactions and simulations of such interactions. The fact that the authors' method, of introducing a large charge at $t = 0$ caused large oscillations in the value of the potential in the plasma which persited for several ω_p^{-1} suggests that a better simulation would be done if this oscillation could be prevented by introducing the test charge in some gradual fashion. There is also the direct extension of this work which can

be done if a test particle moving with $\zeta > 1$ can be successfully simulated and its wake observed. Other possibilities arise such as performing similar analyses with either a different plasma velocity distribution function, or in the presence of a magnetic field $\underline{B}$.

Work concerning the case of a different plasma velocity distribution function has been done theoretically by Whipple (40). Numerical calculations by the present author using these theoretical results have been done, as have a small number of simulations, but the results are of too preliminary a nature to describe here.

The case where a magnetic field is present is gone into in some detail in Chapter 5 below.

(3) (b) Significance of Results Concerning Test Particles

The work described in Ref (8) and the present work are probably the only cases in which, in a computer plasma simulation, by the expression "test particle" is meant an extra-large superparticle moving in the plasma. Most other investigators who use the concept and give "test particle" results adopt a different approach. They have a one or two component plasma which is set off from an initial condition and allowed to evolve with time, without a large test charge and its possible attendant transients embedded in it. In these cases when it is desired to find the potential due to a test charge (eg Okuda, Ref (36)), the authors select all particles in the plasma at or near the chosen velocity and note the potentials at grid points on either side of them. Then an average is taken of corresponding points, and a graph can be plotted showing what is taken to be the potential due to a test charge moving at the given velocity. It is probable that this gives reasonable answers in the case of Ref (36) because, firstly, his simulation is one-dimensional and so he can afford more grid points, thus achieving greater detail, and secondly, his average charge cloud occupies up to a Debye length or more, and so can be expected to have more influence over distances comparable with the scale lengths of the variations of potential in Fig (7b). In our case, with two dimensions, and the charge 'cloud' occupying one grid rectangle, which itself is much ($^1/16$) less than a Debye square, we do not expect a similar method to be useful. Another drawback if OKUDA's method was employed in two dimensions is that great inaccuracies would come in because the particles are not conveniently moving parallel to the grid lines. This would mean that the potentials at pre-selected distances from them along their lines of motion could not be easily read off but would have to be obtained from interpolation.

Accordingly, in two dimensions, in order to produce a "test particle" effect which can be easily seen the method is implemented of using one large charge and mass. The greatest convenience of this is that only one potential distribution has to be measured.

Another result of the fact that the test particle is given a large charge is that the forces acting on it will be very much larger than if it was a sample particle from the background simulation plasma. This is because the forces acting on it, for example the drag due to the charge which it induces in the plasma, are such that

$$\underline{a} \propto -\frac{q_T^2}{m_T}$$

q_T = test charge, m_T : test particle mass, $\underline{a}$ is the acceleration.

Thus if q_T is greater than the charge q of a typical 'electron' in the plasma, then if m_T has not been increased as the square of q_T, the force acting will be increased. This is useful, for it enables, by a suitable choice of m_T, the slowing down of a particle to be observed in a reasonably short time, a time in which any sample electron from the plasma will not have appreciably slowed.

The concept of a 'dressed test particle' was introduced by Rostoker (Ref (26)), and defined to be a charge plus its attendant polarisation cloud. He uses it to obtain certain expressions concerning the collective behaviour of a system by the superposition of many of these entities, but it is not known at present how widely applicable this technique might be. He introduces a test particle, in his analysis, into the plasma using an 'adiabatic switching factor': that is he lets the charge density be given as

$$\rho_{ext} = \lim_{\lambda \to 0} \rho(k,\omega) \exp(i(\underline{k}.\underline{x} + \omega t))_e{}^{\lambda t}$$

where λ approaches zero from below. It was this that led us to the

procedure adopted in the simulations described below, of gradually increasing the charge on the test particle from $t = 0$ to a maximum value at $t = \tau_p$. This proved markedly beneficial in the reduction of the amplitude of transients in the system.

(4) (a) Introduction to Results of Electrostatic Plasma Simulation

In general, in each simulation described below, similar parameters were employed as in the work done in Ref (8), and beside the description of each individual simulation, should be found the data which relates to it.

A typical program, compiled and composed by the I.C.L. System 4 Multijob system, occupied some 410 - 450 kilobytes of core store. The upper limit occurred when 'on-line graphics' was included. This program was large enough for the simulation of the motion of 16,384 particles. Since each particle has four co-ordinates, all requiring a word of store, and since there are four bytes per word, this means that 16 bytes are required to describe one particle. Thus since the maximum limit of store available is 500 kilobytes, we can only fit in about 3,000 more particles in the remaining storage space. Thus with 16,384 particles we are working close to the limits of the machine, in that it would be impracticable to increase the number of particles in the simulation by more than 20%, whereas a change in particle number which would give noticeably finer resolution would probably require an order of magnitude increase. Thus we are getting almost the best detail possible with the core space available.

In every section of this chapter is included the additional theory required (where this is the case) and a description of the results of the simulations associated with it, as well as any other calculations which may have been performed.

Because of the desirability of minimising the storage occupied by the program in the computer, instead of using the standard GHOST system contour plotting routine, a simpler one was written by the

author, and this proved quite adequate for the purpose. Any contour plot reproduced below was generated using this routine. It uses straightforward linear interpolation to find points on contours, and joins up these points with straight lines.

(4) (b) Stationary Test Particle: Starting Procedures for Simulations

Before any of the calculations involving a moving test-particle were done, a preliminary numerical experiment was done to test a proposed method of introducing the test-particle "adiabatically" into the plasma. This was prompted by the idea of the use of the 'adiabatic switching factor' by Rostoker (26) to describe the introduction of his test particle into a plasma. The object of this is to ascertain whether the large fluctuations in the potential observed in GALAXY runs Ref (32) over the first several ($\sim$ 8 or more) $\times \omega_p^{-1}$ and which can be ascribed to the transient effects set up by the sudden introduction of the test charge at $t = 0$, can be eliminated or reduced.

In the GALAXY runs, however, the overall shape of the potential distribution remained the same once the dynamic screening had been set up; only the unwanted transient effects caused the values of potential over the whole distribution to oscillate upwards and downwards in step. The fact that the overall shape of the distribution remained the same meant that this did not adversely affect the results. However, in the numerical experiments below, where, for example, we want to set off a particle with a given initial velocity and observe its slowing down under the effect of the reaction of the plasma, we would prefer to have transient effects eliminated, in order to prevent any possible adverse effects on the results.

Since the NOVA program is written in modular form in FORTRAN, the modification required to perform an experiment to decide whether the adiabatic introduction of a test charge is advantageous, is simple. In fact a switch was built in so that the tests could be data-driven.

What was in fact done was straightforward. It was decided that the charge on the test-particle should increase with time such that, for times less than the plasma period the charge $q(t)$ is given by

$$q(t) = CHMAX * t / \tau_p \qquad (1)$$

where CHMAX = maximum charge, τ_p = plasma period, t = time elapsed. For times greater than τ_p, the charge was held constant at the value CHMAX.

It was also hoped that after a time τ_p had passed, the local charge distribution would have rearranged itself, such that the expected shielding would be set up. This is of importance for later experiments when we do not want to allow the drag force, due to the charge induced in the plasma, to act on the test particle until such time as the induced charge has been fully established. An early test run gave an indication of likely errors in a calculation of drag on a particle, starting with $q = CHMAX$ at $t = 0$

The following two runs were implemented subsequently

(1) The test particle was set up with charge equal to CHMAX at $t = 0$ as follows:

MESH DIMENSIONS	64 x 64
PHYSICAL DIMENSIONS OF PLASMA	16 x 16 DEBYE LENGTHS
TIMESTEP DT	0.25
NO. OF 'PARTICLES' IN PLASMA	16384
CHARGE ON TEST PARTICLE	200 UNITS

(2) The test particle was originally given a charge of one unit, the same as the plasma particles, and this was gradually increased to CHMAX = 200.0 . The other data remained the same.

A graphical analysis of the results clearly demonstrates that transient oscillations are almost eliminated in the second case, where the charge is entered adiabatically.

In case (1), where the test charge is introduced with its maximum value at the beginning of the simulation, it can be seen from Fig (9) that oscillations of a large amplitude are set up, which show little sign of damping as time passes, as far as the simulation proceeds, that is, a total of 17.5 plasma times (ω_p^{-1}) . This graph shows the value of the potential, in arbitrary units, at the co-ordinates of the test-particle, and it can be seen that the amplitude of the unwanted oscillations is about $\frac{1}{3}$ of the average value of the potential. The period of the oscillations was estimated to be about $2.5\ \omega_p^{-1}$.

We should like to check that shielding has occurred before a time of τ_p has elapsed in the simulation.

According to theory, the unshielded charge in two dimensions gives rise to a potential distribution $\phi(x) \sim \log(x)$, while the shielded charge gives rise to a potential distribution $\phi(x) \sim K_0(x)$ where K_0 is the modified Bessel function of order 0 . For various values of elapsed time t , the potential distribution in the region of the test charge was plotted against $-\log x$ and against $K_0(x)$ It was found that shielding had been already set up after 10 timesteps, ie after $2.5\,\omega_p^{-1}$ .The plot of the potential $\phi(x)$ against $K_0(x)$ Fig (10) for $t = 2.5\omega_p^{-1}$ shows good linearity, demonstrating that shielding has taken place in the expected manner. Thus shielding will certainly have taken place by $\tau_p = 2\pi\omega_p^{-1}$, as had been hoped.

For case (2) with gradual increase of test-particle charge, the potential at the position of the test particle was plotted as a function of time, and this is reproduced in Fig (12). It can be seen that, as was hoped, there do not occur the large amplitude oscillations which dominated the behaviour in Fig (9). One can see clearly the gradual increase in potential with increasing test-particle charge, and once the maximum charge has been established, it is noticeable that there is merely an oscillation of small amplitude which is quickly damped leaving the potential at a value which remains almost constant with time.

In this case also, the potential distribution near the test particle was plotted against $\log(x)$ and $K_0(x)$ for a chosen value of t. Examination of Fig (14) and Fig (13) show that by $t = \tau_p$ the line of $\bar{\phi}(x)/\log(x)$ has deviated from linearity while $\bar{\phi}(x)/K_0(x)$ appears to be a good straight line. For the purposes of comparison, a graph of $K_0(x)$ against $\log(x)$ is shown in Fig (11), which indicates that the plot of $\bar{\phi}(x)$ against $\log(x)$ in Fig (14) has taken up a form which one might expect for a shielded potential distribution. This, in addition to the results above give us the utmost confidence that full electrostatic shielding of the test charge will have been set up by $t = \tau_p$

The results of this preliminary work are satisfactory, and enable us to proceed with confidence to further numerical experiments where the reduction of transients, which we can now achieve, ensures that the physical effects in which we are interested will not be obscured or adversely modified.

Mathematically, what is now being done is the following.

Instead of the term $4\pi q\,\delta(x-ut)$ in the equation (3a(2)) we now have $4\pi q(t)\,\delta(x-ut)$ where

$$q(t) = qt/T \;:\; 0 < t \leq T$$
$$q(t) = q \qquad :\; T \leq t \tag{2}$$

When we perform a Fourier-Laplace transform on this new function we obtain, where $\mathcal{F}$ means Fourier transform, $\mathcal{L}$ means Laplace transform.

$$\gamma = \mathcal{F}\mathcal{L}\,4\pi q(t)\,\delta(x-ut) = 4\pi q \int_0^\infty \exp(-pt)\int \exp(-i\underline{k}.\underline{x})\int \exp(ik_1(x-ut))\,dk_1\,dk \tag{3}$$
$$= \int_0^\infty 4\pi q(t)\exp(-(p+i\underline{k}.\underline{u})t)\,dt$$

Splitting this up into two integrals from 0 to T and from T to ∞ we obtain

$$\gamma = \frac{4\pi q}{T(p+i\underline{k}.\underline{u})^2}\left[1 - \exp(-(p+i\underline{k}.\underline{u})T)\right] \tag{4}$$

which tends to $4\pi q/(p+i\underline{k}.\underline{u})$ as $T \to 0$, and which becomes very small as T becomes very large. When we deal with the pole in the inverse Laplace transform in equation (3a7), at $p = -i\underline{k}.\underline{u}$, this term tends to $4\pi q$ as before, but the oscillating terms derived from the roots of $\epsilon(k,\omega) = 0$, and assumed to be damped in the analysis of Ref (8) such that they do not affect the large time solution, are modified so that their initial amplitudes, compared with what it would be in the case of the sudden switch-on of test particle at $t = 0$, are reduced by a factor $\sim 1/T$. The potential is given by (see Ref 8)

$$\Phi(x,t) = \frac{q}{\pi}\int \frac{\exp[ik.(x-ut)]\,dk}{k^2\epsilon(k,-i\underline{k}.\underline{u})} + [\text{damped oscillatory terms}] \tag{5}$$

Using the procedure outlined above, this becomes

$$\underline{\Phi}(x,t) = \frac{q}{\pi}\int \frac{\exp[i\underline{k}\cdot(\underline{x}-\underline{u}t)]\,d\underline{k}}{k^2\,\epsilon(k,-i\underline{k}\cdot\underline{u})} + \gamma\left[\begin{matrix}\text{damped oscillatory}\\ \text{terms}\end{matrix}\right] \quad (6)$$

where $\gamma = O\left(\frac{1}{T}\right)$.

Intuitively, and demonstrably, the longer the time T, the more the amplitude of oscillating terms would be expected to be reduced. However the longer the time T the greater the computing time required. The present value of $T = 2\pi/\omega_p$ seems quite adequate for the purpose of bringing down the amplitude of unwanted oscillations in the level of the potential in the simulation plasma.

(4) (c) Moving Test Particle: No Reaction of Plasma Upon Test Particle

In part this section is a repeat of previous work (Ref 8), serving as a check upon the performance of the NOVA program.

(1) A test particle of greater than thermal velocity was introduced into the simulation plasma at $t = 0$, and the resulting potential distribution after a time when transients had been eliminated somewhat, was noted, with special interest in the cross section parallel to the direction of motion. Some relevant simulation parameters were:

MESH DIMENSIONS	64 x 64
PLASMA DIMENSIONS	16 x 16 DEBYE LENGTHS
TIMESTEP DT	0.25
NO. OF PARTICLES IN PLASMA	16384
VELOCITY OF TEST PARTICLE	

The above mentioned potential distribution cross-section after 70 steps was plotted, but is not reproduced here, and was found to compare favourably with that in Fig (7b), which is the result of a run in (8). This was one of the preliminary testing runs with the full NOVA code on the I.B.M. 370/165 at A.E.R.E. Harwell.

After this result had been obtained, it was decided to repeat the run with a gradually increasing charge on the test particle, and this was successful in reducing transients as before. A slightly smoother collection of potential values through which to draw another curve as in Fig (7b) was obtained, and a good similarity was obtained, though, again, this curve is not reproduced here.

As in 4(b), in the first part of this experiment the potential value at the test particle fluctuated wildly as time progressed, while in the second part, once the charge had been established, fluctuations were of much smaller amplitude.

The next part of this section concerns the verification of the predictions of Ref (8) concerning a test particle in a plasma moving with a velocity greater than any of the velocities simulated by the authors of that paper, using GALAXY. Their analysis, like that of earlier work (Refs 24, 25, 27) predicts that the test particle will leave a wake in the form of a plasma oscillation behind it as it moves with a high velocity, this wake being damped slightly. In order to allow a suitable physical length along the direction of motion of the test charge, in which to observe the wake, which will be much longer than the strongly damped one observed in earlier runs with smaller test particle velocities, the computation had to be switched to a simulation of a rectangular two-dimensional plasma. This involved a few changes in coding.

It was decided that no pair of sides of the rectangle should be less than eight Debye lengths, in order to ensure the suppression of boundary effects; also it was decided to keep a plasma of the same physical properties, and to keep, in the new case, a computational mesh in the same relation to the physical lengths as previously. Accordingly, the number of mesh steps and Debye lengths were doubled in the x-direction and halved in the y-direction, to give a 128 x 32 computational grid, and a 32 x 8 Debye length rectangle. Thus there are still four mesh steps per Debye length, and 64 particles per Debye square ($N_D = 64$).

It would be preferable to have a rectangle which represents a physically longer area, but this produces problems. This is because we can only have a grid of a number of meshes which is a power of 2 because the Poisson-solvers require this constraint. Therefore, we would need a grid which was 256 mesh lengths in the x-direction, while retaining 32 in the x-direction, say, if we wanted to increase, in the slightest, the number of mesh steps along the direction of motion of the particle. The motive behind increasing the number of mesh lengths would be to ensure that there were a suitable number of grid steps per Debye length, when we increase the physical length of the simulation plasma. The present level of 4 grid lengths per Debye length is near the lowest limit which can usefully be used if shielding properties are to be represented accurately. When we double the number of mesh squares, if we retain the same number of simulation particles, we are reducing N_{λ_D} by a factor of 2, noticeably altering plasma properties. However it would be outwith the storage capabilities of the computer to double the number of plasma particles, or even to increase it by more than a few thousand, in order to try to keep plasma properties the same as previously. Thus any proposed simulation with a longer physical area must be affected by the fact that the system which will be simulated on the computer, will be a less accurate representation of a plasma of the type of interest.

Having a rectangle of 32 Debye lengths end to end, we are clearly somewhat limited in the length of test-particle wake we can hope to simulate. This is because the calculation has periodic boundary conditions, and if the wake is of the same order of magnitude as the length of the rectangle, the test particle will interfere with the end of its own wake. Thus we have to ensure that we would not be dealing with wakes of such a length (unless interested in the interaction

of a test particle with a wake?). Thus however long the lightly damped oscillatory wake may be that is left behind a particle, which is travelling at velocity v, in the steady state, we cannot describe it in the simulation after more than 32 Debye lengths of it have been generated by the test particle.

The first run which was performed was with a test particle of velocity $2.0\, v_{e_{th}}$, where $v_{e_{th}} = 1.0$ in scaled units. The form of the cross section of the potential distribution parallel to the direction of motion of the particle after 70 steps is given in Fig (15). It can be seen that the 'wake' is still quite strongly damped, as in the previous results. The value of $\xi = \sqrt{2}$ used here is larger than the greatest value $\xi = 1$ used in any of the actual simulations in Ref (8), so that, at this point we have gone beyond the work of that paper. Data for this run were as follows.

MESH DIMENSIONS	128 x 32
PHYSICAL DIMENSION	32 x 8 Debye Lengths
TIMESTEP DT	0.125
NO. OF 'PARTICLES' IN SIMULATION	16384
VELOCITY OF TEST PARTICLE	2.0

This run completed and the results noted, it was decided to attempt another run with a higher test-particle velocity of $v = 2.5$ This means a value of ξ of 1.78. The results show that the test-particle is now moving fast enough to generate a wake, and the cross-section of the potential distribution after 80 steps is shown in Fig (16). The latter shows the state where the 'bow wave' in front of the particle has almost caught up with the end of the 'wake'. This is as far as the calculation proceeded. The fact that this wake

occupies 32 Debye lengths and probably would require many more to simulate it in its entirety, leads one to the conclusion that for higher velocities, specifically in order to compare simulation with the analytic result Ref (8) for $\gamma = 1.4$, a prohibitively long rectangle would be required if identical plasma properties are to be maintained in a simulation and if wake interference is to be avoided.

It was, however, decided to attempt a simulation which could describe a longer wake, by using the same number of simulation plasma particles and the same computational grid, but changing the physical scaling from a 32 x 8 Debye length rectangle to a 43 x 10 Debye length rectangle. The hope here was that one could describe more of the wake without any interference occurring between the end of the wake and the build-up of potential in front of the test particle. A NOVA run was implemented with the same data as the last one described, except for the new 43 x 10 λ_D scaling.

The potential distribution which had been set up by the time that 80 steps of $\Delta t = 0.15\omega_p^{-1}$ had passed is represented in Fig (17) where the cross section of the potential distribution along the line of motion of the particle is plotted. Consideration of this diagram reveals 2 noticeable minima behind the test particle, at about 2 and 17 Debye lengths distant from the test particle. This is a good indication of the tendency toward the setting up of a spatial oscillation of potential behind the test particle with respect to the test particle position. Any indication of how strong damping effects may be at this velocity, is unclear from the data, but it is evident that they have largely disappeared compared with the slow test particle case.

Further increase in the number of Debye squares simulated by the 128 x 32 grid mesh and the 16000 particles, will have two deleterious

effects. Because of the decrease in the number of grid cells per Debye cell the effective 'size' of each particle will increase, tending to make the plasma more collisional. The decrease in the number of particles per Debye square will have a similar effect, as well as reducing relaxation times. Together these two effects act towards making the simulation a poorer representation of a collisionless plasma, and results obtained begin to have doubtful validity. Because of these considerations it was decided that little would be gained by 'diluting' the plasma in the simulation any further especially since the main motive for this would be to simulate a wake in something much nearer its entirety than in any of the above examples. The fact that this would require an order of magnitude increase in physical plasma length indicates the amount of 'dilution' which would have to be done.

This does not detract from the fact that we have here demonstrated that for fast-moving particles in the plasma a more pronounced oscillatory wake is set up behind them as they move than in the case of subthermal particles. However due to the lightness of the damping of the wake, and the periodicity and finite length of the simulation plasma it is impractical to simulate the whole wake, the best quantitative description of which must be given by calculations along the same lines as those in (8).

(4) (d) Slowing of a Test Particle in a Plasma

In the purely electrostatic case the shielding of a test particle in a plasma is equivalent to its inducing an equal and opposite charge in the plasma; this induced charge reacts upon the test particle, producing a drag opposing its motion.

In order to work out the value of this drag force we proceed as follows.

The potential $\underline{\Phi}(\underline{r})$ in the plasma, where $\underline{r}$ is the distance of the point of measurement from the test particle, is given by the sum of two terms, which we refer to as the 'self term' and the 'induced term'. The self term is just the potential which would be measured if the plasma was not present, while the induced term is the potential due to the equal and opposite charge induced in the plasma by the test particle. So

$$\underline{\Phi} = \underline{\Phi}_{induced} + \underline{\Phi}_{self} \qquad (1)$$

We know from Chapter (3) an expression for $\underline{\Phi}$ and we also know that for $\underline{\Phi}_{self}$, the vacuum potential, so that we can write, using equation (3a(9))

$$\underline{\Phi}_{induced} = \frac{q}{\pi} \int e^{i\underline{k}.\underline{r}} \left(\frac{1}{k^2 \epsilon} - \frac{1}{k^2} \right) d\underline{k} \qquad (2)$$

Therefore, the induced electric field is given by

$$\underline{E}_{induced} = -\frac{iq}{\pi} \int \underline{k} e^{i\underline{k}.\underline{r}} \left(\frac{1}{k^2 \epsilon} - \frac{1}{k^2} \right) d\underline{k} \qquad (3)$$

Now, the drag force at the position of the particle will be given by

$$F = q E_{induced}(+) \tag{4}$$

where r = 0. Thus from (8)

$$F = -\frac{iq^2}{\pi}\int_0^{2\pi} d\phi \cos\phi \int_0^{\infty} k^2 dk \left(\frac{1}{k^2 + k_D f} - \frac{1}{k^2}\right) \tag{5}$$

where $f = f(\cos\phi) = 1 + \xi\cos\phi\, Z(\xi\cos\phi)$ where ξ is defined as previously. This result is for the two-dimensional case.

$$F = \frac{iq^2}{2} k_D \int_0^{2\pi} d\phi \cos\phi \left[1 + \xi\cos\phi\, Z(\xi\cos\phi)\right]^{-\frac{1}{2}} \tag{6}$$

A graph of this function, which was obtained by numerical integration, is reproduced in Fig (18). It has a maximum round about $\xi = 1.55$, and goes to zero for very small and very large values of ξ. In the case of a slow test particle, ie $\xi \ll 1$, the expression (6) reduces to the following form, if the Debye length is taken as the unit of length

$$F = -\frac{\pi^{3/2}}{4} q^2 \xi \tag{7}$$

This differs from the expression obtained in Ref (25) for example, but this can be explained by the fact that not only are collisions considered, but the analysis is for 3 dimensions, and the approximation mentioned in Chapter (1b) has been made. In fact there are few grounds for comparison at all.

For large velocities $(\xi \gg 1)$ the limiting expression for F is given by

$$F = -\frac{\pi q^2 k_D}{\sqrt{2}} \frac{1}{\xi} \tag{8}$$

It is notable that this result differs from the three-dimensional case, where there is a log divergence for large k, and a cut-off k_{max} is usually taken at distance of closest approach $d = \sqrt{e^2/kT}$

A small program was written to solve the simultaneous equations of motion, where q_T is the charge on the test particle,

$$\frac{dv}{dt} = \frac{1}{m_T} F(v, q_T) \tag{9}$$

$$\underline{v} = \frac{dz}{dt} \tag{10}$$

where v = velocity, m_T = mass, z = position of test particle respectively. These describe the motion of the test charge in a plasma in two-dimensions acted on only by the drag force given in equation (6) above. The particle was given an initial velocity V and the equations were solved using a Runge-Kutta technique (Ref 39). The result is plotted in Figs (20) and (21) showing the distance travelled by the particle in Debye lengths and the reduction of its velocity as it moves. The data used in the plot of velocity against time were now used to plot $\log(\underline{v})$ against time, in order to demonstrate graphically the range of v over which linearity could be expected in the function $F(v)$
For if we let $F(v) = -kv$ then

$$m\frac{dv}{dt} = -kv \tag{11}$$

Then $V = Ae^{-\beta t}$, A and B constants, so that the graph of $\log(v)$ against t would be a straight line. The result of this plot is given in Fig (19) where it can be seen that linearity holds for v up to at least $v_{eff} (= 1)$.

This result having been obtained from straightforward Vlasov theory, it was now an opportune moment to run the NOVA code with appropriate input data in order to see whether the linear theory we have used, which essentially treats the plasma as a dielectric medium with frequency and wavelength dependent dielectric constant, is sufficient to describe the slowing of a test particle in a plasma. It turns out that this is, in fact, the case over most of the range of velocity used, as is shown below.

A run was set up with the following data.

MESH DIMENSIONS	64 x 64
PHYSICAL DIMENSIONS	16 x 16 DEBYE LENGTHS
TIMESTEP DT	0.25 ω_p^{-1}
NUMBER OF PLASMA PARTICLES	16,384
CHARGE ON TEST PARTICLE	200 UNITS
MASS OF TEST PARTICLE	1000 UNITS
VELOCITY OF TEST PARTICLE	$\sqrt{2}$ ELECTRON THERMAL

The I.C.L. 4/70 was used for these runs. The first twenty-five timesteps were occupied in establishing the full charge on the test particle, so that data was taken from the 26th step onwards. Since, by this time, according to the results of 4(b), shielding will have occurred, ie, the induced potential will have been set up, we perform this numerical experiment in the confidence that the force acting on the test particle will be attributable to an equal and opposite induced charge in the plasma. After the run described above, two other runs were made with different timesteps $DT = 0.2$, and initial velocities , and respectively, and the results were merged to give the one graphs of Figs (22) and (23). The parameters used

were such that the slowing down was quite gradual, and quite a long time would have been necessary to follow the whole of the particle trajectory in one calculation - a run of such a length that there might have been delay in getting it implemented on the machine. The plots in Figs (22) and (23) compare well with the results of the calculations from the analytic formula. Therefore we can be confident that in the calculations of test-particle interactions, the drag force acting on the particles at least at velocities which are the order of or less than v_{th} , will be that given by the derived formula.
It is of interest here to repeat the plot of the variation of the logarithm of velocity of the test particle with time, to compare with the theoretical result. For the NOVA run described above, this was done, and a straight line was obtained which included almost all values of ξ used, from 1.4 downwards. This is shown in Fig (24) where only points representing high velocities ($\xi \approx 1.0$) and points representing low velocities show any deviation. In the former case this can be ascribed to the non-linearity of the force law for larger ξ , and in the latter case the deviations can be ascribed to fluctuations.

There is a good comparison here with results of Fig (19) especially since the data points seem to deviate from linearity at the same place on the straight line at the high velocity end. This shows a good agreement between theory and simulation.

It is noticeable from the results obtained, that the test particle does not keep moving parallel to the direction in which it was set off at first. The amount by which it is deflected is not large in comparison with the total distance it travels, and the transverse velocities it develops are not large compared with its velocity parallel to its original direction of motion. The forces causing the test charge to

leave its original vector direction of motion are due to fluctuations in the transverse electric field which it experiences along its path; only here, since the force is proportional to q_T^2/m_T and this ratio is much great (a factor of 40) than the same ratio for a plasma particle, the deflection in a given time for a test particle moving with a given velocity, is much greater than that for a plasma particle. In other words the deflection time τ_D for a test particle is much shorter than that for a plasma particle, where τ_D is defined to be the time required for a moving particle to be deflected by $\pi/2$. Deflection times in simulations of this type, as discussed in Hockney (32) are shorter than in real plasmas, so these larger deflections, experienced by the test particles, are a non-physical product of the simulation, which can only be reduced by having smaller fluctuations in the field. This in its turn requires smaller fluctuations in density, which in turn requires either many more particles in the simulation, or some form of 'quiet' start, where as even as possible a distribution of particles in phase space is set up in order to generate force fields which are as even as possible.

The effects of field fluctuations were most noticeable in a run with mass and charge of test particle put equal to 200 units. This gives a scaled value of $q_T^2/m_T \doteq 1/4$, as compared with $1/20$ for the previous case and $1/800$ for the plasma particles, where in the test particle case the charge q_T is 200 units. In this case one can clearly see fluctuations on top of the general line of the slowing-down graphs in Fig (25) where both position and velocity are plotted as function of time. The fluctuations in the parallel field clearly affect the shape of the slowing-down graph, and when a plot of $\log(v)$ against t was roughly sketched, a very poor result was obtained with respect to linearity.

Consideration in more detail of the results shows that the fluctuations begin to have a serious effect long before thermalisation of the test particle has been reached. By thermalisation we mean the state where the test charge has lost kinetic energy to the plasma to an extent where $\frac{1}{2} m_T v_T^2 \doteq \frac{1}{2} m_e v_{e_{th}}^2$ where $m_e, v_{e_{th}}$ are simulation electron mass and thermal velocity respectively, and m_T, v_T are mass and velocity of the test particle.

At the stage where the particle has been slowed to $v_T \sim 0{\cdot}2 v_{e_{th}}$ it is noticeable from numerical output that changes in kinetic energy, under the effect of the fluctuations in field, are of the same order of magnitude as the kinetic energy of the test particle itself. There are changes, over times $\sim \omega_p^{-1}$, in the transverse kinetic energy (perpendicular to original direction of motion) of the same order of magnitude once the test particle has slowed.

These fluctuation effects are disastrous from the point of view of simulating the slowing of a test particle in the plasma due to collective interactions. When the larger mass of $m_T = 1000$ units was used, however, as described above, the factor of 5 in mass proved enough to remove these computational effects to an extent where the results that are produced, are satisfactory.

It is evident from the foregoing that in discussing the reliability of 2-particle interaction simulations, allowance will have to be made for the amount by which a particle may be deflected from its path merely by local variations in the electric field E, and this will be borne in mind later.

At this point it is of interest to discover whether the presence of ions in the plasma will affect the slowing of a test charge in the plasma, at the velocities which are considered here, which are of the order of magnitude of the electron thermal velocity.

The analysis is a straightforward adaptation of that given in Ref (8). Another (Vlasov) equation is required, to describe the effect of the ions. The Fourier-Laplace transformed equation is

$$(p + i\underline{k}.\underline{v})\bar{f}_{1i} + \frac{iq}{m_i}\bar{\Phi}\,\underline{k}.\frac{\partial f_{0i}}{\partial \underline{v}} = 0 \qquad (12)$$

where $\bar{f}_{1i}$ is the transformed 1st order perturbation in the ion distribution function. If we let $\bar{f}_{1e}$ be that for the electrons, we can express Poisson's equation, transformed, as in chapter 3 as

$$k^2\bar{\Phi} = 4\pi e\int \bar{f}_{1e}\,d\underline{v} - 4\pi e\int \bar{f}_{1i}\,d\underline{v} + \frac{4\pi q}{(p + i\underline{k}.\underline{u})} \qquad (13)$$

Using these two new equations in the analysis as before, we obtain

$$\epsilon(k,p) = 1 - \frac{4\pi i e^2}{m_e}\int \frac{\underline{k}.\frac{\partial f_{0e}}{\partial \underline{v}}\,d\underline{v}}{(p + i\underline{k}.\underline{v})} - \frac{4\pi i e^2}{m_i}\int \frac{\underline{k}.\frac{\partial f_{0i}}{\partial \underline{v}}\,d\underline{v}}{(p + i\underline{k}.\underline{v})} \qquad (14)$$

As in Ref (8), this leads to the expression for the potential distribution due to the test charge

$$\Phi(r,\theta) = \frac{q}{\pi}\int_0^\infty k\,dk\int_0^{2\pi} \frac{\exp(ikr\cos(\theta - \phi))\,d\phi}{k^2 + k_{De}^2 f_e(\cos\phi) + k_{Di}^2 f_i(\cos\phi)} \qquad (15)$$

where

$$f_i(\cos\phi) = 1 + \xi_i\cos\phi\, Z(\xi_i\cos\phi)$$

for the ions and similarly for the electrons, and the definition of ξ_i, ξ_e are as for ξ before, for the two species.

If ions and electrons are at the same temperature, we get

$k_{Di} = k_{De} = k_D$, and when we follow the same procedure as outlined earlier in this section, we get the drag force on the test particle as

$$F = \frac{iq^2}{2} k_D \int_0^{2\pi} d\phi \cos\phi \left[2 + \xi \cos\phi Z(\xi\cos\phi) + \alpha \xi \cos\phi Z(\alpha\xi\cos\phi) \right]^{-\frac{1}{2}} \quad (16)$$

here ξ is ξ_e and α is given by $\sqrt{\frac{m_i}{m_e}}$. For the case where the plasma is fully ionised hydrogen where the molecule is ionised into protons and electrons, we have $m_i/m_e = 1800$ giving $\sqrt{\frac{m_i}{m_e}} \gtrsim 40$ If we examine the contribution from the two 'f' terms in the expression (14) by taking the asymptotic large velocity expression for the ion and the low velocity expression for the electrons, we can estimate when the contribution due to the ions equals in importance that of the electrons for test particle slowing purposes. The reason why we adopt this procedure is that the ions can be expected to have a contribution which is peaked at a much lower velocity than that for the electrons, so that that part of the distribution described by the asymptotic expression will certainly apply over the range of velocities of the order of electron thermal.

Thus, we are comparing

$$\frac{\pi q^2 k_D}{\sqrt{2}} \frac{1}{\alpha \xi_e} \quad : \quad \frac{\pi^{3/2}}{4} q^2 k_D \xi_e$$

With $\alpha = 40$, we obtain $\xi_e \doteq 0.2$, or $u \doteq 0.3$ where u is the test particle velocity in units of electron thermal. Thus for the lightest possible ions, the electron contribution to test-particle slowing is greater for $u \gtrsim 0.3$, than the ion contribution. Thus we can feel justified in leaving out the ions from the analysis since they will not seriously affect the slowing-down

results for the velocities which we have investigated above. From theory and simulation therefore this chapter has given an adequate quantitative description of the slowing of a test particle in a collisionless plasma.

(4) (e) Symmetric Slow Collision of Test Particles in 2-Dimensions

Using the expressions for the potential derived in Ref (8), and the expression for the drag force due to the plasma derived in the previous section, we can derive equations of motion for the interaction of two test particles in a plasma (Ref (44)).

It is assumed that as the test particles approach, slow down and collide, the change in their velocities leads to changing potentials with negligible transients. We give to the two test-particles space co-ordinates $\underline{r}_1, \underline{r}_2$ and velocities $\underline{v}_1, \underline{v}_2$ respectively.

The equilibrium potential field at $\underline{r}_1$ due to the second test particle (T.P.2) is

$$\underline{\Phi}_{12}(\underline{r}_1, \underline{r}_2, \underline{v}_2) = \frac{q}{\pi}\int \frac{\exp(i\underline{k}.(\underline{r}_1 - \underline{r}_2))}{k^2 \epsilon(\underline{k}, -i\underline{k}.\underline{v}_2)}\, dk \qquad (1)$$

where, again ϵ is given by the expression in equation (6) Chapter (3a).

Similarly, the potential field at $\underline{r}_2$ due to T.P.1 is

$$\underline{\Phi}_{21}(\underline{r}_2, \underline{r}_1, \underline{v}_1) = \frac{q}{\pi}\int \frac{\exp(i\underline{k}.(\underline{r}_2 - \underline{r}_1))}{k^2 \epsilon(\underline{k}, -i\underline{k}.\underline{v}_1)}\, dk \qquad (2)$$

As in Ref (8) the distribution function for the plasma is taken to be Maxwellian in form so that ϵ is independent of position, and $\underline{\Phi}_{12}, \underline{\Phi}_{21}$ are functions of $\underline{r}$ only, where $\underline{r} = \underline{r}_1 - \underline{r}_2$

$$\underline{\Phi}_{12}(\underline{r}, \underline{v}_2) = \frac{q}{\pi}\int \frac{\exp(i\underline{k}.\underline{r})\, dk}{k^2 \epsilon(\underline{k}, -i\underline{k}.\underline{v}_2)} \qquad (3)$$

$$\underline{\Phi}_{21}(\underline{r}, \underline{v}_1) = \frac{q}{\pi}\int \frac{\exp(-i\underline{k}.\underline{r})\, dk}{k^2 \epsilon(\underline{k}, -i\underline{k}.\underline{v}_1)} \qquad (4)$$

$\underline{\Phi}_{12}$ is a scaler function of r^2, v_2^2 and $\underline{r}.\underline{v}_2$. For small velocities, relative to the electron thermal speed, $\underline{\Phi}_{12}$ can be expanded in the form

$$\underline{\Phi}_{12}(\underline{r}, \underline{v}_2) = a(r) + b(r)\, \underline{r}.\underline{v}_2 \qquad (5)$$

+ higher order terms.

Also $\underline{\Phi}_{21}(\underline{r},\underline{v}_1)$ is obtained from $\underline{\Phi}_{12}(\underline{r},\underline{v}_2)$ by interchanging and v_1 and v_2, $r \Rightarrow -r$. Thus to lowest order in v_1

$$\underline{\Phi}_{21}(r,v_1) = a(r) - b(r)\,\underline{r}.\underline{v}_1 \qquad (6)$$

The equations of motion for test particle (1) is given by

$m_1 \dot{v}_1 = F = -q\dfrac{\partial \Phi}{\partial r}(r, v_2)$, and similarly for the other.

This gives, for small v_1, v_2

$$\begin{aligned} m/q^2\,\dot{\underline{v}}_1 &= -\frac{a'}{r}\underline{r} - \frac{b'}{r}\underline{r}(\underline{r}.\underline{v}_2) - b\underline{v}_2 - F(\underline{v}_1) \\ m/q^2\,\dot{\underline{v}}_2 &= \frac{a'}{r}\underline{r} - \frac{b'}{r}\underline{r}(\underline{r}.\underline{v}_1) - b\underline{v}_1 - F(\underline{v}_2) \end{aligned} \qquad (7)$$

$F(v)$ is a linear function of v for small velocities, as shown in the previous section; we shall write, for convenience, $F(v) = Fv$ where $F = \pi^{3/2}/4\sqrt{2}$, having chosen unity for the scaling of thermal velocity, and Debye length. Introducing a relative velocity $\underline{v} = \underline{v}_1 - \underline{v}_2$ we can get

$$m/q^2\,\dot{\underline{v}} = -\frac{2a'}{r}\underline{r} + \frac{b'}{r}\underline{r}(\underline{r}.\underline{v}) + (b-F)\underline{v} \qquad (8)$$

Also, if we introduce a centre of mass velocity $\underline{V} = \frac{1}{2}(\underline{v}_1 + \underline{v}_2)$ we get

$$m/q^2\,\dot{\underline{V}} = -\frac{b'}{r}\underline{r}(\underline{r}.\underline{V}) - (b+F)\underline{V} \qquad (9)$$

Thus the drag coefficient is increased if $b > 0$ in the equation for centre of mass motion, and there is also a drag aligned along $\underline{r}$ in this case. Similarly for relative motion the drag is modified, as is the force acting along the relative co-ordinate $\underline{r}$.

If we take the cross-product of the equation for relative motion $\underline{V}$ with $\underline{r}$, and let $\underline{L} = \underline{r} \times \underline{v}$ we obtain

$$\frac{m}{q^2}\,\underline{r}\times\dot{\underline{v}} = \left(\frac{d}{dt}\underline{L} - \dot{\underline{r}}\times\underline{v}\right)\frac{m}{q^2} = \frac{m}{q^2}\frac{dL}{dt} = (b-F)L \qquad (10)$$

In the special case of a symmetric collision $\underline{v}_1 = -\underline{v}_2$, and so $\underline{V} = 0$. Thus if we use a polar co-ordinate system (r, θ) , we obtain

$$\frac{m}{q^2}(\ddot{r} - L^2/r^3) = -2a' + b' r\dot{r} + (b-F)\dot{r} \qquad (11)$$

$$\frac{m}{q^2}\dot{L} = (b-F)L \qquad (12)$$

a and b can be obtained from Ref (8), by comparing, for $q = 1$

$$\bar{\Phi}(r, V) = 2(A_0 + A_1 \cos\theta) \qquad (13)$$

with $$\bar{\Phi}(r, v) = a + b(r.V)$$

This gives $a = 2I_0^0 \; ; \; b = 2\pi^{1/2} I_1^1$ so that

$$a = 2K_0(r) \; , \; b = 2\pi^{1/2} r \int_0^\infty \frac{x J_1(x)\,dx}{(x^2+r^2)^2} \; , \qquad (14)$$

the unit of length being taken as the Debye length. Knowing functional forms for a and b it is possible now to solve the equations (11) and (12) numerically along with the equation $\frac{dr}{dt} = \dot{r}$ (15) These are three simultaneous equations in three dependent variables and one independent variable, and they were tackled successfully using a Runge-Kutta method. By varying parameters such as the effective charge and mass of the test particle, it was attempted to find an

estimate of the parameters which would best suit a computer simulation of the same event. The points made in the previous section concerning fluctuations in field, etc, had to be borne in mind carefully here.

In order to ensure that the potential energy due to the coulomb repulsion between the two test charges was great enough that they did not approach within $0{\cdot}25\lambda_D$ (one grid mesh length), a suitably small initial velocity was taken in the simulations. A NOVA run was now initiated, with the following details.

MESH DIMENSIONS	64 by 64
PLASMA DIMENSIONS	16 x 16 DEBYE LENGTH
NUMBER OF PARTICLES IN PLASMA	16384
TEST PARTICLE CHARGE	100
TEST PARTICLE MASS	1000
INITIAL RELATIVE VELOCITY	0.5 ELECTRON THERMAL

What was done was as follows. The test particles were set up, with zero charge, some distance apart, the distance being pre-calculated and dependent on the relative velocity $-0{\cdot}5v_{eA}$. The particles were allowed to approach each other at constant velocity, until such time as their charge had attained its maximum, when they were approximately $2\lambda_D$ apart. At this point they were treated as any other plasma particle, being advanced in time using the standard particle pusher which is used for all the other plasma particles. It proved impossible to use the standard particle pusher to perform a 'head-on' collision, because even with $M_T = 1000.0$ there are deflections perpendicular to particle trajectories due to field fluctuations, and once the particles have been deflected from their head-on course their mutual interaction causes them to be deflected even further.

The results of the Runge-Kutta solution were processed with the view of comparing them with a set obtained from the simulation. The particle trajectories were drawn for each case, and one example is shown in Fig (26). We can see from these that we have but a moderately good comparison between analytic prediction and simulation for the two slow test particle collision in the symmetric collision case. Other values of impact parameter tended to give similar discrepancies.

Factors which can have given rise to the disparity between the two trajectories are as follows:

(a) The fluctuations in transverse electric field which the particles experience as soon as the force is switched on could cause them to be deflected from their paths more than otherwise, giving an effectively larger impact parameter.

(b) The fact that we have only taken the term $O(v)$ in the expansion in the theoretical case could lead to inaccuracy though one would not expect much error at these low velocities.

(c) It may be that the assumption of negligible transient effects, when the particles collide, is erroneous.

(5) Single Test Particle in a Magnetic Field

(a) Derivation of Potential Distribution

It was considered of interest to examine the shielding of a test particle in a constant magnetic field, by means of plasma simulations in two dimensions using NOVA. The magnetic field in question is uniform, constant, and perpendicular to the plane of the plasma.

Plasma dielectric functions in the case of a uniform magnetic field in 3 dimensions have been known for some time, and have been used to deduce oscillation modes of the plasma. The current state of the art is given in Ref (41) in a long review article. However, the only authors who claim to have used the strictly 2-dimensional form to give the field due to a test particle are Montgomery and Tappert (Ref 19), who only give a value of G for the large field limit and who do not give their analysis, which they promise to present at a later date. It is therefore of interest to derive the form of the field due to a test particle in a two-dimensional magnetised plasma, and to investigate whether there are any phenomena, in the case of less strong magnetic fields, which are noticeable and which serve to differentiate the shielding in this case from that in the electrostatic case. By less strong fields is meant those where the Debye length λ_D is of the order of the Lasmor radius a_i. In particular, we anticipate a priori that for weak fields the test particle may be shielded in a manner similar to that which pertains in the electrostatic case, and that, therefore, there must be some intermediate region between this and the strong field situation in which the authors of Ref (19) predict that shielding will have disappeared, a region where the potential will take some transitional form between the $K_0(r)$ of electrostatic shielding, and the $-\log(r)$ of the unshielded case.

Therefore in this case there is motivation for performing some analysis, and also motivation for being prepared to do a plasma simulation in the event of the analysis becoming intractable, or to support the results obtained.

An analysis similar to that of Ref (42) was followed in the early part of the derivation of the test-particle potential.

As usual the plasma is assumed collisionless, and the equation governing the evolution of the distribution function f is Vlasov's equation

$$\frac{\partial f}{\partial t} + \underline{v} \cdot \frac{\partial f}{\partial \underline{x}} + \frac{e}{m}\left(\underline{E} + \frac{\underline{v} \times \underline{B}}{c}\right) \cdot \frac{\partial f}{\partial \underline{v}} = 0 \qquad (1)$$

If we linearise as follows,

$\underline{E} = 0 + \underline{E}_1 \; ; \; B = B_0 \; \therefore \; f = f_0 + f_1$ then, where θ is the angle between v and the $+ve$ x-direction, we obtain

$$\frac{\partial f_1}{\partial t} + \underline{v} \cdot \frac{\partial f_1}{\partial \underline{x}} - \Omega \frac{\partial f}{\partial \theta} = -\frac{e}{m} \underline{E}_1 \cdot \frac{\partial f_0}{\partial \underline{v}} \; , \qquad (2)$$

where $\Omega = \frac{eB_0}{mc}$, the Larmor frequency. This simplified form of the equation has appeared because we are considering a strictly two-dimensional case: there are no velocity components perpendicular to the plane of the plasma.

On the assumption that $f_0 = f_0(v)$, which holds, for example, for a Maxwellian distribution, we can perform a Fourier-Laplace Transform in space and time on this equation, as follows

$$(p + i\underline{k} \cdot \underline{v}) \bar{f}_1 - \Omega \frac{\partial \bar{f}_1}{\partial \theta} = ie \bar{\Phi} \underline{k} \cdot \frac{\partial f_0}{\partial \underline{v}} \qquad (3)$$

$$= H(\theta)$$

where

$\bar{f}_1$ is the Fourier-Laplace transform of f , and the equation $\underline{E}_1 = -\underline{\nabla}\bar{\Phi}$, has been used.

The equation (3) can be solved using the integrating factor

$$F = \exp\left[-\int_{\theta_0}^{\theta}\left(\frac{p+i\underline{k}.\underline{v}}{\Omega}\right)\theta''\right] \tag{4}$$

as follows.

$$F(\theta)\,\bar{f}_1(\theta) = -\int_{\pm\infty}^{\theta} F(\theta')\left(\frac{ie}{m\Omega}\right)\underline{k}.\frac{\partial \bar{f}_0}{\partial \underline{v}}(\dot{\theta})\,\bar{\Phi}\,d\theta' \tag{5}$$

the lower limit being chosen to be appropriate later on.

$$\bar{f}_1(\theta) = \int_{\pm\infty}^{\theta} G\left(\frac{ie}{m\Omega}\right)\underline{k}.\frac{\partial \bar{f}_0}{\partial \underline{v}}\,\bar{\Phi}\,d\theta' \tag{6}$$

where

$$G = \exp\left[\int_{\theta'}^{\theta}\left(\frac{p}{\Omega} + ik v\cos(\theta''-\phi)\right)d\theta''\right] \tag{7}$$

where ϕ is the angle between $\underline{k}$ and $\underline{x}$ - direction. Again, adhering to strict two-dimensionality, the only components of the wave-vector $\underline{k}$ are those in the plane of the plasma. So

$$G = \exp\left[\frac{p}{\Omega}(\theta-\theta') + \frac{ikv}{\Omega}\left(\sin(\theta-\phi)-\sin(\theta'-\phi)\right)\right] \tag{8}$$

As in 3(a), we have Poisson's equation to solve for $\bar{\Phi}$, where the linearised, Fourier-Laplace transformed equation is

$$k^2\bar{\Phi}_1 = 4\pi e\int \bar{f}_1\,dv + \frac{4\pi q}{(p+i\underline{k}.\underline{u})} \tag{9}$$

Thus, in order to solve for $\bar{\Phi}_1$, we will require the integral

$$\int f_1\,dv = \int_0^{\infty} v\,dv\int_0^{2\pi} d\theta\,\bar{f}_1(v,\theta) \tag{10}$$

The first necessity is to evaluate the function $f_1(v,\theta)$. This is given by

$$f_1(v,\theta) = -\frac{e}{m}\frac{\partial f_0}{\partial v}\exp\left(\frac{\rho}{\Omega}\theta + \frac{ikv}{\Omega}\sin(\theta-\phi)\right)\int_{\pm\infty}^{\theta} k\cdot\frac{\partial f_0}{\partial v}\exp\left(-\frac{\rho}{\Omega}\theta' - \frac{ikv}{\Omega}\sin(\theta'-\phi)\right)d\theta' \quad (11)$$

Now $\frac{\partial f_0}{\partial v}$ is parallel to v if $f_0 = f(v^2)$, so the θ' integral becomes, using

$$\exp(iab\sin\alpha) = \sum_{n=-\infty}^{\infty} J_n(ab)\exp(in\alpha) \quad (12)$$

$$I = \left[\frac{k}{2}\frac{\partial f_0}{\partial v}\sum_{n=-\infty}^{\infty} J_n\left(\frac{kv}{\Omega}\right)\exp(in\phi)\right]\int_{\pm\infty}^{\theta}\exp\left(-\frac{\rho}{\Omega}\theta' - n\theta'\right)\left(\exp(i(\theta'-\phi)) + \exp -i(\theta'-\phi)\right)d\theta' \quad (13)$$

which gives, if ρ has a real part, and the lower limit is chosen appropriately,

$$I = [\ \ ]\left[\frac{\exp\left(-i(n+1)\theta - \rho/\Omega\,\theta + i\phi\right)}{-i(n+1) - \rho/\Omega} + \frac{\exp\left(-i(n-1)\theta - i\phi - \rho/\Omega\,\theta\right)}{-i(n-1) - \rho/\Omega}\right] \quad (14)$$

Taking the factor $e^{in\phi}$ into the exponential in each case we get $I = S_n^{n+1} + S_n^{n-1}$

where

$$S_n^{n+1} = -\frac{k}{2}\frac{\partial f_0}{\partial v}\sum_{n=-\infty}^{\infty} J_n\left(\frac{kv}{\Omega}\right)\left[\frac{\exp\left(-i(n+1)\theta - \frac{\rho}{\Omega}\theta + i(n+1)\phi\right)}{\rho/\Omega + i(n+1)}\right] \quad (15)$$

and similarly for S_n^{n-1}, with $n-1$ in place of $n+1$. In order to express the two sums S_n^{n+1} and S_n^{n-1} in a form which can be dealt with, we use

$$J_n\left(\frac{kv}{\Omega}\right) = (n-1)\frac{\Omega}{kv}J_{n-1}\left(\frac{kv}{\Omega}\right) - J'_{n-1}\left(\frac{kv}{\Omega}\right) \quad (16) \text{ and}$$

$$J_n\left(\frac{kv}{\Omega}\right) = J'_{n+1}\left(\frac{kv}{\Omega}\right) + (n+1)\frac{\Omega}{kv}J_{n+1}\left(\frac{kv}{\Omega}\right) \quad (17)$$

in the sums S_n^{n-1} and S_n^{n+1} respectively. This gives two infinite

sums which when we respectively perform the displacements $n-1 \to n$ and $n+1 \to n$ we can easily add together, noting that the terms in J_n' cancel, so getting

$$I = -k\frac{\partial f_0}{\partial v}\sum_{n=-\infty}^{\infty} J_n\left(\frac{kv}{\Omega}\right)\frac{n\Omega}{kv}\,\frac{2\pi p(-in\delta - p\delta/\Omega + in\phi)}{p/\Omega + in} \qquad (18)$$

We are now in a position to perform the δ - integration in (10), and so we include the factors which have been omitted up till now, in the integrand. The δ - integral is

$$\Theta = \frac{\bar{\Phi} ie}{m\Omega}\int_0^{2\pi} d\theta \exp\left(\frac{p\theta}{\Omega} + \frac{ikv}{\Omega}\sin(\theta-\phi)\right)k\frac{\partial f_0}{\partial v}\sum_{n=-\infty}^{\infty} J_n\left(\frac{kv}{\Omega}\right)\frac{n\Omega}{kv}\,\frac{2\pi p(-in\delta - p\delta/\Omega + in\phi)}{in + p/\Omega} \qquad (19)$$

Again using (12), and performing the integration, we find that the result is

$$\Theta = \bar{\Phi}\sum_{n=-\infty}^{\infty} \frac{ie\,\frac{\partial f_0}{\partial v}\,n\Omega}{m(p+in\Omega)v}\,2\pi J_n^2\left(\frac{kv}{\Omega}\right) \qquad (20)$$

Thus we now have only the v integral in equation (10) to perform. Now if we choose f_0 to be an isotropic Maxwellian distribution function in 2-dimensions we have $f_0(v) = \frac{1}{2\pi v_{e_{Rh}}^2} e^{-v^2/v_{e_{Rh}}^2}$ where $v_{e_{Rh}}$ is the electron thermal velocity.

Thus $$\frac{\partial f_0}{\partial v} = -\frac{v}{v_{e_{Rh}}^2}\left(\frac{1}{2\pi v_{e_{Rh}}^2}\right)e^{-v^2/v_{e_{Rh}}^2} \qquad (21)$$

The integral is

$$\int f_1\,dv = \int_0^{\infty} v\,dv\;\Theta$$

$$= \sum_{n=-\infty}^{\infty} A\int_0^{\infty} v\,dv\,\frac{-v}{v_{e_{Rh}}^2}\,e^{-v^2/v_{e_{Rh}}^2}\,J_n^2\left(\frac{kv}{\Omega}\right) \qquad (22)$$

(where all non v - dependent factors are collected in A)

$$= \sum_{n=-\infty} - \frac{A}{V_{e}^{2}{}_{A}} v_{enA}^{2} \exp\left(-\frac{k^2 v_{eA}^2}{\Omega^2}\right) I_n\left(\frac{k^2 v_{eA}^2}{\Omega^2}\right)$$

$$= -\bar{\Phi} \sum_{n=\infty}^{\infty} \frac{ien\Omega}{m(p+in\Omega)v_{eA}^2} \exp\left(\frac{-k^2 v_{eA}^2}{\Omega^2}\right) I_n\left(\frac{k^2 v_{eA}^2}{\Omega^2}\right) \quad (23)$$

Thus, rearranging Poisson's equation (9) in order to solve for $\bar{\Phi}$, we have

$$\bar{\Phi}(k,p) = \frac{4\pi q}{(p + i\underline{k}.\underline{u})k^2 \epsilon(k,p)} \quad \text{where} \quad (24)$$

$$\epsilon(k,p) = 1 + \frac{k_D^2 i}{k^2} \sum_{n=-\infty}^{\infty} \frac{n\Omega}{(p+in\Omega)} \exp\left(\frac{k^2}{k_c^2}\right) I_n\left(\frac{k^2}{k_c^2}\right) \quad (25)$$

where $k_D = 1/\lambda_D$, the Debye wave number and $k_c = 1/a_i$, the Larmor wave number.

We now have to consider the application, first of an inverse Laplace transform, then of an inverse Fourier transform, upon the potential function $\bar{\Phi}(k,p)$.

This is not so simple as in the electrostatic case, because of the nature of the function $\epsilon(k,p)$ in the denominator. In the derivation of Landau damping (eg Montgomery and Tidman, Ref 31), it is shown that all the zeros of ϵ are to the left of the imaginary p-axis. However, in the present case, it is a straightforward matter to demonstrate that there is an infinite set of zeros of ϵ which lie on the imaginary p-axis. For

$$\epsilon(k,p) = 1 + \frac{k_D^2}{k^2} i \sum_{n} \frac{n\Omega}{p+in\Omega} \exp\left(\frac{-k^2}{k_c^2}\right) I_n\left(\frac{k^2}{k_c^2}\right) \quad (26)$$

Now $I_n(z) = I_{-n}(z)$ for all z, so that we can group together terms with n and $-n$. The term with $n = 0$ disappears and we obtain

$$\epsilon(k,p) = 1 + \frac{k_D^2}{k^2} \sum_{n=1}^{\infty} \frac{2n^2\Omega^2}{p^2+n^2\Omega^2} \exp\left(-\frac{k^2}{k_c^2}\right) I_n\left(\frac{k^2}{k_c^2}\right) \qquad (27)$$

If p is purely imaginary, $p = i\omega$, the denominator of each term in the sum is $-\omega^2+n^2\Omega^2$. It is obvious that for every n, there will be a point, as ω varies, where this factor is zero, making $\epsilon \to +\infty$ if this point is approached from the left, and $\epsilon \to -\infty$ if approached from the right. Given continuity of the function ϵ between these 'poles' of ϵ, there must be a value of ω, between every point $\omega = n\Omega$ and $\omega = (n+1)\Omega$ where $\epsilon = 0$. These zeros of ϵ, are poles of $\bar{\Phi}(k,p)$ and because ω has no imaginary part, represent undamped oscillations. It is to be noted that if $p = +i\omega_n$ is a pole of $\bar{\Phi}$ then $p = -i\omega_n$ is also. There is an infinitely denumerable set of poles with zero real part in the p-plane in the expression for $\bar{\Phi}$. To help complete a description of ϵ, a graph has been drawn (Fig 27) showing $\epsilon(k,\omega)$ for $k = 1$, out to $\omega = \pm 4\Omega$ A very similar graph occurs in Ref (41), in which the authors are dealing with longitudinal modes of plasma oscillation in a constant magnetic field. When they consider perpendicular propagation $(k_{\parallel} = 0)$ they demonstrate the existence of essentially the same infinity of undamped modes as occur here. As ω increases, ϵ tends to a constant value near unity between its poles, rising very sharply at the multiples of Ω. Also, as ω increases, ω_n, between $n\Omega$ and $(n+1)\Omega$, tends towards $n\Omega$, though never quite reaches it.

Thus the Fourier transform of the potential will be given by

$$\bar{\bar{\phi}}(k) = 4\pi q \left[\frac{e^{-i\underline{k}\cdot\underline{u}t}}{\epsilon(k,-i\underline{k}\cdot\underline{u})} + \left(\sum_i \frac{e^{i\omega_i t}}{(i\omega_i + i\underline{k}\cdot\underline{u})\frac{\partial\epsilon}{\partial\rho}(k,i\omega_i)} - \frac{e^{-i\omega_i t}}{(-i\omega_i + i\underline{k}\cdot\underline{u})\frac{\partial\epsilon}{\partial\rho}(k,-i\omega_i)} \right) \right] \quad (28)$$

where, by inspection, $\frac{\partial\epsilon}{\partial\rho}(k,-i\omega) = -\frac{\partial\epsilon}{\partial\rho}(k,i\omega)$

The question of what amplitude the purely oscillatory terms will have once a Fourier transform has been applied, is of importance. It was to be hoped that they would, in the stationary test particle case at least, leave the plasma with a background of noise of an amplitude dependent upon whatever perturbation (in this case the test charge) has caused the disturbance, this noise element being produced by some form of phase mixing of modes as the k- integration is performed.

In the case of a moving test charge we would hope for the same sort of effect to take place. Whether these things are what takes place, it was hoped to demonstrate from runs of NOVA with a constant magnetic field included.

The potential in real space is given by

$$\phi(x,t) = \frac{q}{\pi} \int \frac{\exp(i\underline{k}\cdot\underline{x})}{k^2} \frac{\bar{\bar{\phi}}(\underline{k})}{4\pi} d\underline{k} \quad (29)$$

as before.

(b) Test Particle With Zero Velocity

If we take the special case of $u = 0$, that is, a stationary test particle, we get

$$\phi(x,t) = \frac{q}{\pi} \int \frac{\exp i(\underline{k}.\underline{x} + \underline{k}\underline{u}t)\ dk}{k^2 + 2k_D^2 \sum_{n=1}^{\infty} \exp\left(-\frac{k^2}{k_c^2}\right) I_n\left(\frac{k^2}{k_c^2}\right)} + \text{other terms} \quad (1)$$

Using the relationship

$$\exp(z\cos\theta) = I_0(z) + 2\sum_{n=1}^{\infty} I_n(z)$$ we obtain

$$\phi(x,t) = \frac{q}{\pi} \int \frac{\exp i\,k.(x-ut)\ dk}{k^2 + k_D^2\left(1 - \exp\left(-\frac{k^2}{k_c^2}\right) I_0\left(\frac{k^2}{k_c^2}\right)\right)} + \text{etc} \quad (2)$$

Here we can recover the claimed result of Ref (19), for if we consider the denominator, which is $k^2 \epsilon(k,0)$ in the limit of large k_c^2 where k_c is proportional to the field B, we obtain the form $\sim k^2\left(1 + k_D^2/k_c^2\right) = k_c^2\left(1 + \omega_p^2/\omega_c^2\right)$ where $\omega_c = \Omega$.

for large ω_c , the claim is made that ϵ is independent of k and that, therefore the form of the potential is $-q\log(r)/\left(1+\omega_p^2/\omega_c^2\right)$ What this represents is the partial disappearance of shielding, which disappears altogether as $\omega_p/\omega_c \to 0$, and the potential $\phi \to -q\log r$, the unshielded potential due to a charged rod in two dimensions. However, this is only in the large ω_c limit, and there is more information which can be obtained about shielding if we actually perform the integration in equation (2).

First of all, the results of a 'NOVA' run would be of interest to quote here since they serve to confirm some of the propositions concerning background noise put forward above. A simulation was performed using the following parameters.

COMPUTATIONAL MESH DIMENSIONS	64 x 64
'PLASMA' DIMENSIONS	16 x 16 DEBYE LENGTH
NUMBER OF PARTICLES IN PLASMA	16384
TEST PARTICLE CHARGE	200 UNITS
MAGNETIC FIELD FACTOR ω_c/ω_p	1.0
TEST PARTICLE VELOCITY	0.0

An identical run, without magnetic field, had already been performed (see 4b) so that there were grounds for comparison of, say, the total potential energy in these runs. Accordingly, a graph was drawn showing the time variation of the potential energy in all modes as calculated in the NOVA diagnostic routines, for both the run with $\omega_c/\omega_p = 1.0$ described above, and for the earlier run, described in Chapter 4(b) and using identical parameters, (Fig 28). It is noticeable at once that the mean value of potential energy in the plasma is significantly higher in the magnetic case. It is in fact greater by a mean of some 20%. Using the expected result, then, that there will be an amount of background noise due to the undamped modes of the two-dimensional plasma, we can explain this discrepancy in the values of potential energy, and can see also that 20% of the potential energy in the magnetised simulation plasma is in these modes.

A subsequent figure was drawn (Fig (29))showing the variation of the potential at the test particle position with time, for the same two cases for which data of potential energies were plotted in Fig (28). Again it is noticeable that the potential values in the magnetic case are significantly greater than in the non-magnetic situation, here by some 20-25%.

Again, similar data became available for a run with a non-'adiabatic' start procedure, and this was then directly comparable with the previous run (Chapter 4(b)) in the electrostatic case. A graph comparing the mode potential energies for the magnetic, $\omega_c/\omega_p = 1$, case, with this previous run, is reproduced in Fig (30). The mean values of the two potential energies are within 5%, but in the magnetic case the time-variation of amplitude has a much longer period.

For the particular 'NOVA' run described above, it was found by plotting a graph that the potential distribution was not quite the same as in the electrostatic case; it was thought that any dissimilarities would be accentuated if the magnetic field was increased.

Accordingly a similar run to the above was done with $\omega_c/\omega_p = 2.0$ and a stationary test particle. We have plotted thepotential, at points close to the test particle, against $(\omega g(x)$ and it can be seen that something very close to a linear relationship has been obtained (Fig 31).

From these preliminary simulations, it is to be expected that analytic results for the shielding of a stationary test particle in a magnetic field will be noticeably different from those for the electrostatic case, in two dimensions.

The next part of the work to be described is the evaluation of the potential given by the integral in equation (2), on the assumption that the other terms merely give rise to background noise, and can be ignored for the purposes of evaluation of the form of the shielding of the stationary test-charge.

If we use polar co-ordinates (k, θ) we have

$$\phi(x,t) = \frac{q}{\pi}\int_0^\infty k\,dk \int_0^{2\pi} \frac{\sum_m i^m J_m(kx)\, e^{im\theta}\, d\theta}{\left(k^2 + k_D^2\left(1 - \exp\left(-\frac{k^2}{k_c^2}\right) I_0\left(\frac{k^2}{k_c^2}\right)\right)\right)} \qquad (3)$$

$$= 2q \int_0^\infty \frac{J_0(kx)\, k\, dk}{\left(k^2 + k_D^2\left(1 - \exp\left(-\frac{k^2}{k_c^2}\right) I_0\left(\frac{k^2}{k_c^2}\right)\right)\right)}$$

On inspection of this integral we see that as $k \to 0$, the denominator tends to $\left(k^2 + k_D^2\left(1 - 1 + k^2/k_c^2 \ldots\right)\right) = k^2\left(1 + k_D^2/k_c^2\right)$. Since $J_0(kx) \to 1$ as $k \to 0$, we have demonstrated that the integrand goes to infinity as $k \to 0$. However, we know that the Fourier

transform of $J_0(kx)/k^2$ in two dimensions is $-\log|x|$, inasmuch as this is the form of the potential of a charged rod in two dimensions, found by Gauss' law. So we adopt the tactics of subtracting this, suitably normalised by $1/(1+k_D^2/k_c^2)$ from the integrand, performing the integration numerically, and adding the factor $-\log x/(1+k_D^2/k_c^2)$ to the result. That is we propose to subtract the term $\frac{J_0(kx)\,k\,dk}{k^2(1+k_D^2/k_c^2)}$ from the integrand in (3). By the rules of mathematical analysis, this is not integrable; yet it is derivable from the form of the Fourier transform of $1/(k^2(1+k_D^2/k_c^2))$ by using the expansion used in (3). The reason why this is not integrable is because of the infinity in the integrand at $k=0$, which manifests itself in the fact that $\log(x)$ is not normalisable. But since it can be shown from Gauss' law that the potential due to a charged rod is $-q\log(x)$, we can use this result in the full confidence that if the Fourier transform could be done and normalised this would be the answer. Evidently the result would be $\sim -\log x + \log b$ where the second term is indeterminate, though Gauss's law's renormalisation makes $b=1$. If we were working with the electric field here we would not have this integrability problem since the functions are all better behaved; but it is the form of the potential which we are interested in elucidating directly.

The integral which we now perform numerically, then, is

$$\Phi' = \int_0^\infty \frac{J_0(kx)\,k\,dk}{k^2+k_D^2(1-\exp(-k^2/k_c^2)I_0(k^2/k_c^2))} - \frac{J_0(kx)\,k\,dk}{k^2(1+k_D^2/k_c^2)} \qquad (4)$$

By subtracting these two we are effectively cancelling the unknown normalisation constants, which were mentioned above. We get

$$\Phi' = \int_0^\infty \frac{J_0(kx)\left(k^2\frac{k_D^2}{k_c^2} - k_D^2\left(1-\exp\left(-\frac{k^2}{k_c^2}\right)I_0\left(\frac{k^2}{k_c^2}\right)\right)\right)dk}{k\left(1+\frac{k_D^2}{k_c^2}\right)\left(k^2+k_D^2\left(1-\exp\left(-\frac{k^2}{k_c^2}\right)I_0\left(\frac{k^2}{k_c^2}\right)\right)\right)} \qquad (5)$$

As $k \to 0$ now, this goes as $\sim k$, so that we have no integrability problems at this point. Let $\hat{r} = x$,

If we express $x = k\hat{r}$, $a = k_D\hat{r}$, $b = k_c\hat{r}$, we get

$$\Phi' = \int_0^\infty \frac{J_0(x)\left(x^2\frac{a^2}{b^2} - a^2\left(1 - \exp\left(-\frac{x^2}{b^2}\right) I_0\left(\frac{x^2}{b^2}\right)\right)\right) dx}{x\left(1 + a^2/b^2\right)\left(x^2 + a^2\left(1 - \exp\left(-x^2/b^2\right) I_0\left(x^2/b^2\right)\right)\right)} \quad (6)$$

To get $\phi(\hat{r}, t)$ we have to add to this the term

$$-\log a / \left(1 + a^2/b^2\right).$$

The computation was performed for a range of values of the ratio a/b. a is the radial distance from the test particle measured in Debye lengths, while b is the same distance measured in Larmor radii. This ratio is the same as k_D/k_c. The results of numerical integration of the expression (6) are graphically presented for values of a out to 7.0 in Fig (32). A plot of $K_0(a)$ is also sketched in. It can be seen that for strong magnetic field $k_D/k_c \leq 1$, the potential is tending to large negative numbers as a increases. From the actual numbers produced it can be seen that in every case, once a certain value of a has been reached, the dependence of the potential on a becomes more and more that of $-\log a/\left(1+a^2/b^2\right)$, which is $-\log a\left(\left(1 + k_D^2/k_c^2\right)\right.$ or $-\log a^{\left(\frac{1}{1 + k_D^2/k_c^2}\right)}$. For k_D/k_c large eg 10 as in the diagram, this is a very slowly decreasing function of a, while for k_D/k_c small eg $\frac{1}{3}$ as in the diagram, it tends to large negative numbers almost as quickly as $-\log a$ itself. For $k_D/k_c = 10$, in fact, we can see that for small a the function is very close to $K_0(a)$, the result for the electrostatic case, but as a increases the log dependence eventually takes over.

The fact that, at large distances for non-zero field the form of the potential is $-q\log a/\left(1+\frac{k_D^2}{k_c^2}\right)$ indicates that incomplete shielding has

occurred. This represents the potential due to a line charge $q/(1+k_b^2/k_c^2)$ in a vacuum. In other words the charge q has induced a charge $-(q-q/(1+k_b^2/k_c^2))$ ie $q\,\frac{k_b^2}{k_c^2}/(1+k_b^2/k_c^2)$ in the plasma and so is not completely shielded in the two-dimensional case in the presence of a magnetic field. As the field increases while the electrostatic plasma properties remain the same, it is evident that the charge induced in the plasma will decrease accordingly.

Thus in the magnetic field case we have got away altogether from the $\phi \sim K_0(a)$ dependence for the potential which exists in two dimension electrostatic shielding. In this non-magnetised case the particle could always be shown to be completely shielded by the plasma, while here we have demonstrated that the particle is never completely shielded in the presence of a magnetic field perpendicular to the plane of the plasma, though except in the infinite field case shielding will never disappear entirely.

Our numerical results show that the potential distribution is very close to $K_0(a)$ for small field at points near the particle, while for large field it is very close to $-\log a$ in its dependence.

Next, to see whether simulation and theory agreed for the magnetised, stationary test-particle case, a graphical comparison was done. For $\omega_c/\omega_p = 1.0$ and $\omega_c/\omega_p = 2.0$, the values obtained from theory were plotted against those from the appropriate NOVA run, and the graphs obtained are reproduced in Fig (33). It can be seen at once from these that good linearity has been obtained in the relationship. This shows that (a) the expression (3) describes adequately the potential distribution about a stationary test particle in a two-dimensional magnetised plasma and that (b) it is justifiable to state that the only effect that the undamped modes have is to provide a noise background

which does not affect the form of the potential distribution.

The fact that the test particle (and therefore, by implication, any given particle) is not completely shielded is a similar type of result to one derived in Ref (18). Here the authors solve for the motion of 2 line charges from the two-dimensional plasma interacting in the field of each other and also in the constant magnetic field perpendicular to the plane of the plasma, when all other charges are removed. It is found that the geometrical relationship between them is a periodic function of time. The authors deduce that this indicates that two particle correlations will not disappear with time in the two-dimensional magnetised plasma, a result similar in nature to ours, above, which says that as a consequence of incomplete shielding the presence of a test charge can be felt by any other charge in the plasma.

(c) Non-Zero Test Charge Velocity

The case when $u \neq 0$ provided more complications analytically than the previous case of $u = 0$. When the Laplace transforms have been done we have to integrate

$$\Phi(x,t) = \int_0^{\infty} k\,dk \int_0^{2\pi} d\phi\, e^{ik.x} \frac{2}{\pi} \left[\frac{e^{-ik.ut}}{(k^2 \epsilon(k, -ik.u))} + \frac{1}{k^2} \sum \frac{e^{p_i t}}{(p_i + ik.u)\frac{\partial \epsilon}{\partial p}(k,p_i)} - \frac{e^{-p_i t}}{(-p_i + ik.u)\frac{\partial \epsilon}{\partial p}(k,p_i)} \right] \quad (1)$$

Now the first term here will have a pole on the real k axis every time that $p_i = -ik.u$ as k varies for all i. However, there will always be a term in the sum over i which cancels this out. For

$$\frac{\partial \epsilon(k,p_i)}{\partial p} = \lim_{p \to p_i} \frac{\epsilon(k,p) - \epsilon(k,p_i)}{p - p_i} = \lim_{p \to p_i} \frac{\epsilon(k,p)}{(p - p_i)} \quad (2)$$

and as $k \Rightarrow$ a value such that $p_i + ik.u \Rightarrow 0$, then the appropriate term in the sum is

$$\lim_{\substack{p \to p_i \\ ik.u \to -p_i}} \frac{e^{p_i t}}{\frac{(p_i + ik.u)}{(p - p_i)} \epsilon(k,p)} = \frac{e^{-ik.ut}}{-k^2 \epsilon(k, -ik.u)} \quad (3)$$

if we take the limits appropriately, which exactly cancels the first term in the expression for Φ above, (Equation (1)).

If we assume as in the previous case that for long times, the time varying terms give only noise, then we can demonstrate a general property of the first term in the integral in equation (1) which serves to differentiate shielding in the magnetic case for a moving particle from the result for the purely electrostatic case. We consider that the time-varying terms, as demonstrated above, remove the contributions from the poles of the first term as we integrate along the real k- axis,

but that their contribution does not otherwise affect the general form of the potential. If we include an analysis such as in 4(b) of the gradual introduction of the test charge, we can consider the amplitude of the noise terms to be proportional to $1/T$ compared with the principal terms. For if we express $\underline{\phi}(x,t)$ as in Chapter 4(b)6, we have

$$\underline{\phi}(x,t)=\int_0^{\infty} k\,dk \int_0^{2\pi} d\phi\, e^{i\underline{k}.\underline{x}} \frac{q}{\pi}\left[\frac{\exp(-i\underline{k}.\underline{u}t)}{k^2\epsilon(k,-i\underline{k}.\underline{u})}+\frac{\gamma}{k^2}\left[\left(\frac{\exp(p_i t)}{(p_i+i\underline{k}.\underline{u})\frac{\partial\epsilon}{\partial p}}-\frac{\exp(-p_i t)}{(-p_i+i\underline{k}.\underline{u})\frac{\partial\epsilon}{\partial p}}\right)\right]\right] \quad (4)$$

where $\gamma = 4\pi q\left[1-\exp-(p+i\underline{k}.\underline{u})T\right]/\left[T(p+i\underline{k}.\underline{u})^2\right]$

The factor γ, which is due to the gradual introduction of the test charge into the plasma, is of order $1/T$, and becomes smaller as T becomes larger, so that in the limit of very slow introduction of the particle, the 'noise' terms arising from the undamped modes have negligible amplitude. This applies except at or near the points where the contribution from these terms are required to cancel the large contribution from the first term.

Consider, then, the first term only

$$\underline{\phi}(x,t) = \frac{q}{\pi}\int_0^{\infty} k\,dk \int_0^{2\pi} \frac{\exp i\underline{k}.(x-ut)\,d\phi}{k^2\epsilon(k,-i\underline{k}.\underline{u})} \quad (5)$$

ϕ is the angle between $\underline{k}$ and $\underline{u}$; let $\tau = x-ut$, expand $\exp(i\underline{k}.\underline{r})$ and $\epsilon(k,-i\underline{k}.\underline{u})$, to give

$$\phi(x,t) = \frac{q}{\pi}\int_0^{\infty} k\,dk \int_0^{2\pi} \frac{\sum_m i^m J_m(k\tau)\exp(im(\theta-\phi))\,d\phi}{k^2+2k_D^2\sum_{n=1}^{\infty}\frac{1}{1-\frac{k^2\xi^2}{k_c^2 n^2}}\cos^2\phi\,\exp\left(\frac{-k^2}{k_c^2}\right)I_n\left(\frac{k^2}{k_c^2}\right)} \quad (6)$$

where $\xi = u/\omega_{pn}$, and θ is the angle between x and k .

We now show that this is of the form $\sum_{\ell=0}^{\infty} a_{2\ell} \cos(2\ell\theta)$

The denominator of each term in the sum over m, is, by inspection, even in ϕ. Let us group the terms in m and $-m$ together, noting that $J_m(kr) = (-1)^m J_{-m}(kr)$, $i^m = i^{-m}(-1)^m$, and ignoring for the moment the $\int_0^{\infty} dk$. We have for these 2 terms

$$\int_0^{2\pi} d\phi \frac{\left(i^m\right) J_m(kr)\exp(im(\theta-\phi)) + i^m(-1)^m(-1)^m J_m(kr)\exp(-im(\theta-\phi))}{k^2 + 2ik_D^2 \sum_{n=1}^{\infty} 1/\left(1 - \frac{k^2\xi^2\cos\phi}{n^2 k_c^2}\right) \exp(-k^2/k_c^2) I_n(k^2/k_c^2)} \quad (7)$$

$$= \int_0^{2\pi} \frac{i^m J_m(kr)\, 2\cos m(\theta-\phi)\, d\phi}{\text{denominator (even in } \phi)}.$$

This is non-zero only for even m by a straightforward argument, so that we can express the function

$$\phi(r,\theta) = \sum_{\ell=0}^{\infty} a_{2\ell}(r)\cos 2\ell\theta \qquad \text{where} \qquad (8)$$

$$a_{2\ell}(r) = \frac{2\varepsilon}{\pi}\int_0^{\infty} k\,dk \int_0^{2\pi} \frac{(-1)^{\ell} J_{2\ell}(kr)\cos 2\ell\phi \; d\phi}{k^2 + 2ik_D^2 \sum_{n=1}^{\infty} 1/\left(1 - \frac{k^2\xi^2\cos^2\phi}{k_c^2 n^2}\right) \exp\left(-\frac{k^2}{k_c^2}\right) I_0\left(\frac{k^2}{k_c^2}\right)} \quad (9)$$

$$a_0(r) = \frac{\varepsilon}{\pi}\int_0^{\infty} k\,dk \int_0^{2\pi} \frac{J_0(kr)\, d\phi}{k^2 + 2ik_D^2 \sum_{n=1}^{\infty} 1/\left(1 - \frac{k^2\xi^2\cos^2\phi}{k_c^2 n^2}\right) \exp\left(-\frac{k^2}{k_c^2}\right) I_0\left(\frac{k^2}{k_c^2}\right)} \quad (10)$$

By showing that only even multiples of θ appear in the expression for $\underline{\phi}$, on the assumption that the undamped terms produce noise which is of low amplitude and isotropic, we have demonstrated that the potential distribution due to a moving particle in a magnetic field in two dimensions takes a significantly different form from that in the

electrostatic case. The significant difference is that in the present instance, while we still have symmetry about the line of motion of the particle, we also have symmetry about the line $\theta = \pi/2$. In other words, the result implies that the distribution is such that $\underline{\phi}(a,0) = \underline{\phi}(a,\pi)$, for example. The potential 'in front' of the particle takes the same form as the 'wake' behind it. It will be recalled that in the electrostatic case $\underline{\phi}(a,0) \neq \underline{\phi}(a,\pi)$, the distribution in front and behind the particle being significantly different.

We could demonstrate the symmetry of the potential distribution along the line of motion of the particle equally well by noting that we can express the r.h.s. of (6) as $\underline{\phi}(\tilde{r})$. The fact that $\underline{\phi}(\tilde{r}) = \underline{\phi}(-\tilde{r})$ shows that the potential distribution is identical whether the direction of motion is along $\theta = 0$ or $\theta = \pi$.

Care should always be taken in taking limits as certain parameters vary, in such expressions as those in equations (9,10). Tentatively, we examine what happens in the large field limit, and get

$$a_0 \Rightarrow \frac{q}{\pi} \int_0^\infty k\,dk \int_0^{2\pi} \frac{J_0(kr)\,d\phi}{k^2(1 + k_D^2/k_c^2)} \qquad (11)$$

exactly the form of the large-β potential for $u = 0$, while we get

$$a_{2\ell} \Rightarrow \frac{q}{\pi} \int_0^\infty k\,dk \int_0^{2\pi} \frac{(-1)^\ell J_{2\ell}(kr)\cos 2\ell\phi\,d\phi}{k^2(1 + k_D^2/k_c^2)} \qquad (12)$$

This will give finite values for small r and as r increases will become very small, leaving only the a_0 term. Thus for large field the potential distribution at large distances will be of the same form as that for the stationary test charge. So, not surprisingly, there is no increase in the total shielding in the moving particle case, and the particle is still incompletely shielded.

The integrals in equations (9) and (10) are intractable by analytic or numerical means as they stand. Thus it would be of interest to investigate by means of plasma simulation, whether the conclusion of the symmetries holds, and whether the assumption of a noise level which has not an adverse affect on the analysis, is justified. It would also be of interest if any details of the distributions could be elucidated, especially for moderate fields where $\omega_p \sim \omega_c$; for in the high field case we do not, after the rough limit-taking above, expect anything of interest. Also, the case $\omega_p \sim \omega_c$ is most convenient to deal with by simulation because (a) for the high field case we need to use a small timestep with respect to $1/\omega_p$ in order to follow particles properly as they move in their orbits round field lines, and this means very much computing time before we even compute for one plasma period, and we want to compute for 'a few' plasma periods. (b) For the low-field case we need to compute for many plasma periods before a particle has completed an orbit, and it needs to complete some few orbits before we can reasonably claim to be simulating the 'long time' state of the system in terms of magnetic effects. In other words the most convenient part of parameter space, in which we minimise the computing time required to include effects both on timescales $1/\omega_p$ and $1/\omega_c$ is when these two timescales are of the same order of magnitude.

For the case $\omega_c = \omega_p$ a NOVA run was initiated, and the parameters used were as follows.

COMPUTATIONAL MESH DIMENSIONS	64 x 64
PLASMA DIMENSIONS	16 x 16 DEBYE LENGTH
NUMBER OF PLASMA PARTICLES	16,384
CHARGE ON TEST PARTICLE	200 UNITS
VELOCITY OF TEST PARTICLE	ELECTRON THERMAL

Because of technical problems, the program with a square computational area was used here, although the rectangular plasma would have been preferable in that it gives more physical space for the potential distribution to set itself up in along the direction of test-particle motion. Fig (34) shows the cross-section along the line of motion of the test particle after 70 timesteps have passed. At this point there is a slight beginning of interference between the front and back of the potential distribution. However, examination of Fig (34) shows that a distribution has been set up different in character to that set up in the electrostatic case. As the theory predicted, the distribution is symmetrical about the particle along its line of motion, to within statistical fluctuations. This is another instance where the 'quiet start' procedure would have helped to give better detail.

A similar run was done for $\omega_c/\omega_p = 2.0$, using a timestep of $\Delta T = 0.125$ in order to ensure that particle motion in orbits around magnetic fields was as well simulated as previously. The results here also tend to confirm the symmetry of the distribution between $\theta = 0$ and $\theta = \pi$. Fig (35) shows a cross-section of the potential along the line of motion of the particle, while Fig (36) gives a contour plot of the entire distribution. From these it can be seen that the claim of symmetry is indeed well-founded to within simulation fluctuations. However, in this case it is noticeable that spatial variations in the potential at

distances greater than a few Debye lengths from the test particle are of a smaller amplitude than in the lower-field case of $\omega_c/\omega_p = 1.0$

It would also be of interest here to perform a comparison, similar to Figs (28) and (29) of potential energy variations with time, between magnetised and unmagnetised cases for a test-particle velocity $V_T = V_{e_{th}}$. The appropriate comparison graph is given in Fig (37), where again there is 20% greater potential energy in the modes in the magnetic case than there is in the electrostatic case, indicating the presence of an extra noise background in the magnetic case. The next graph Fig (38) compares values of potential at the test-particle position for the two cases, and again the values in the magnetic case are some 20-25% greater than in the other case.

We now investigate whether any other diagnostic output from the two NOVA runs would be of interest to compare. We had available as output at each timestep the normalised mode amplitudes for a small number of selected modes, one of which is that for which in two dimensions $k_x = 1$, $k_y = 0$; sine and cosine modes were available. We present here a plot Fig (39) of the comparison between the sine mode amplitude in the magnetised case where $\omega_p/\omega_c = 1.0$, and the amplitude of the same mode in the electrostatic case. From this plot it is evident that on average the mode amplitude in the magnetic case was greater. A similar result holds for the cosine modes. Both of these were in the run where the test particle velocity was $V_T = V_{th} = 1.0$ in scaled units. The fact that the amplitude is greater in the magnetic case can be construed as being due to the lack of damping of modes which was demonstrated earlier, and this greater amplitude in each mode will contribute to the greater potential energy (and background noise) in the magnetic case compared with the electrostatic case.

These two NOVA runs having been made, which confirm the general results of equation (8), and our assumptions about noise, it was now thought a reasonable proposition to attempt to integrate the leading term in equation (1) in order to ascertain whether any numerical results could be obtained which would give further quantitative detail on the potential distribution.

If we express this as in equation (5) we can proceed to expand $\epsilon(k, -i\underline{k}\cdot\underline{u})$ in the following way in powers of ζ^2

$$\epsilon(k, -i\underline{k}\cdot\underline{u}) = 1 + 2\frac{k_D^2}{k^2}\sum_{n=1}^{\infty}\left(1 + \frac{k^2\zeta^2\cos^2\phi}{k_c^2 n^2} + \frac{k^4\zeta^4\cos^4\phi}{k_c^4 n^4}\right) \times \exp\left(-\frac{k^2}{k_c^2}\right) I_n\left(\frac{k^2}{k_c^2}\right) \qquad (13)$$

By the rules of mathematical analysis this expansion is valid when $\frac{k^2\zeta^2\cos^2\phi}{k_c^2} < 1$, that is, $\frac{k^2\zeta^2}{k_c^2} < 1$. Thus, the smaller the value of ζ, the larger the range of k in terms of k_c for which there is validity. If $k_c \gtrsim k_D$, then since $k_c = \frac{1}{a_i}$ and $k_D = \frac{1}{\lambda_D}$ by taking small ζ we have validity over wavelengths from the largest down to significantly less than λ_D. Since shielding is a phenomenon whose typical scale length is that of λ_D or greater, it is evident that all important wavelengths will be included even if we cut off the integral at a value of k just below the value $k = k_c/\zeta$, which is what we propose to do here, though the functions obtained after the expansion is completed, are numerically integrable over the whole range of k, by means of the manipulation of section (b). In order to claim a meaning for the results obtained numerically below, we have to assume that the contribution to the integral from values of $k \geq k_c/\zeta$ is negligible, and that the effects of the infinities in the integrand are

nullified as outlined above. These infinities all occur for $k > k_c/\xi$

We proceed to expand the newly-expanded denominator of in (5) and obtain, using $2\sum I_n(z)\exp(-z) = 1 - I_0(z)\exp(-z)$,

$$\Phi(r,t) = \int_0^\infty \frac{k\,dk}{k^3}\int_0^{2\pi} \exp i\underline{k}.(\underline{x}-\underline{u}t)\left[\frac{1}{1+\frac{k_D^2}{k^2}\left(1-\exp\left(-\frac{k^2}{k_c^2}\right)I_0\left(\frac{k^2}{k_c^2}\right)\right)} - \right.$$

$$\frac{\frac{2k_D^2}{k^2}\sum_{n=1}^{\infty}\left(\frac{k^2\xi^2}{k_c^2 n^2}\right)\cos^2\phi\exp\left(\frac{k^2}{k_c^2}\right)I_n\left(\frac{k^2}{k_c^2}\right)}{\left(1+\frac{k_D^2}{k^2}\left(1-\exp\left(-\frac{k^2}{k_c^2}\right)I_0\left(\frac{k^2}{k_c^2}\right)\right)\right)^2} + \frac{\xi^4\cos^4\phi\left(\frac{2k_D^2}{k^2}\sum_n \frac{k^2}{k_c^2 n^2}\exp\left(-\frac{k^2}{k_c^2}\right)I_n\left(\frac{k^2}{k_c^2}\right)\right)^2}{\left(1+\frac{k_D^2}{k_c^2}\left(1-\exp\left(-\frac{k^2}{k_c^2}\right)I_0\left(\frac{k^2}{k_c^2}\right)\right)\right)^3} \quad (14)$$

$$\left. - \frac{\xi^4\cos^4\phi\,\frac{2k_D^2}{k^2}\sum_n \frac{k^4}{k_c^4 n^4}\exp\left(-\frac{k^2}{k_c^2}\right)I_n\left(\frac{k^2}{k_c^2}\right)}{\left(1+k_D^2/k_c^2\left(1-\exp\left(-k^2/k_c^2\right)I_0\left(k^2/k_c^2\right)\right)\right)^2}\right] d\phi$$

to order ξ^4 . Thus we can express Φ as $A - B\xi^2 + F\xi^4$ where the definitions of A, B, F are evident, and $F = F_1 - F_2$ As before we put $\underline{r} = \underline{x} - \underline{u}t$ and define θ to be the angle between the observer and the direction of motion $\underline{u}$, the latter chosen in the x direction, so that we get

$$\exp i\underline{k}.(\underline{x}-\underline{u}t) = \exp ik.r\cos(\theta-\phi) = \sum_{m=-\infty}^{\infty} i^m J_m(kr)\exp im(\theta-\phi) \quad (15)$$

In an integral over 2π , this factor, multiplied by $\cos^l\theta$ picks out only terms with l or $-l$. In particular, for $\cos^2\phi$ we have

$$\int_0^{2\pi} \exp im(\theta-\phi)\cos^2\phi\,d\phi = \begin{cases} \pi/2 & : m = -2 \\ \pi & : m = 0 \\ \pi/2 & : m = 2 \end{cases}$$

Thus from the sums in (15) we get after the ϕ integration,

$$\pi\left[J_0(kr) - J_2(kr)\cos 2\theta\right] \quad (16)$$

For the $\cos^4\phi$ term, the expression remaining is

$$\tfrac{3}{4}\pi J_0(kr) - \pi J_2(kr)\cos 2\theta + \tfrac{1}{4}\pi J_4(kr)\cos 4\theta \qquad (17)$$

If we include only terms up to order ζ^2 we have

$$\bar{\Phi} = A - B\zeta^2 = A - \zeta^2(C - D\cos 2\theta) \qquad (18)$$

It is brought out most clearly here that, as in the expressions for $\bar{\Phi}$ previously, only even terms in ζ^2 occur and only angular variations about the direction of motion by even multiples of θ . This is in contrast to the non-magnetic case where all powers of ζ are included and all multiples of θ .

The terms in the expression are as follows.

$$A = 2q\int_0^{k_{max}} \frac{J_0(kr)\,k\,dk}{k^2 + k_D^2\left(1 - \exp(-k^2/k_c^2)\,I_0(k^2/k_c^2)\right)} \qquad (19)$$

$$C = 2q\int_0^{k_{max}} \frac{k^3 k_D^2 \sum_{n=1}^{\infty} \frac{\exp(-k^2/k_c^2)\,I_n(k^2/k_c^2)}{k_c^2 n^2}\, J_0(kr)\,dk}{\left(k^2 + k_D^2\left(1 - \exp(-k^2/k_c^2)\,I_0(k^2/k_c^2)\right)\right)^2} \qquad (20)$$

$$D = 2q\int_0^{k_{max}} \frac{k^3 J_2(kr)\left(\sum_{n=1}^{\infty} \frac{\exp(-k^2/k_c^2)\,I_n(k^2/k_c^2)}{k_c^2 n^2}\right)\,dk}{\left(k^2 + k_D^2\left(1 - \exp(-k^2/k_c^2)\,I_0(k^2/k_c^2)\right)\right)^2} \qquad (21)$$

The integral for A is very similar to that for the stationary particle case apart from the upper integration limit, as we would expect; for when $\zeta \to 0$, every other term disappears because of the coefficients ζ^{2l} , and also the limit in the integration tends to infinity. If we assume that it is allowable to extend the range of integration beyond k_{max} , for mathematical convenience assuming the normal mode terms to deal with the poles, we can deal with the integrals in A and C by

the same and similar means, respectively, as were employed in part (b). These give rise to a log variation at large a. The term D does not have any divergence problems, so can be integrated in a straightforward manner.

It should be emphasised that this calculation is not being presented as a definitive analysis of the form of the potential due to the test charge, merely as an indication of what sort of distribution one can expect the formula to give rise to, to second order in ξ. The fact that there is no first order term indicates that for small ξ at least, one can expect a distribution very similar to the stationary test charge; however, it is difficult to tell anything about the case of slightly larger ξ, and in the large ξ limit there does not seem to be any expansion of the denominator which one can use, for moderate field strengths.

The function C is similar in general form to A, but D is somewhat different. It is plotted in Fig (40) for a few field strengths, and it is noticeable that the value of $D(a)$ at any point decreases as the field increases, showing that there is a smaller perturbation from the stationary-particle form the larger the field becomes. For reduction of D will tend to give symmetry ϕ in space about any line through the test charge, as the effect of the angular dependence is thus reduced. The form of D shows that it may be possible, for certain values of parameters, to obtain a potential distribution showing 'bumps' as in Fig (34), but no parameters used in the calculation gave anything like so pronounced an effect.

The results of forming the sum $A - B\xi^2$ for moderate values of B were that, keeping ξ small, no spatial oscillations of an amplitude comparable with those in Fig (34) were observed.

As B increases, to a point where $\omega_c/\omega_p = 2.0$, the simulation shows that for $V_T = V_{ph}$ the amplitude of the spatial variations at distances far from the test particle has decreased markedly. This implies that they would have decreased even more for even higher magnetic field. In this limit the expansion technique even for moderate velocities was seen to give results closer to the simulation's results.

The conclusion is that for such parameters as make the expansion valid, and given k_{max} a high enough value so as to include the range of wave numbers required to completely describe the physics, the expansion (14) is a satisfactory way of calculating from analysis the test particle's potential distribution. The parameter range which gives this validity is $\gamma \ll 1$ and $\omega_p/\omega_c \gg 1$. However for these values of the parameters, the potential distribution around the test-particle is very similar to that for the stationary test particle case, and is thus of no great interest.

In general terms however, given that we know that the potential distribution is going to take the form (8)

$\Phi(r,\theta) = A'(r) + B'(r)\cos 2\theta$ plus other terms, we can make one or two general comments about its shape. If we make the not unreasonable assumption, that the form of $B'(r)$ might be similar to the $D(r)$ of equation (21), for non-negligible velocities, then we might expect to see a distribution such as is outlined by the rough sketches in Fig (41).

The first of these shows the cross-section of potential distribution along the line of motion of the particle if the function B' was of sufficient amplitude, as it might well be for a sufficiently high test-particle velocity. The 'contour' map shows a plan view of

what the distribution might be, where the dotted contours represent either minima or some kind of quasi minima or 'areas of inflexion' in the downward trend of the potential value.

In conclusion, what can now be stated about the potential distribution about a moving test charge in a two-dimensional magnetised Maxwellian plasma is as follows. The shielding of the particle is incomplete just as in the stationary test particle case. The potential distribution according to theory exhibits symmetry about the line through the particle perpendicular to the direction of motion. Both these facts are in contrast to the situation in the electrostatic case. The claim of symmetry is supported by simulation. However, due to the analytic difficulties involved it did not prove possible to produce from the theory a quantitative description of the potential distribution around the test-particle for moderate values of magnetic field and non-negligible test particle velocities.

(d) Test Particle in Three-Dimensional Magnetised Plasma

Expressions for the dielectric function of a three-dimensional magnetised plasma have been known for some time (Refs 41,43). If we take the expression given in Ref (43) for longitudinal modes

$$\epsilon(k,\omega) = 1 + \frac{4\pi e^2}{k^2 m} \sum_{n=-\infty}^{\infty} \int \frac{J_n^2\left(\frac{k_\perp v_\perp}{\omega_c}\right) d\underline{v}}{(\omega - k_z v_z - n\omega_c)} \left[n\frac{\omega_c}{v}\frac{\partial f_0}{\partial v} + k_z \frac{\partial f_0}{\partial v_z} \right] \quad (1)$$

We can follow an analysis which leads to the result of Ref (19) for $\epsilon(k,0)$, and Ref (26) for stationary test particle.

If we integrate in cylindrical co-ordinates in velocity space, we obtain

$$\epsilon(k,\omega) = 1 + \frac{k_D^2}{k^2} \sum_n \int_{-\infty}^{\infty} \frac{f_z \left[-(n\omega_c + k_z v_z) \right] dv_z}{\omega - k_z v_z - n\omega_c} \left[\exp\left(-\frac{k_\perp^2}{k_c^2}\right) I_n\left(\frac{k_\perp^2}{k_c^2}\right) \right] \quad (2)$$

where we chose f_0 to be Maxwellian, $f_0 = \left(\frac{1}{2\pi v_{e_{th}}^2}\right)^{3/2} \exp\left(-v^2/2v_{e_{th}}^2\right)$, and where $v_z^2 + v_\perp^2 = v^2$, $f_z = \frac{1}{(2\pi v_{e_{th}}^2)^{1/2}} \exp\left(-v_z^2/2v_{e_{th}}^2\right)$

From (2) we get

$$\epsilon(k,\omega) = 1 + \frac{k_D^2}{k^2} \sum_n \left(1 - \omega \int_{-\infty}^{\infty} \frac{\exp\left(-v_z^2/2v_{e_{th}}^2\right) dv_z}{\omega - k_z v_z - n\omega_c} \right) \exp\left(-\frac{k_\perp^2}{k_c^2}\right) I_n\left(\frac{k_\perp^2}{k_c^2}\right) \quad (3)$$

After a change of variable we obtain

$$\epsilon(k,\omega) = 1 + \frac{k_D^2}{k^2} \sum_n \left(1 - \omega \int_{-\infty}^{\infty} \frac{\exp(-x^2)\, dx}{-x - \frac{n\omega_c}{\sqrt{2}k_z} + \frac{\omega}{\sqrt{2}k_z v_{e_{th}}}} \right) \exp\left(\frac{k_\perp^2}{k_c^2}\right) I_n\left(\frac{k_\perp^2}{k_c^2}\right) \quad (4)$$

Assuming that $\epsilon(k, -i\underline{k}.\underline{v})$ is going to be the term of interest in the test-particle shielding case, that is, that there are no unstable modes

and that undamped modes have suitably low amplitude because we consider the gradual introduction of the test-particle, we now consider what form this function takes.

We have

$$\epsilon(k_1 - \underline{k}.\underline{u}) = 1 + \sum_n \frac{k_D^2}{k^2}\left(1 - \frac{k.\zeta}{\sqrt{n}} Z\left(-\frac{n k_z}{\sqrt{2}k_z} - \frac{k.\zeta}{k_z}\right)\right) \times \exp\left(-\frac{k_\perp^2}{k_z^2}\right) I_n\left(\frac{k_\perp^2}{k_z^2}\right) \qquad (5)$$

Here ζ takes the value it had in Ref (8); ie $\zeta = \frac{u}{\sqrt{2}V_{eA}}$, and $Z(x)$ is given in Ref (37).

Thus for $\omega = 0$, we obtain

$$\epsilon(k,0) = 1 + k_D^2/k^2 \qquad (6)$$

Thus shielding in this case, for a stationary test particle in a magnetic field, is the same as it is in the electrostatic case. This agrees with Ref (19).

In the case of non-zero ζ, we can show immediately from (5) that we do not obtain the same fore-and-aft symmetry about the line perpendicular to the test-particle direction of motion. For $\epsilon(k_1 - \underline{k}.\underline{u}) \neq \epsilon(k, \underline{k}.\underline{u})$, by inspection, using the known properties of the plasma dispersion function Z (Ref (37)), showing that if the velocity vector is reversed the distribution will be different.

Inspection of (1) shows that if either $k_z = 0$, (the field being in the z direction) or no component of particle velocity is allowed in the z-direction, the expression of $\epsilon(k,\omega)$ reduces to the expression arrived at in 5(a) for the two-dimensional case.

Thus the presence of physical effects along the field lines causes the removal of the lack of total shielding, and the symmetry of potential distribution about a test particle. These effects which occur in the two-dimensional case indicate at least two ways in which the two-dimensional plasma used in many simulations differs from a real plasma where a magnetic field is present.

Acknowledgements

The author would like to thank Dr E W Laing for suggesting this project and for many interesting discussions. Thanks are also due to Dr A Lamont for pointing out some of the difficulties of earlier work. A large fraction of the computational results described above would not have been obtained but for the assistance of members of the staff of the U.K.A.E.A. Culham Laboratory. Principally, the author would like to thank Brendan McNamara, for the provision of his plasma simulation program and for his help in decyphering the secret code error messages from the I.C.L. 4/70. For help in this latter respect thanks are also due to D Fox, J Davis, A Sherwood and W Holman, without whose assistance one would still be struggling with the manuals.

Finally, the author would like to thank Dr K V Roberts for the provision of the Computational Physics Contract between Culham Laboratory and Glasgow University, which provided the financial support for this work, and Professor J C Gunn for providing research facilities at the University of Glasgow.

References

(1) O. Buneman: Phys. Rev. Vol. 115, p 503 (1959).

(2) J. Dawson: Phys. Fluids, Vol. 5, p 445 (1962).

(3) R.W. Hockney: Phys. Fluids, Vol. 9, p 1826 (1966).

(4) P. Burger: J Appl. Phys., Vol. 36, p 1938 (1965).

(5) R.W. Hockney: J. Assoc. Comput. Mech., Vol. 12, p 95 (1965).

(6) R.W. Hockney: Article in "Methods of Computational Physics", Edited by Alder et al, Vol. 9, Academic Press.

(7) J. Boris, K.V. Roberts: J Comput. Phys., Vol. 4, p 552 (1969).

(8) E.W. Laing, A. Lamont, P. Fielding: J. Plasma Physics, Vol. 5, No. 3, p 441 (1971).

(9) B. McNamara, A.B. Langdon: To be published.

(10) A. Hasegawa, H. Okuda: Phys. Fluids, Vol. 11, 9, (1968), p 1995.

(11) J. Dawson: Princeton University Plasma Physics Laboratory Report, Matt-894, April 1972.

(12) B. McNamara: Private communication.

(13) A. Riviere, Vth European Conference on Plasma Physics and Nuclear Fusion, Grenoble, 1972.

(14) I. Cook, B. McNamara, A. Sykes, J Boris: European Conference on Plasma Physics, Utrecht, 1969.

(15) J. Byers, M. Grewal: Phys. Fluids, Vol. 13, 7, p 1819 (1970).

(16) J.B. Taylor, B. McNamara: Phys. Fluids, Vol 14, p 1492 (1971).

(17) J. Dawson, H. Okuda, R. Carlile: Phys. Rev. Letters, 27, p 491 (1971).

(18) G. Vahala, D. Montgomery: J. Plas. Phys., Vol 6, 2, p 425 (1971).

(19) D. Montgomery, F. Tappert: Phys. Fluids, Vol 5, 4, p 683 (1972).

(20) J.B. Taylor, W.B. Thompson: Culham Laboratory Report CLM-p 286.

(21) D. Montgomery, C.S. Liu, G. Vahala: Phys. Fluids, Vol 15, 5, p 815 (1972).

(22) W.B. Thompson: An Introduction to Plasma Physics, Pergamon, 1964.

(23) L. Landau: Journal of Physics, Vol X, No. 1, 1946.

(24) D. Bohm, D. Pines: Phys. Rev. Vol. 85, 2, p 338 (1952).

(25) J. Neufeld, R. Ritchie: Phys. Rev., Vol. 98, 6, p 1632 (1955).

(26) N. Rostoker: Nuclear Fusion Vol. 1, p 101 (1961).

(27) W.B. Thompson, J. Hubbard, Rev. Mod. Phys. Vol 32, p 714 (1960).

(28) G. Joyce, D. Montgomery: Phys. Fl. 10, 9, p 2017 (1967).

(29) D. Montgomery, G. Joyce, R. Suzihara: Plasma Phys., Vol 10, p 681 (1968).

(30) G. Cooper: Phys. Fluids, Vol. 12, p 2707 (1969).

(31) D. Montgomery, M. Tidman: Plasma Kinetic Theory, McGraw-Hill, 1964.

(32) R.W. Hockney: Invited Paper to Culham Conference on Computational Physics, 1969.

(33) R.C. Singleton: Communications of the A.C.M., 10 (10), 1967.

(34) C. Birdsall, A.B. Langdon, H. Okuda: Article in Methods of Computational Physics, Vol. 9; Editors, Alder et al, Academic Press, 1970.

(35) Hung, S. Private communication.

(36) H. Okuda: Phys. Fluids, Vol. 15, 7, p 1268 (1972).

(37) Fried & Conte: The Plasma Dispersion Function, Academic Press, 1961.

(38) A. Lamont, E.W. Laing: Private Communication.

(39) L. Fox, D. Meyers: Computing Methods for Scientists and Engineers, O.U.P.

(40) R.T.P. Whipple: Private Communication.

(41) I. Bernstein et al in Advances in Plasma Physics, edited by W.B. Thompson, A. Simon, (1969) Wiley.

(42) I. Bernstein: Phys. Rev., 109, 1, p 10 (1958).

(43) E. Harris in "Physics of Hot Plasmas" edited by B. Rye, J. Taylor, Oliver & Boyd, 1970.

(44) E.W. Laing, Private Communication.

APPENDIX

HOW TO RUN NOVA FOR 2-D SIMULATIONS ON ICL 4/70

Main reference - McNamara and Langdon - to be published

The basic routines of NOVA existed in August 1972 on cards and on private disc store belonging to user BMCTHE (Brendan McNamara). They are in the main fairly well commented and they are ready to use but for the fact that one has to substitute certain common blocks, etc., by a procedure outlined below. (No doubt, since Alan Sykes was taking over Brendan's code, the routines will now be under user AASTHE).

A list of routines which were needed for the test particle work is attached and there will now follow a description of each of them. Note that there is often a difference between a file name and a routine name.

(1) ('NOVMAI') - main program

(2) UCP - 'Universal Control Package' supposed to be able to control any multistep process and it is the only thing called by main program.

(3) JOBID - This routine not necessary for test runs but this or any other routine containing blank common (substitute into it from NOVCOM(F) can be used to increase the dimension of XV, the vector which holds the co-ordinates of the particles, etc. The usefulness of this lies in the fact that merely by editing and recompiling one routine and re-composing the program we can vary the size of the plasma in the simulation.

One merely edits the common block which is being substituted, renaming it JOVCOM, say, such as to dimension XV to the required value. Since XV is the last item in blank common and since blank common comes at the end of the root segment, no over writing will be done and the only effect will be to increase XV's dimension.
NB: This is not to be done with any other array, anywhere.

(4) AREAWT - is described by its name: assigns charge to computation grid points using CIC method. QWT is an entry point.

(5) MORE - checks if calculation has done enough steps (NSTEPS) returns argument as appropriate.

(6) VALUES - takes account of the plasma scaling chosen which deduces from the values given in YOUSET and calculates scaling factors accordingly. Throws program off if dimension of plasma omitted.

(7) DEFALT - mnemonic title - sets up default values of many parameters (see listing).

(8) FINISH - ends current run but can return an argument (logical) to tell NOVA to start another run.

(9) PROBES - control routine for most of diagnostics, called with many (integer) arguments from many parts of the code.

(10) REPORT - diagnostic routine which prints out several NAMELISTS containing interesting variables dependent on argument (care with REPORT (4) of standard version - it prints out several arrays dimensioned SIDEX*SIDEY: rather paper-consuming if both these equal ~ 64).

(11) POISOL - FORTRAN control of poisson-solvers.

(12) BRENDN, URPFT - poisson-solvers in USERCODE

(13) POTXV - routine which is called when PROBES calls for potential output. If it is required, one can write this routine oneself for onds own specific purposes. If not, it is dummied out (see below).

(14) TESTON - user's own 'particle pusher' if he has a group of particles which cannot be moved by the standard pushers (this corresponds to 'equation 4' when calling HEADIN from YOUSET in the creating phase).

(15) SETACE - sets acceleration matrices, given potential.

(16) PRPTCL - prints every PRTHEM particles' co-ordinates at each step.

(17) UNMAG - electrostatic particle pusher (equation 2).

(18) MAGON - includes constant B perp. to plasma (equation 3).

(19) DOSTEP - controls running of one computational timestep; is called by UCP

(20) RPPFT - connected with poisson solvers.

(21) FMODES - prints out up to 6 selected mode amplitudes (sin and cos) and stores values in FS and FC.

(22) PLMODE - prints out after 50 steps the whole of FC, FS in suitable format and returns printer from 50 to 1 so that FC, FS start filling up again from beginning.

(23) ENERGY - calculates (1) kinetic energy of group , (3) potential energy in modes. (2) print-out of energies at each step.
(24) PLENRG - similar to PLMODE, except prints out energies.
(25) YOUSET - user writes this. It controls the setting up of his particular plasma. He can include any amount of necessary routines to be called by this equation.
(26) RNMAXW, which sets up GALAXY velocity distribution.
(27) CHEKBC - in the setting up (CREATE) phase this checks the boundary conditions to ensure that all particles fall inside the computational grid. Standard version only pulls in erring particles by an amount equal to the linear dimension of the plasma.,
(28) HEADIN - sets up header for particle description in the array XV. It has several arguments which are required, most of which end up in some position in the header.
(29) DONEIT - closes down (parts of) create phase.
(30) CHRGIT - lays down charge of a particle given its co-ordinates.
(31) PTCLIN - puts particle co-ordinates which are in the array (dimensioned 4) which is its argument into the next available 4 co-ordinates in XV.

DATA BLOCKS - file names

(1) DENERG(F) - gives certain data for the common block ENERG
(2) DFMODE(F) - gives some data for common FMOD
(3) DNOVA(S) - gives some data for common NOVPAR
(4) DPOIS(S) - gives some data for common POIS (data for poisson-solvers, eg array dimensions.
(5) DPROBE - gives data for probes routines in PROBIT common

COMMON BLOCKS in (F) files files [AU subroutines are in (S) files.]
Files are as follows:

(1) BUILD(F) - purpose obscure
(2) LANGDP(F) - contains common block (ABLANG?) connected with double periodic poisson-solvers.

(3) NOVCOM(F) - contains blank common and NOVPAR

(4) EQLADP - equivalence statements for LANGDP

(5) TRIBUF - contains common block used in triple buffering mode.

(6) EQPOIS - contains equivalence statements for common block POIS.

(7) EQNOVC - contains equivalence statements for common block NOVCOM.

(8) POISON - contains common block POIS mainly required for poisson-solvers.

(9) GRAFXV - common related to graphical output

(10) DIAGCM - connected with diagnostics

(11) PROBIT - common for probes.

The table shows which segment each routine is usually put into in the program. It also indicates whether the name of the file and the name of the routine are the same. When they are not the same, it is in general because the file contains the double periodic version of the given routine.

In general (S) files are in group NOVA, and compiled files in group NOVCOD. (You do not need to compile BRENDN, URPFT).

Routine name	Appropriate file name if different	Segment	Common block associated	*If there is no need to compile file
MAIN PROGRAM	NOVMAI	ROOT		
UCP		ROOT		
[JOBID		ROOT]		
AREAWT (ENTRY QWT)	SHARED	ROOT		
MORE		ROOT		
VALUES		ROOT		
DEFALT		ROOT		
FINISH		ROOT		
PROBES	PROBED	ROOT		
REPORT		ROOT		
YOUSET		01		
CHEKBC	CHKDP	01		
HEADIN		01		
DONEIT		01		
CHRGIT		01		
PTCLIN		01		
POISOL	DPP01S	02		
BRENDN		02		*
URPFT		02		*
POTXV		02		
TESTON		02		
SETACC	SETACD	02		
PRPTCL		02		
UNMAG		02		
MAGON		02		
DOSTEP		02		
RPPFT	RPPF			
FMODES	FMODED	02		
PLMODE	JJPLMD	02		
ENERGY	ENERGD	02		
PLENRG	JJPLEN	02		

Data block file name	Appropriate file name if different	Segment	Common block associated	*If there is no need to compile file
DENERG(F)		ROOT	ENERG	
DFMODE(F)		ROOT	FMOD	
DNOVA(S)		ROOT	NOVPAR, BLANK	
DPOIS(S)		ROOT	POIS	
DPROBE(S)		ROOT	PROBIT?	
Files containing common block			Common blocks which are contained, or which are associated	
BUILD(F)				
LANGDP(F)			ABLANG?	
NOVCOM(F)			BLANK, NOVPAR	
EQLADP(F)			ABLANG	
TRIBUF(F)				
POISON(F)			POIS	
EQPOIS(F)			POIS	
EQNOVC(F)			BLANK, NOVPAR	
GRAFXV(F)?				
DIAGCM(F)				
PROBIT(F)?				

Setting up a simulation

It is possible to use one of two standard length scalings, or alternatively to set up your own scaling. The procedure to follow if one is using DEBYE length scaling is straightforward - just give the plasma dimensions by setting LXDEBY and LYDEBY. In this scaling a plasma time ($1/\omega_p$) is unity, and the thermal velocity is unity. The scaling factor M* (STARM) is worked out for you. If one decides to include a magnetic field perpendicular to the plasma one gives a value for WC1WPI (ω_c/ω_p) and the extra scaling factor concerned (STARB) is worked out.

Larmor radius scaling is probably equally straightforward to set up. One does not have to think to set up standard scaling, but one certainly will have to when setting up one's own.

Scaling having been decided on, the next move is to decide on the array dimensions required (for the poisson solvers, this must be $(2^n + 1 \times 2^m + 1)$) and edit one's common block files accordingly. This will depend on the particular simulation - fineness of resolution required, number of particles, number of groups of particles, etc. It should always be remembered to edit accordingly equivalence blocks and data blocks as well.

YOUSET will generally need to have both POIS and (BLANK) common blocks in it. It is here that one gives all the parameters of the problem; this is most conveniently done by data reading from an appropriate DSET97 or DSET5. Here also the plasma will be set up by whatever initialisation procedure one thinks fit for the job in hand.

The next consideration is that of diagnostics. These are strongly problem dependent. Probes(n) for n= 1....7 is called at many points in each timestep so that the easiest thing to do is to edit PROBES itself to call routines which one writes oneself, at the appropriate moment, or perhaps to edit or put in one's own version of the routines which PROBES calls as it stands at present. The user will also have to find ways of

switching on and off diagnostics when he wants to - PRDIAG is the logical switch to do this, but the question of operating the switch is left to the user, as is the question of how much it switches off or on. (In test particle work this was done in POTXV. This worked because it was called every timestep.)

Parameters such as TENERG, ... etc., control whether or not PROBES calls ENERGY ... etc., ie every TENERG steps Energy is called. TENERG, etc., can be set in YOUSET if the appropriate common block is there as well.

The actual process for setting up the plasma once the scaling has been established is straightforward.

For the first group HEADIN is called, with appropriate parameters - group number, record number, equation, etc.

Then the 'PSPACE' NCOORD co-ordinates of the first particle are generated by the user, put into XY ( ) and the routine PTCLIN(XY) is called. This puts the co-ordinates into the next PSPACE 4 words of XV and lays down the charge by calling QWT and calls boundary condition check.

This is repeated for all particles in the group.

This is repeated for all remaining groups with a new call to HEADIN for each.

The array XV ends up containing a head and tail for every group, the tail containing the particle co-ordinates. The first few elements of XV are pointers to the beginnings of the other parts in XV. The integer parameter IN is set always to that word of XV which is next to be filled in each part of the create process. At the end of setting up the plasma, the numbers at the beginning of XV should refer to the positions of the start of all the HEAD records, and the last one should indicate the end of the last tail.

All this is given in the report by ABL and BMcN.

TO RUN NOVA USING ICL 4/70

First of all, we require a USERNAME. For the purposes of this it will be GLASGO, password GL8877.
A familiarity with MULTIJOB is useful before commencing, but this can be easily required.

It is assumed that all routines acquired have been written. It is quite useful to test each routine by including it in a NOVA test run instead of testing it in vacuo. The principles outlined below apply both to the test run and to the production run. The basic difference is that for the test one can use standard common blocks (in group NOVA in the BNLTHE space) and for the production run one uses one's own blocks. The standard ones are quite small so the program which is generated will be quite quick.

First of all, a few important points concerning the system.

Each user has a certain amount of private disc space allocated to him, the amount being measured in "Extents" where one extent $\sim \frac{1}{2}$ track and $1\frac{1}{2} - 2$ pages of FORTRAN. In this space he can have various types of Files, 'S', 'F', 'U', 'Y', 'P', 'N'. An 'S' file contains card images of any kind. An 'F' file contains card images, but the 'F' designation informs the compiler that this is a FORTRAN file. 'U' is for usercode. A 'Y' file is any compiled file, and a 'P' file contains a composed program. 'N' files are less common but for example, straightforward calls to GHOST routines will generate 'N' files. Files are allocated to <u>Groups</u> for convenience in handling, so that the full description of a file is

USERNAME: GROUPNAME: FILE NAME (IDENTIFIER/RUN NUMBER)

eg GLASGO: GLASGI. NOVGO (P0340)

BMCTHE: NOVCOD. URPFT(U)

where all names have no more than <u>6 letters</u>.
Before the user can use files in another user's space these files must be protected using the <u>PROTECT</u> command (see A. Sherwood, or manual for details).

A facility which is always used in a NOVA run composition is the ERREXIT facility which is used to insert a dummy subroutine UDUMMY instead of any routine which one does not want to include. Statements which do this for all possible standard routines are in BNCTHE: NOVA. NOVDUM(S). If the subroutine is included the composer ignores the ERREXIT statement.

There are (4) stages in running NOVA (or any other similar program) on the 4/70.

(1) Substitution of common blocks into 'S' files containing the executable statements.

(2) Compilation of such routines as are being changed.

(3) Composition of program (Linkage editing).

(4) Running of program.

(1), (2), (3) are done in 'A' or 'B' stream and (4) is done in 'E' stream. No test program is small enough to fit into A or B. There is a default option for (2) and (3), but (1) is generally done in B for reasons of space.

(1) <u>To substitute common blocks</u>

In the 'S' file which contains the routine, instead of many common statements we merely have, eg.,

```
//␣ SUBSTITUTE ␣ NOVCDM(F)
```

So to get the card images from NOVCOM(F) into this position, we run a program called DMGCSS: PREP. NEWJIP. This can be done from teletype or on cards. Either way, it requires a file giving details of the substitutions to be done. For example, if the user wanted to create a large 'F' file called ROOT which he proposed to compile and put into the 'root' segment, he would set up an 'S' file with run number say, containing the following -

```
//␣ GROUP ␣ FRED
//␣ REPLACE ␣ ROOT(F)
//␣ SUBSTITUTE ␣ NOVA.  PROBED(S)
//␣ SUBSTITUTE ␣ UCP(S)
//␣ SUBSTITUTE ␣ SHARED(S)
    .
    .
    .
//␣ ENDFILE
```

ϕϕϕϕ

If the NEWJIP program acted on this file, it would put all the Fortran cards required into a large file called FRED.ROOT(F). The common blocks would also have to be in group FRED, in this case. UCP and SHARED would also be in FRED.

(2) Compilations

In the same 'S' file, or in another, the following cards will then compile the 'F' files which are quoted

```
//␣ GROUP ␣ JACK  — not needed
//␣ TRIALS
//␣ SCHEDULE  S(TRIALS,, RUN NUMBER
//␣ EXEC TROUT
//␣ FTRAN1 ␣ FRED. ROOT, C,D/MAP,LIST,DEBUG
//␣ FTRAN1 ␣ GROUPNAME, FILENAME, C,D/....
```

'D' deletes the 'F' file.

We can immediately follow this, if desired, by the composition (linkage editing) which as for the compilation is done in the TRIALS system and must have its cards preceded by

```
//␣ TRIALS
```

and followed by

```
//␣ ENDTRIALS.
```

So, either we finish what we are doing by putting a //␣ ENDTRIALS after the last //␣ FTRAN1 card, or we proceed with the composition, which we do as follows.

(3) Composition of a version of NOVA

(//␣ TRIALS ..... understood).

```
//␣ COMPOSE ␣ GROUPNAME. FILENAME (P-----)
```

(name of program to be run eg NOVGO(P1230)

(where --- signify run number)

```
XX OPTION LET, MAP, XREF, TREE
```

(TREE only required if program is segmented)

```
XX  SUBST␣ BMCTHE:  NOVA. NOVDUM
```

(puts in NOVMAI, UDUMMY and ERREXIT cards)

```
*X INCLUDE GROUPNAME, FILENAME, (FILENAME .....)
    .
    .
    .     all compiled modules for root/main segment
    .
    .
*X SEGMENT  01,ONROOT
*X INCLUDE GROUPNAME, FILENAME, (FILENAME)
          all compiled modules for segment 01
*X SEGMENT  02,ONROOT
*X INCLUDE .......
```

after which we must have //U ENDTRIALS, to signify the end of the composition.

In the *X INCLUDE cards one must have all the compiled modules that he wants in the program. The SEGMENT cards signify the start of a segment. The operation of automatic segmentation is far from perfect, however, and it is common to get SYSTEM modules in the wrong segment, or too low down the tree. These have to be explicitly included where they ought to be once their erroneous presence has been found (they cause the program to crunch with negligible error messages).

(4) Running the program

This requires a sequence of control cards which can be either put into a file, and then that file is scheduled, or, alternatively, run from a teletype; or instead of putting them in a file, these cards can be entered as a job directly. Details of what is required can be obtained from manuals (not advisable) or consultants (frequently available) at Culham. In connection with NOVA it should be noted that with 64x64 computational grid it was possible to do a run in core with $\sim$ 2048 particles, in the day-time 'E' stream. This streams can run jobs of up to $\sim$ 396 store units (where 1 store unit = 512 bytes). The large-stream supervisor can run jobs of up to 500K bytes, and is essential in the absence of triple buffering, for a large NOVA code to be runincore. (This is defined as stream 'A', in fact.)

Further points concerning running of program:

The user may have generated in GLASGO space a large number of files which he requires and may find that his private store is getting a bit tight (GLASGO was allocated 600 extents at the end

of August, and the system was full so that there was no chance of getting this increased). He may also find himself wanting to do a large NOVA run, and will realize that the output file DSET99 is stored in his space before it is printed and deleted. If it is too big for the space much output will inevitably be lost. To obviate this a //$_{U}$ FILE card is used (see consultant) to direct the output into the public disc space on 'Volume 4' in group TEMP where to all intents and purposes there is infinite space available, or at least, a great deal more than the user will ever require since this Volume is scribbled completely almost every day by the systems programmers. If this procedure is followed, one need never worry about the size of output files, since the file is put into the print queue as soon as it is established and so will get printed out before the systems people start deleting Volume 4. (Every one automatically has access to Volume 4 because the systems people leave all users, after every clean-up, with one small file on this Volume in group TEMP, so that every file you create in group TEMP will go into Volume 4 and not clutter up your own space.)

Points of use or things for which to watch out

(1) Every time a program is composed, a composition map is generated from which one can tell quite a few things. It gives the size and location of COMMON blocks, SYSTEM routines as well as of the user's own compiled modules. It can help towards optimisation of segmentation in order to minimise the space required.

(2) If mode amplitudes or potential energies are required, it is necessary to ensure that the variable FACMOD, a scaling factor, is set equal to $^{1}/_{STARM}$. This gives the correct scaling between kinetic and potential energies of the NOVA plasma, for example.

(3) A run with 16K particles in a 64 x 64 mesh takes the order of half an hour to do of the order of 100 steps. Accurate numbers for timing are hard to give because the timing is done in ETU (elapsed time counts!) and it is said that this is not a constant, though it is in general $\sim$ 3 seconds.

(4) Triple buffering is probably, even in FORTRAN, not significantly slower than a core calculation. However, since one cannot run jobs of over 100 etu in the 200K 'E' stream during the day, it seems pointless to employ triple buffering while the large stream is available each night. (This is subject to the availability of a night-shift of operators, about which there is, periodically, a deal of doubt.) Another point is that T.B. is just another complication and one would like to keep things as simple as possible.

(5) Those with experience of the Phase-Space plotting package, eg Charlie Hung, are more qualified to discuss the subject than the present writer. Charlie can probably say what routines he calls and with what arguments in order to get his phase space plots. He plots the only two co-ordinates he has (X and V_x) so his case may be simpler than for the 2-D case. There is an extra data block (check with Charlie) to be included, as well as High Level and Low Level Ghost routines (which Brendan has in Files called HIGOST and LOGOST). These latter he recommends to be put in certain segments explicitly; this is more space-efficient than following the procedure in the Ghost manual. It is possible to generate film, etc,, by appropriate use of the package.

(6) Care should be taken if more than two groups of particles are to be used. In the standard common blocks, there are a number of small arrays which are, in fact, dimensioned 2 , where this refers to the number of groups. These dimensions should all be altered accordingly as the number of groups increases.

(7) Difference between a group and a record:
Groups are sets of simulation particles.
Records, consisting of a head and a tail are where all the data concerning these particles is stored.

(8) Brendan had written an ANALYSER package which is intended for use with NOVA. The principle was that there should be two runs - one to generate output and store it some where, eg on disc, the second, another NOVA run, but including only the analysers,was intended to analyse the results in a prescribed manner. Analysers are in files with names beginning JJ. The present writer has no experience with them.

It is to be hoped by this time Alan Sykes, if he has indeed taken over NOVA as JBT wanted him to, will know his way around it pretty well and will be able to advise upon matters connected with it.

FIG (1)

NEAREST GRID POINT

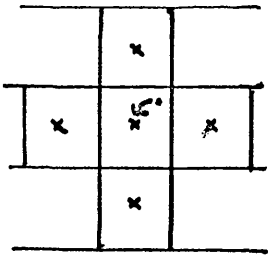

CHARGE DISTRIBUTED AS SHOWN BY ARROW

FIG (2)

CLOUD IN CELL

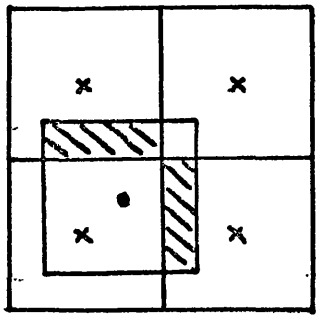

CHARGE SHARED AS SHOWN BETWEEN FOUR GRID POINTS

FIG (3)

N.G.P. FORCE LAW

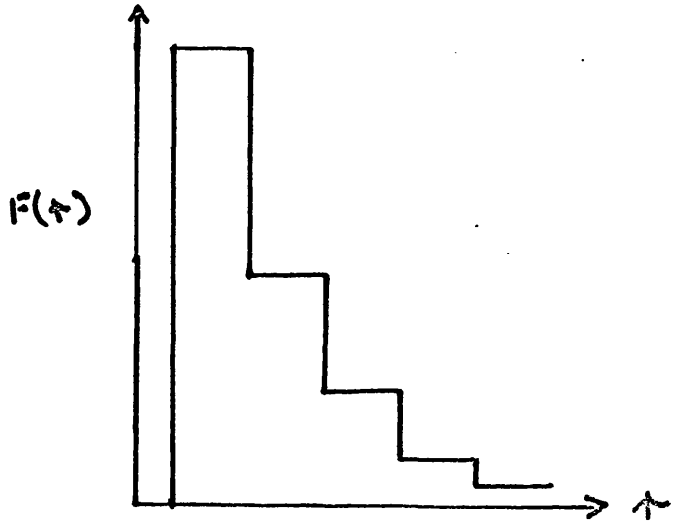

TAKEN FROM HOCKNEY (REF)

FIG(4).

C.I.C. FORCE LAW

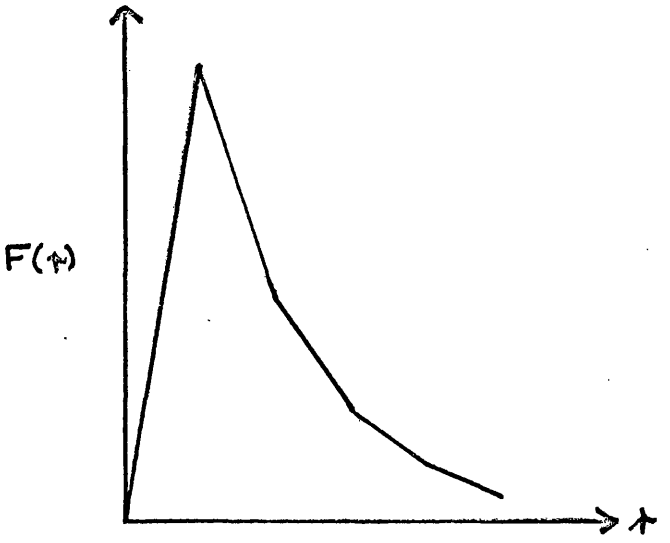

FIG(5).

SIMULATION CHARGE SHAPE FACTOR.

LOOKING PARALLEL TO X OR Y AXIS

THIS GIVES CROSS-SECTION OF CHARGE CLOUD

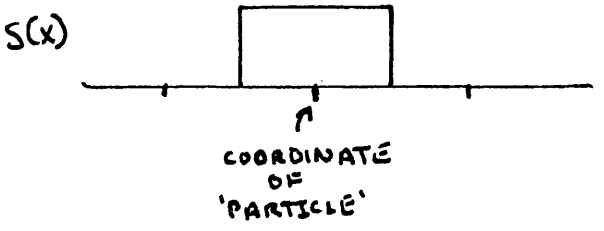

FIG(6)

NOVA SEGMENTATION

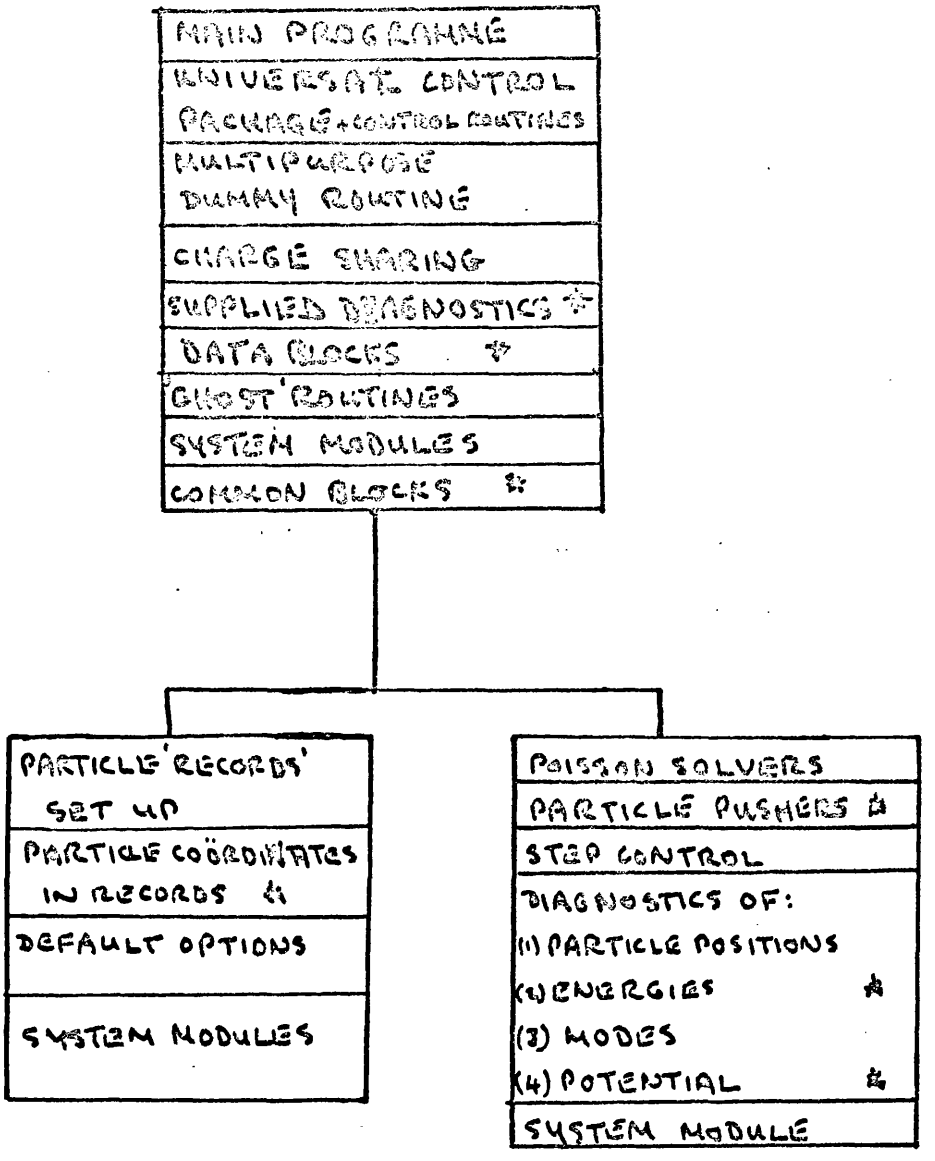

ITEMS ☆ WHOLLY OR PARTLY WRITTEN BY AUTHOR

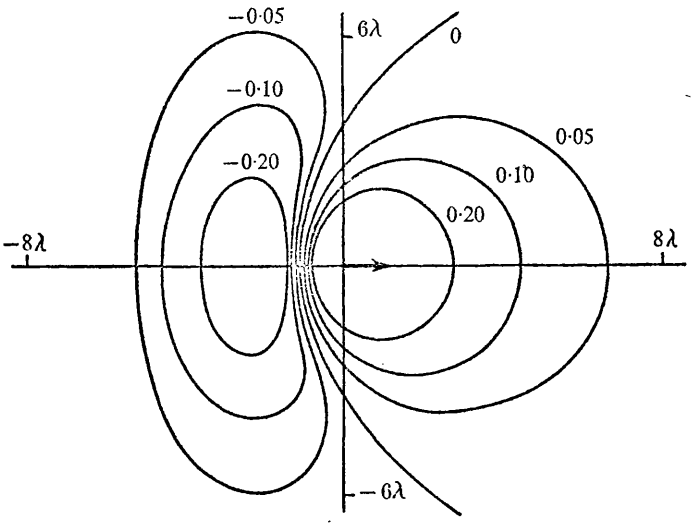

$\phi(\underline{r})$ FOR $\xi = 1$: EXACT COMPUTATION λ = DEBYE LENGTH

FIG(7b)

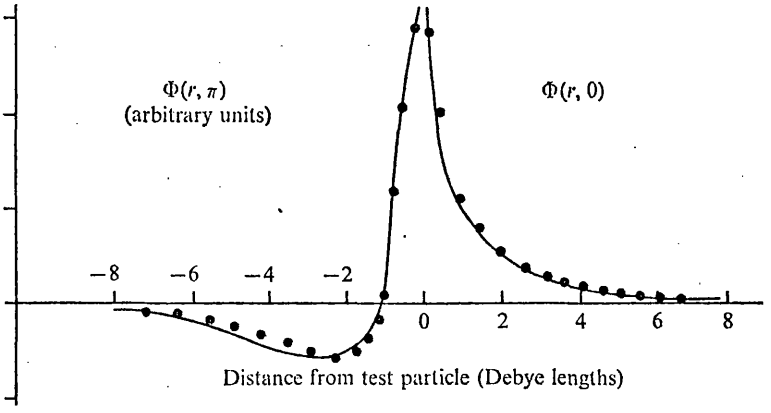

Comparison between theory and simulation, $\xi = 1$:
—, simulation; ••••, theory.

FIG(7c)

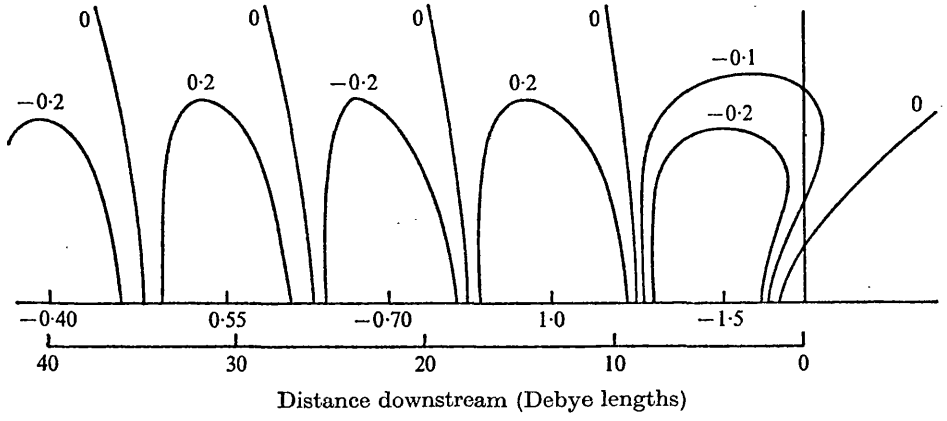

$\phi(\underline{r})$ BY EXACT COMPUTATION FOR $\xi = 2.4$

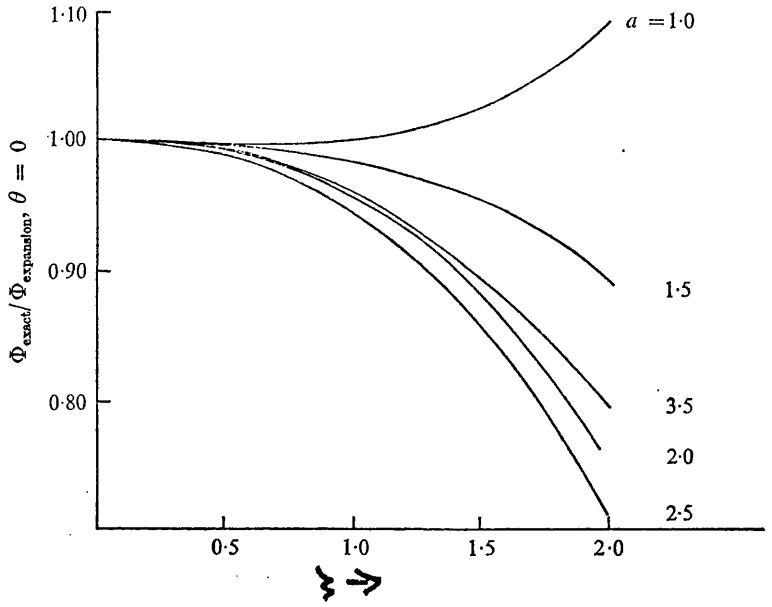

FIG (8B)

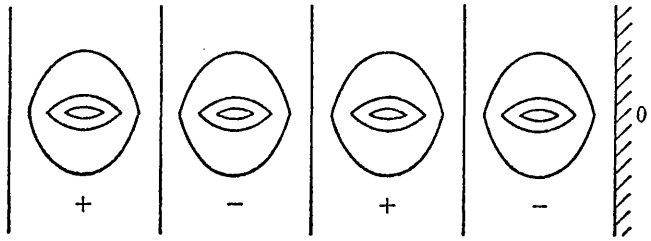

$\phi(\pm)$ FOR $u \gg V_e$

FIG (8C)

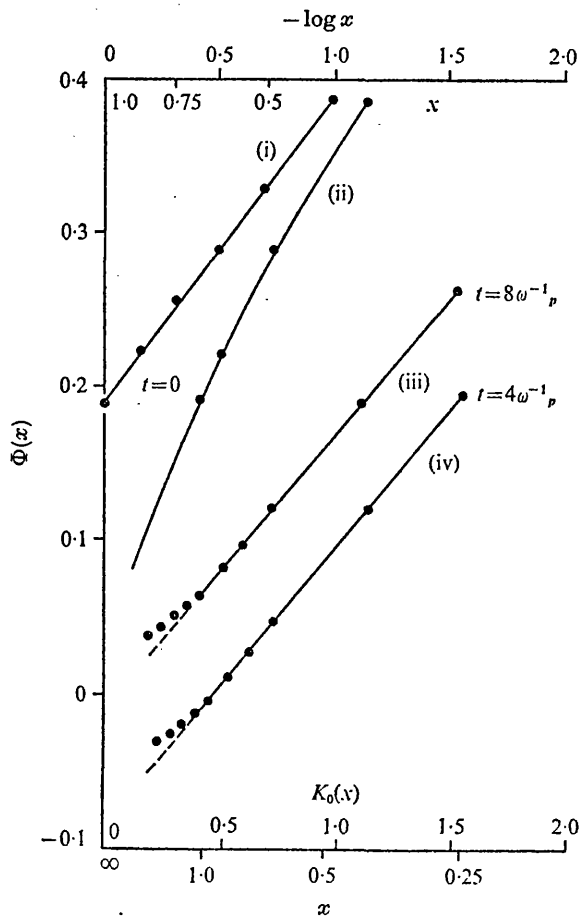

Comparison between theory and simulation, $\xi = 0$:
(i) $\Phi(x)/-\log x$; (ii), (iii), (iv) $\Phi(x)/K_0(x)$.

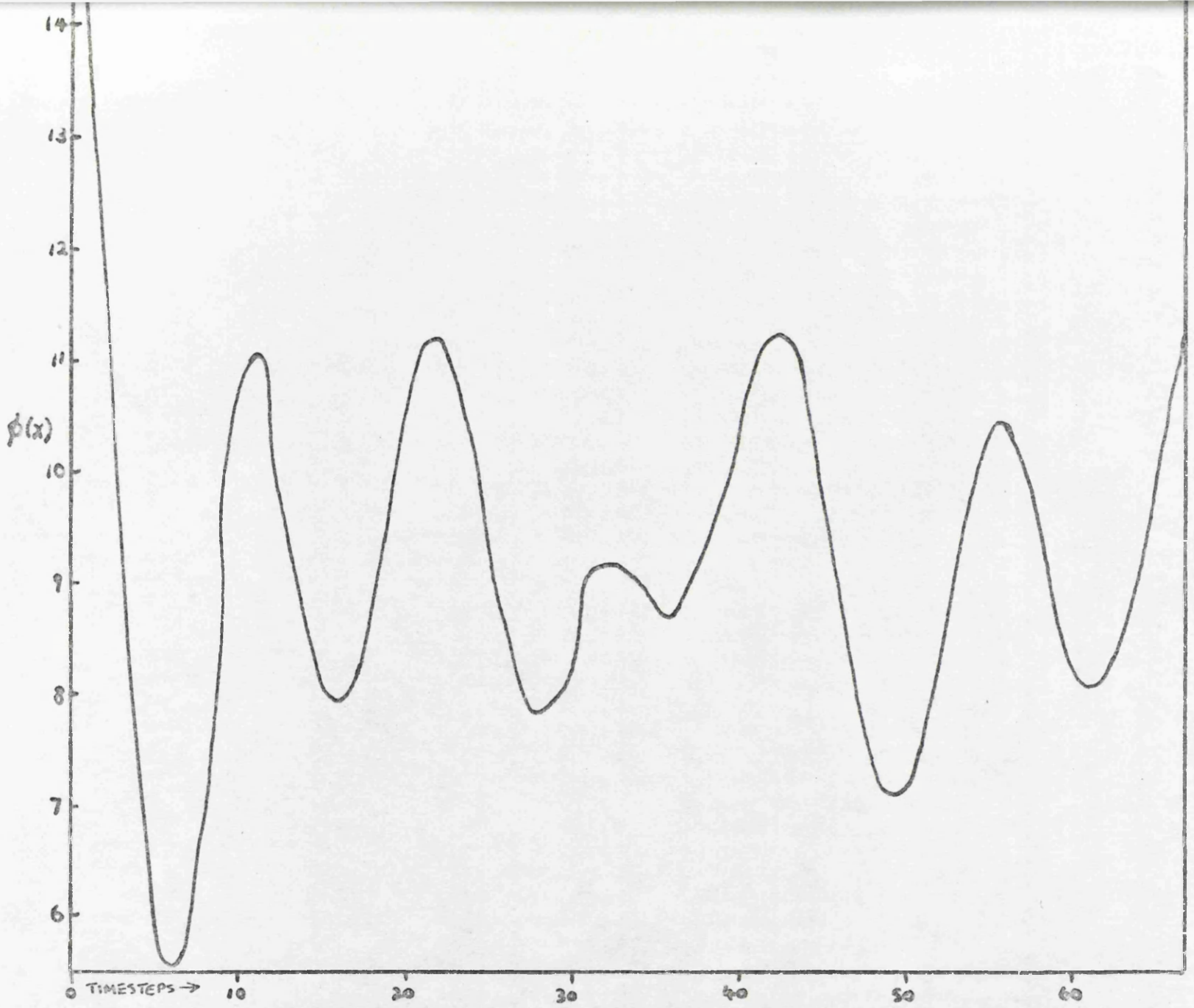

POTENTIAL AGAINST TIME AT POSITION OF TEST PARTICLE : TIMESTEP = 0·25ω_p^{-1}
$\phi(x)$ IN ARBITRARY UNITS: SUDDEN INTRODUCTION OF TEST CHARGE AT T = 0

FIG (9)

FIG(10.)

POTENTIAL $\phi(x)$ NEAR TEST PARTICLE PLOTTED AGAINST $K_0(x)$

TIME = $T = 2{\cdot}5/\omega_p$: X IN DEBYE LENGTH UNITS

$\phi(x)$ IN ARBITRARY UNITS : NON-'ADIABATIC' START

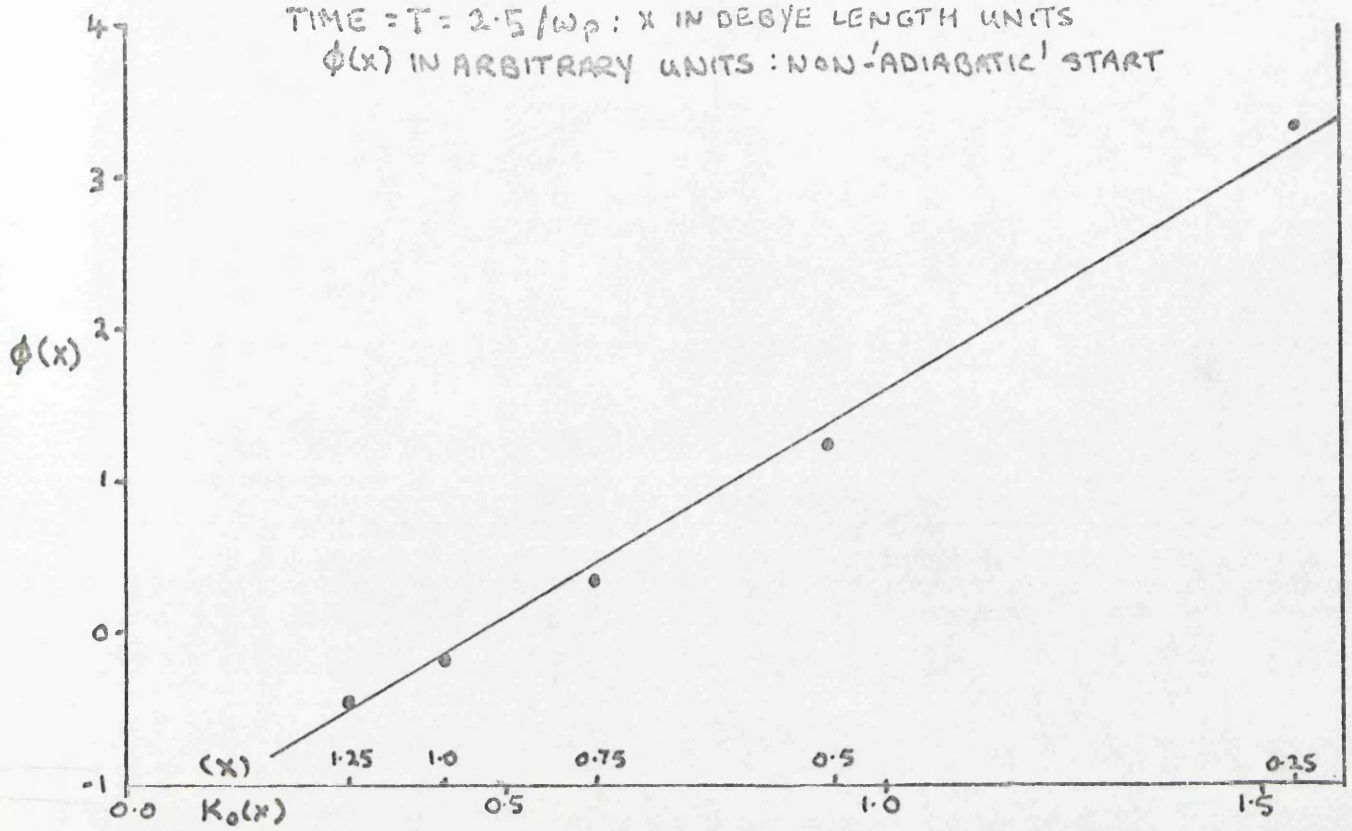

FIG(11.)

PLOT OF $K_0(x)$ AGAINST LOG(X):

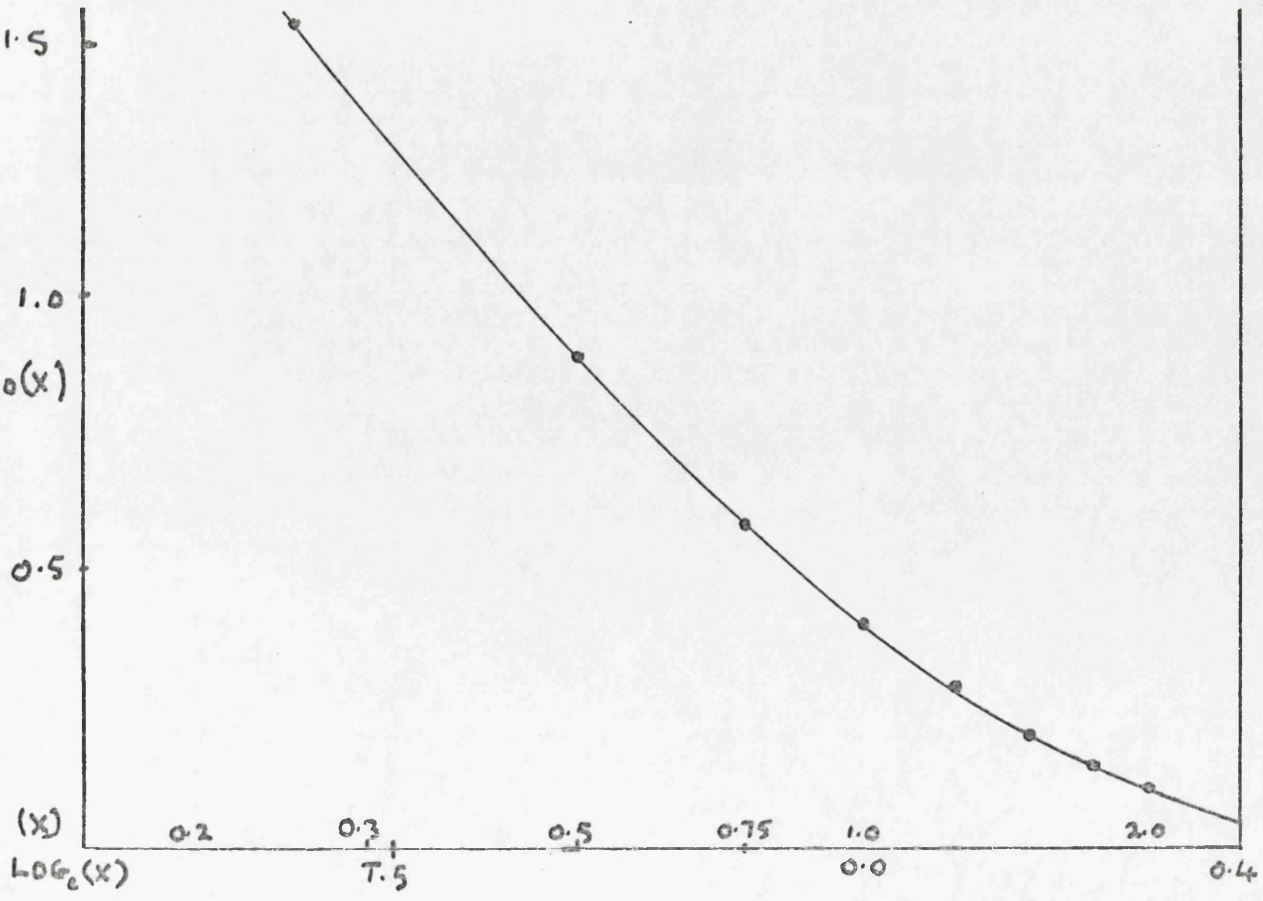

FIG(12)

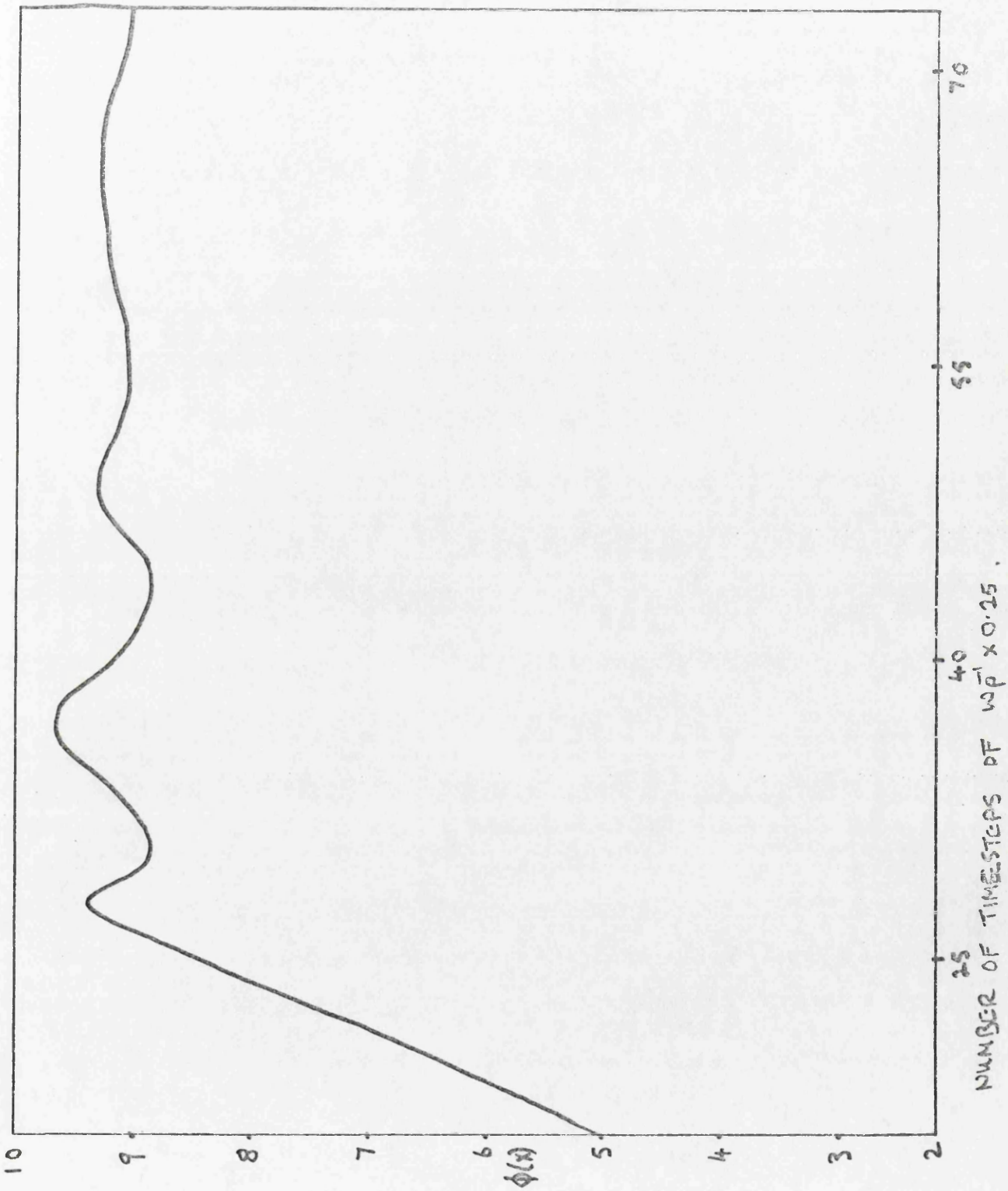

POTENTIAL $\phi(x)$ IN ARBITRARY UNITS AS A FUNCTION OF TIME, FOR ADIABATIC INTRODUCTION OF STATIONARY TEST CHARGE
SAME VERTICAL SCALE AS FOR FIG (9).

FIG(13) POTENTIAL $\phi(x)$ AGAINST $K_0(x)$, POINTS NEAR TEST CHARGE
'ADIABATIC' START
$\phi(x)$ IN ARBITRARY UNITS : x IN DEBYE LENGTHS
TIME $T \doteq 2\pi/\omega_p$

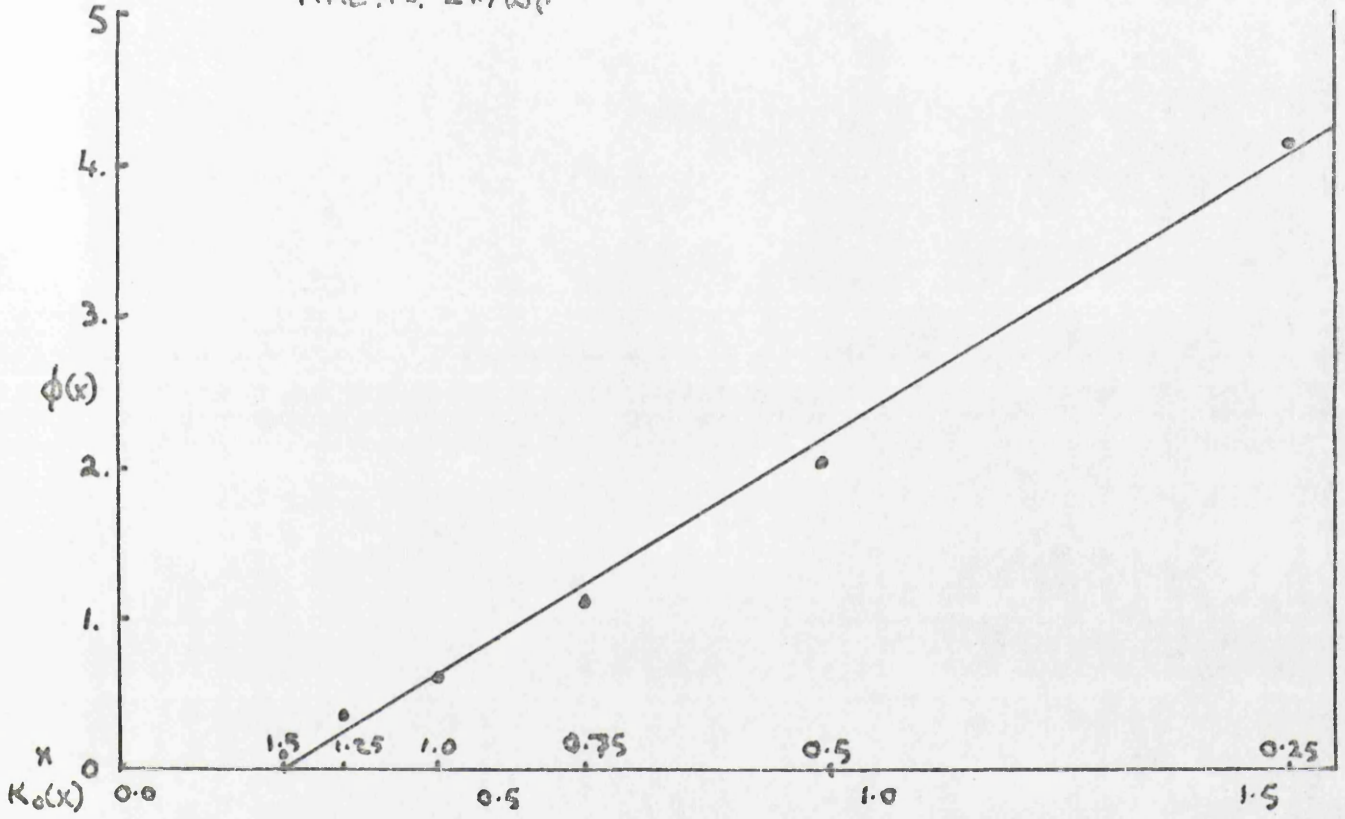

FIG(14) $\phi(x)$ v $\text{LOG}_e(x)$, SAME CASE AS ABOVE

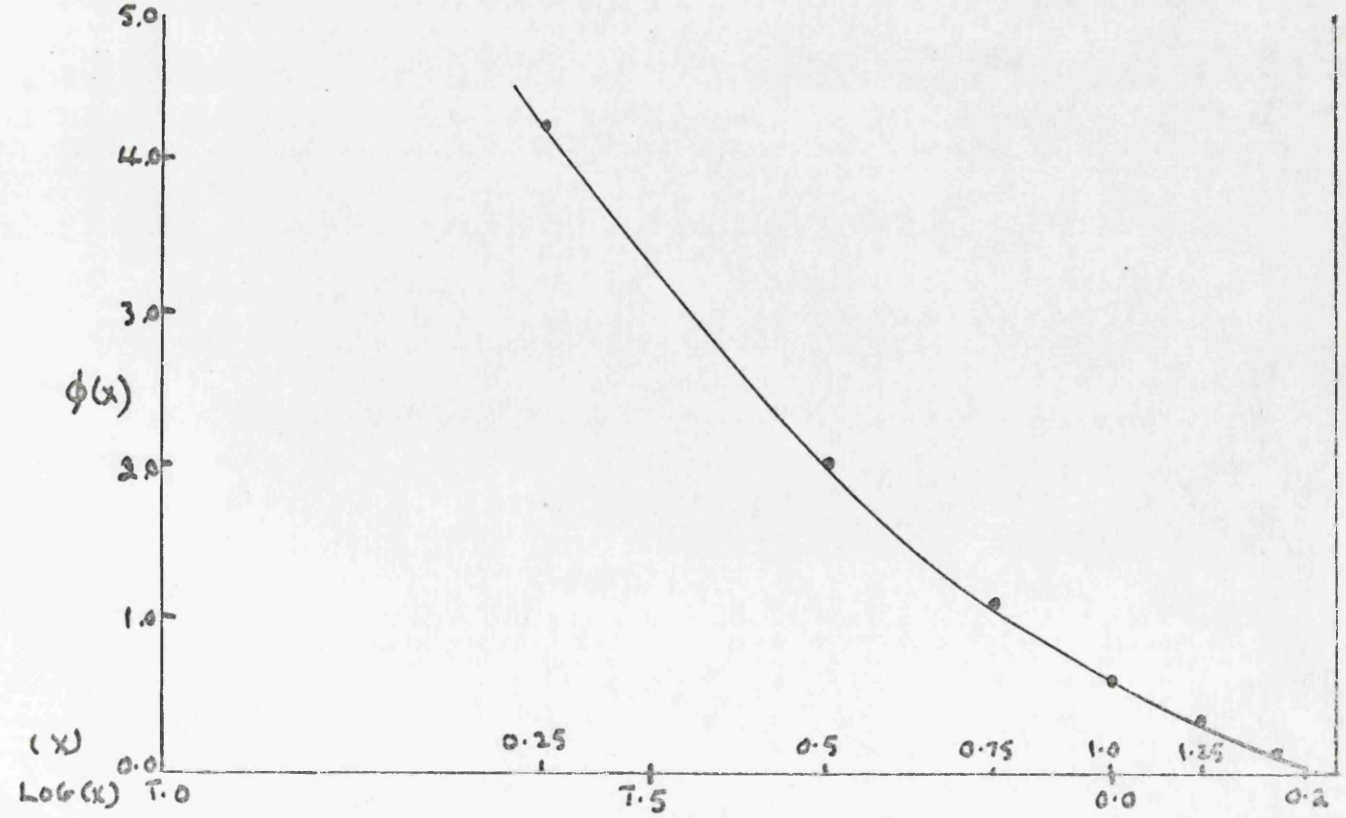

CROSS-SECTION OF POTENTIAL DISTRIBUTION FOR $V = \sqrt{2}\,V_{me}$ $(\tau = \sqrt{2})$: TEST PARTICLE AT 0 :

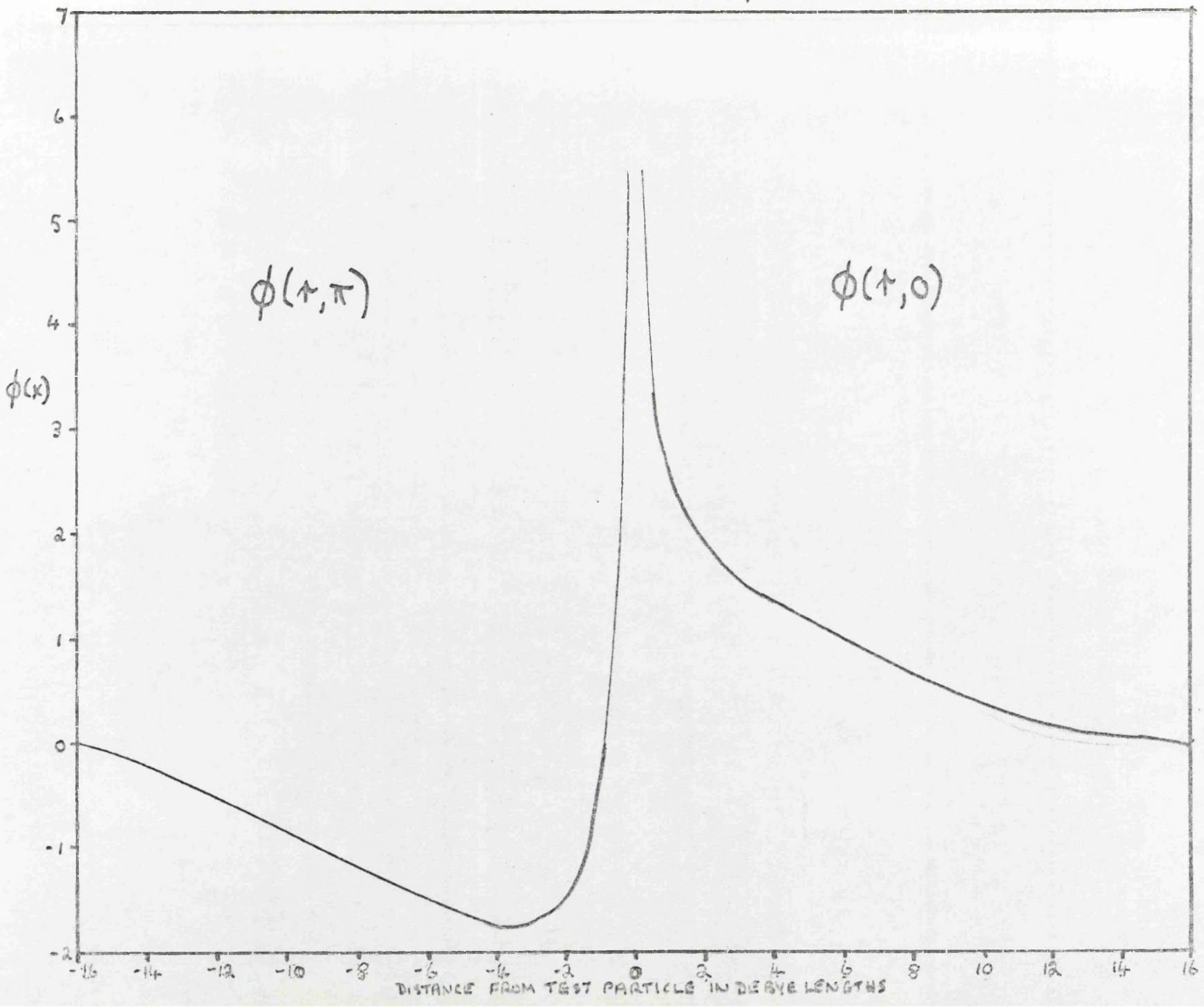

FIG (15)

CROSS SECTION OF POTENTIAL DISTRIBUTION AT $T = 10.1\ \omega_p^{-1}$: $\vec{V} = 2.5$: ϕ IN ARBITRARY UNITS

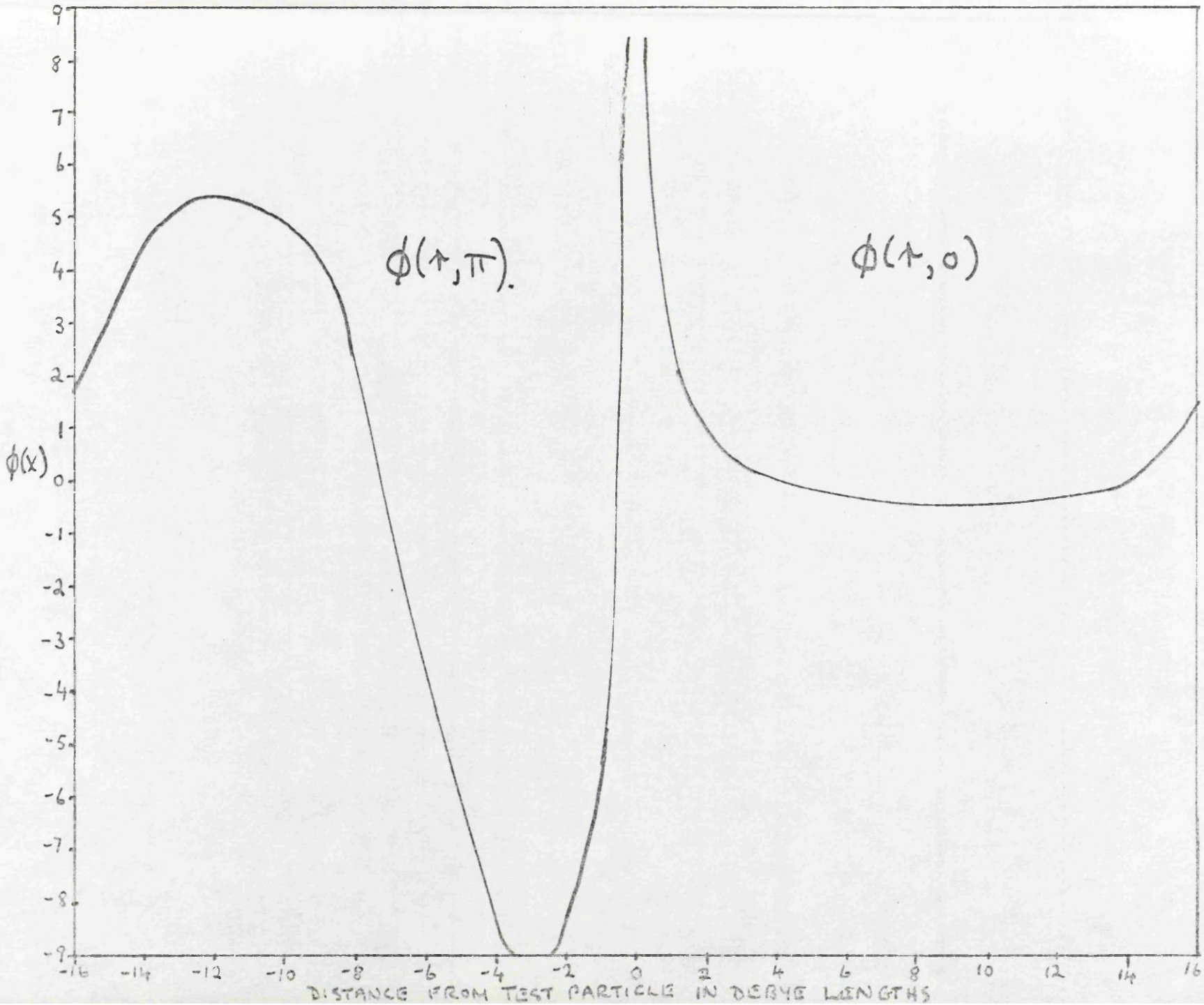

FIG (16)

FIG(17)

POTENTIAL DISTRIBUTION ALONG LINE OF MOTION OF TEST PARTICLE. TEST PARTICLE VELOCITY $V = 2.5 * V_{th}$. ($\frac{v}{c} \doteq 1.7$)

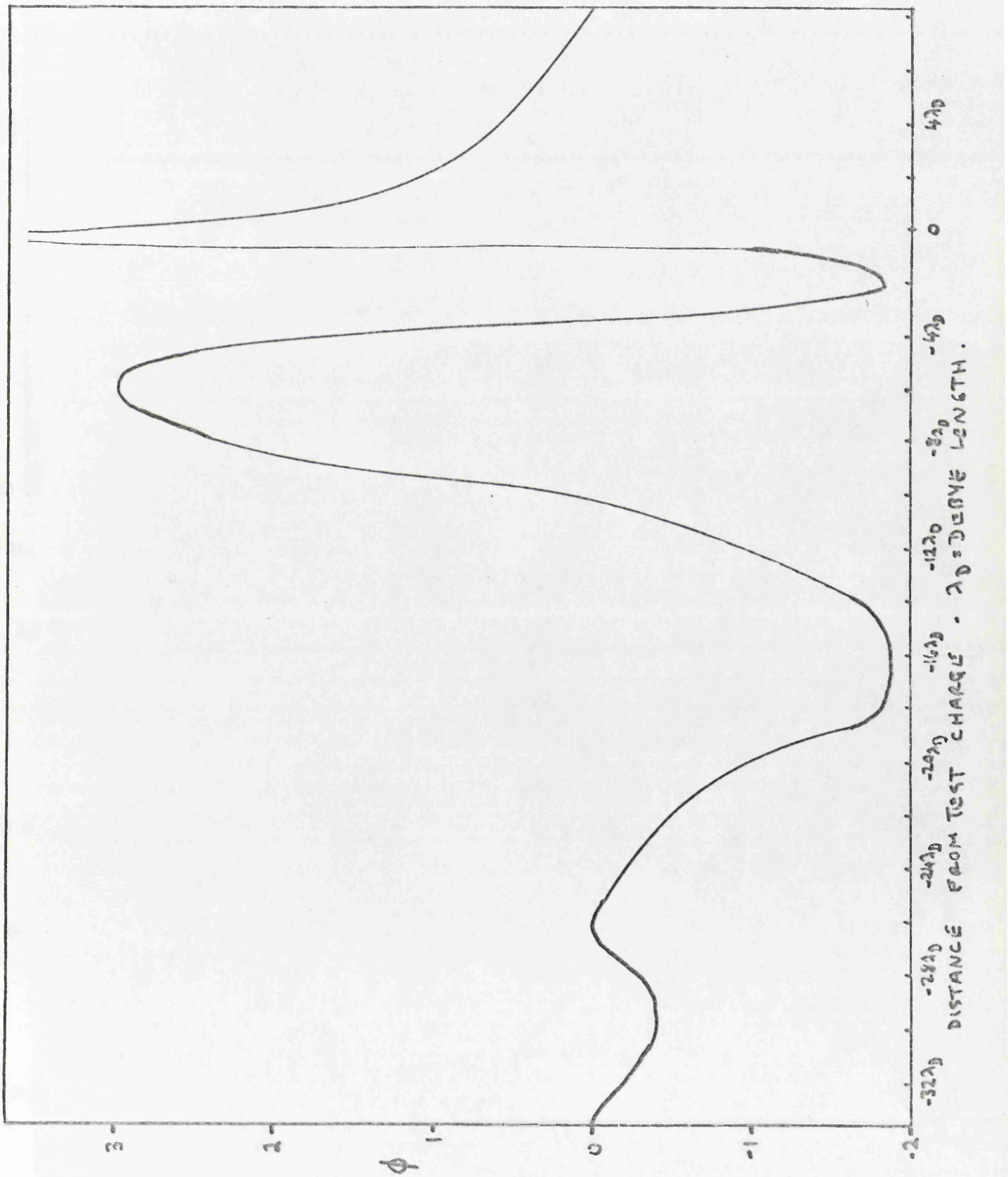

FIG(16) RETARDING FORCE F(V) AS A FUNCTION OF VELOCITY
F IN ARBITRARY UNITS

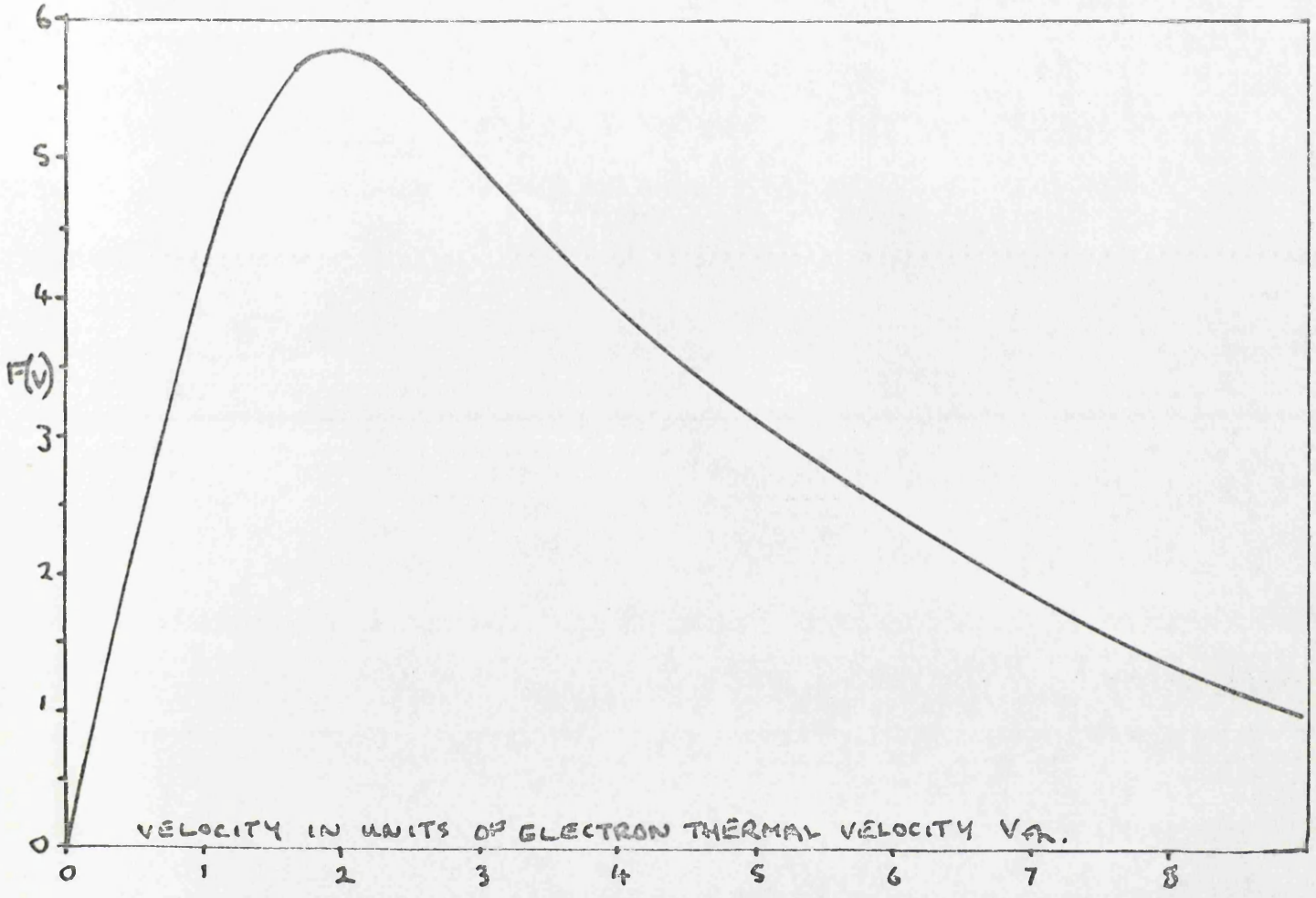

FIG(17) THEORETICAL VARIATION OF $\log_e(V)$ WITH TIME

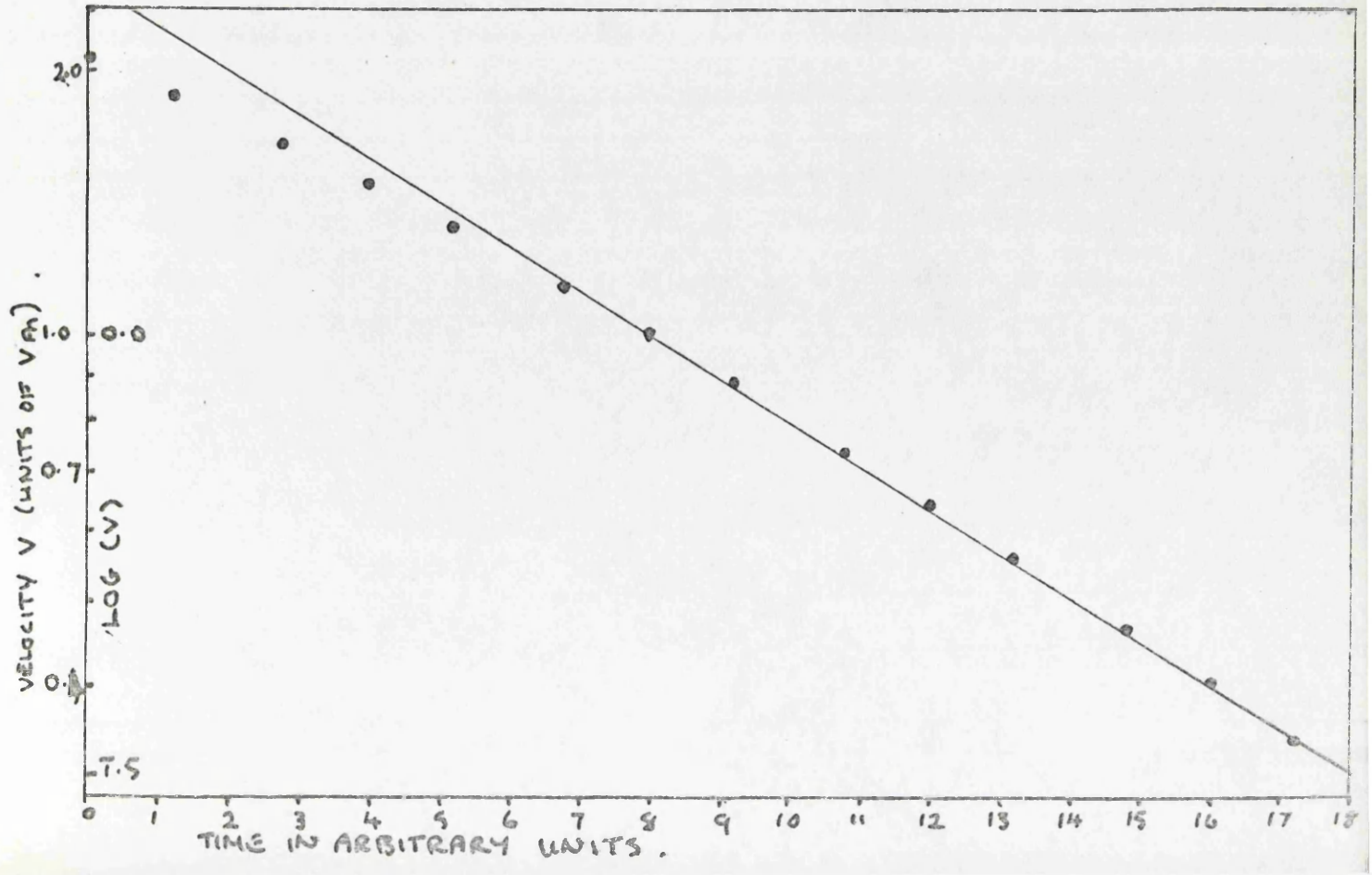

FIG(20) THEORETICAL CALCULATION: DISTANCE TRAVELLED BY TEST PARTICLE AS A FUNCTION OF TIME : $e^2/m = 0.05$

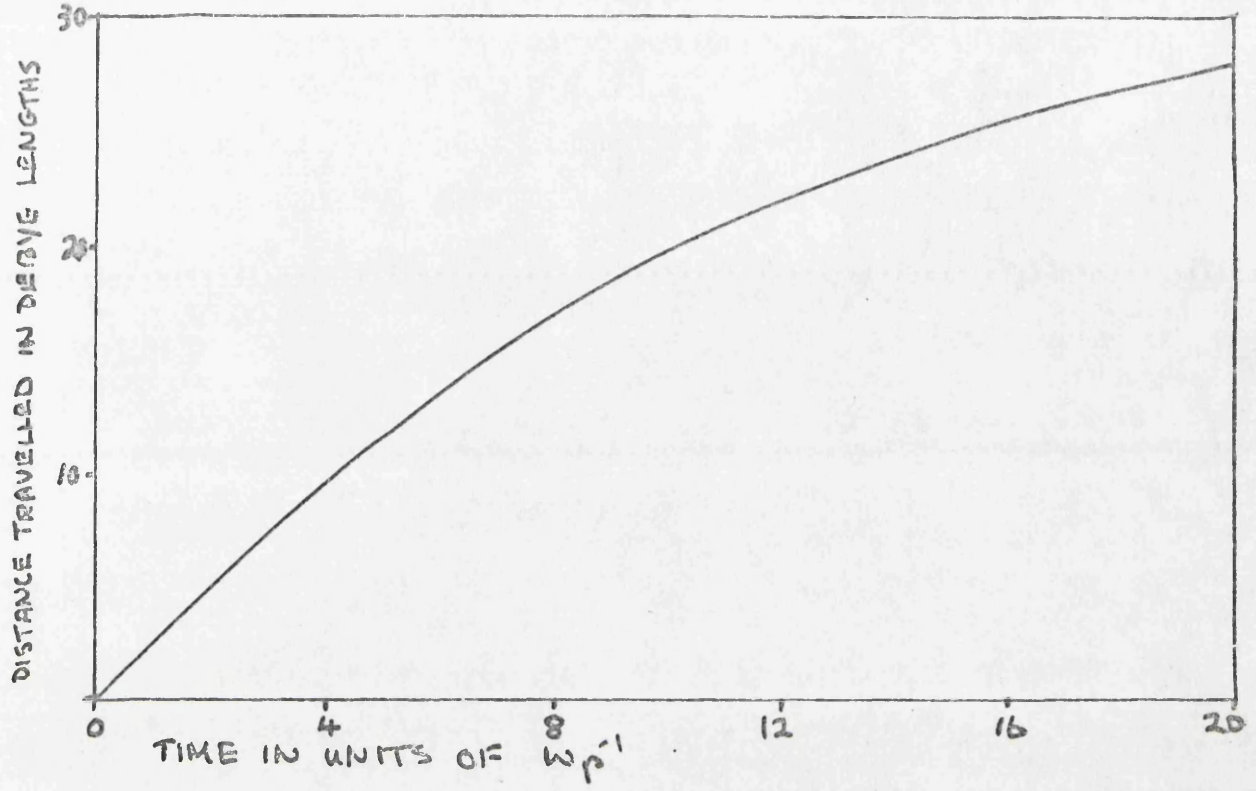

FIG(21) VELOCITY OF TEST PARTICLE AS A FUNCTION OF TIME

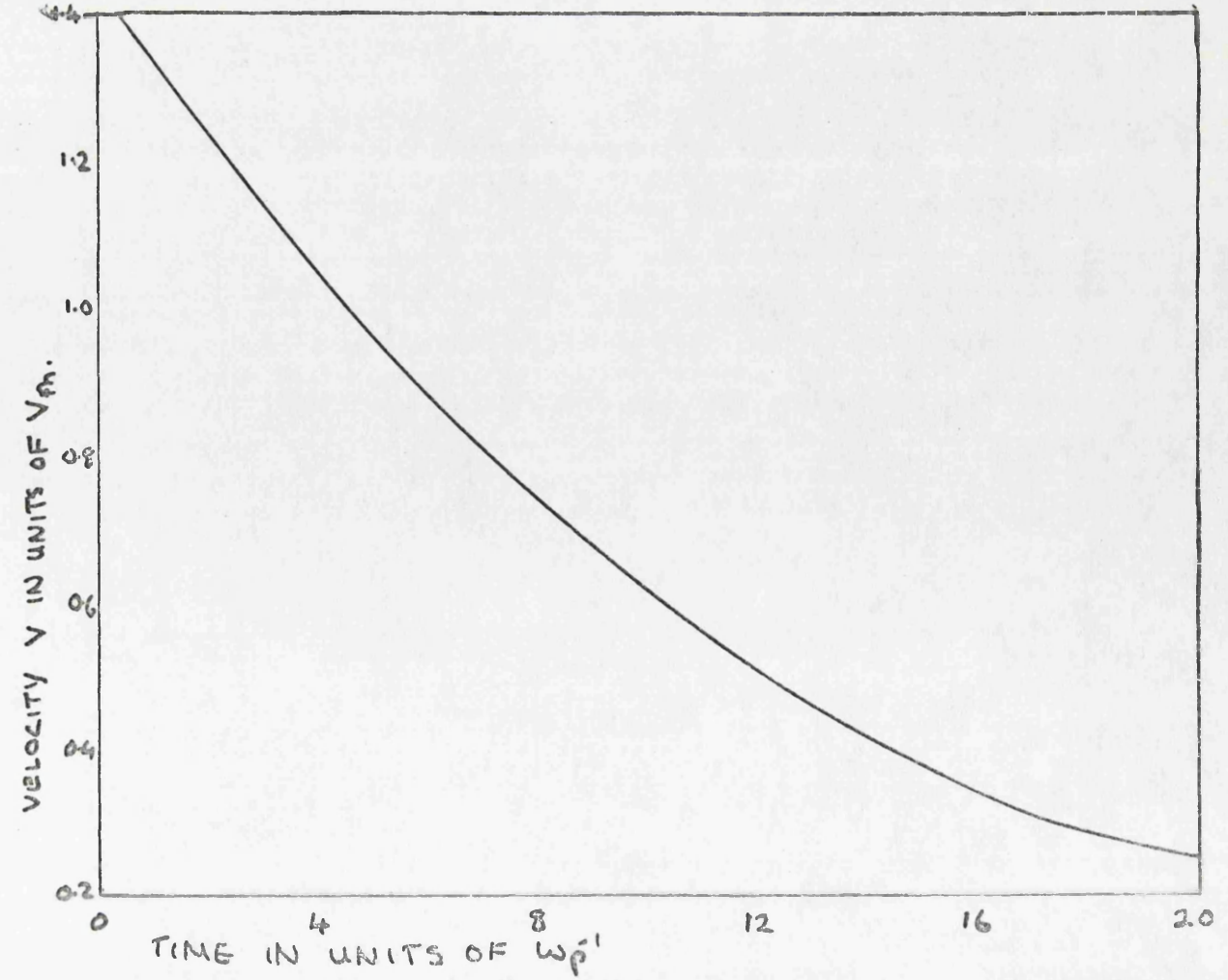

FIG(22). 'NOVA' SIMULATION - DISTANCE TRAVELLED BY TEST PARTICLE AS A FUNCTION OF TIME: $q^2/m = 0.05$

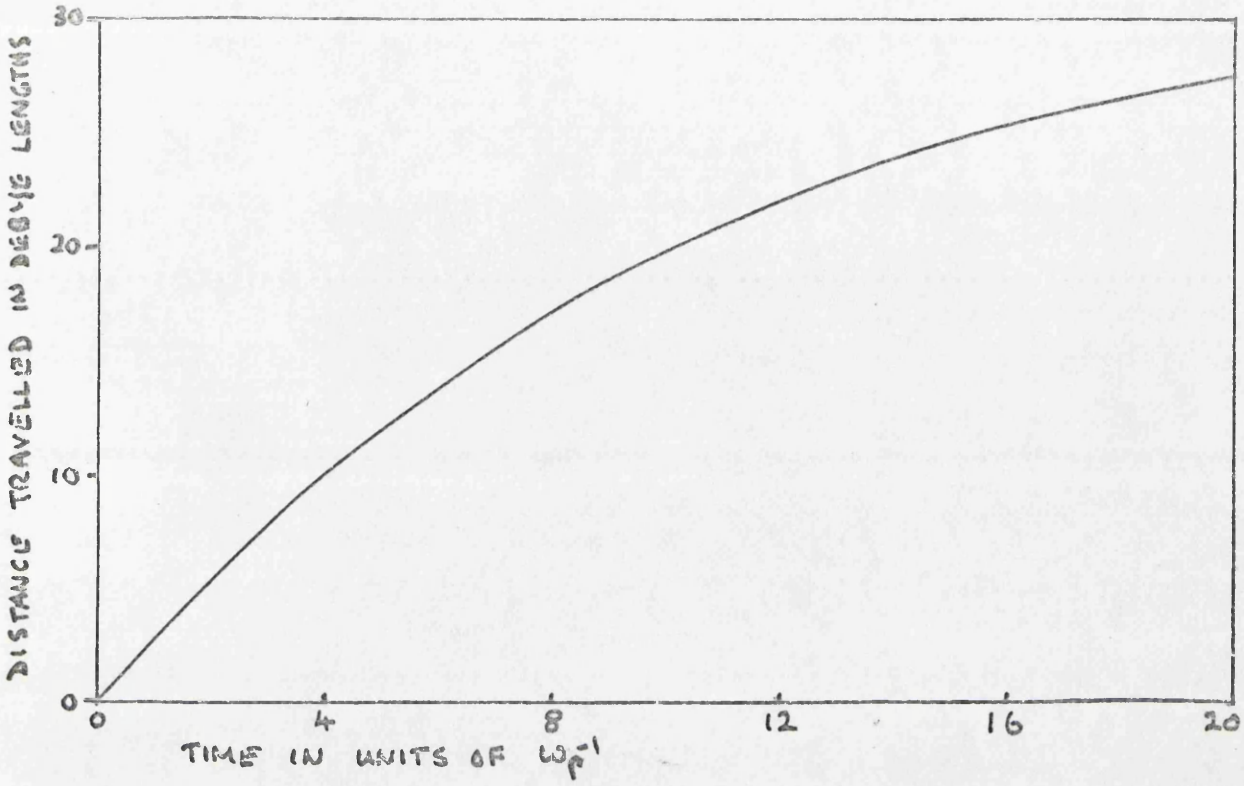

FIG(23) VELOCITY OF TEST PARTICLE AS A FUNCTION OF TIME

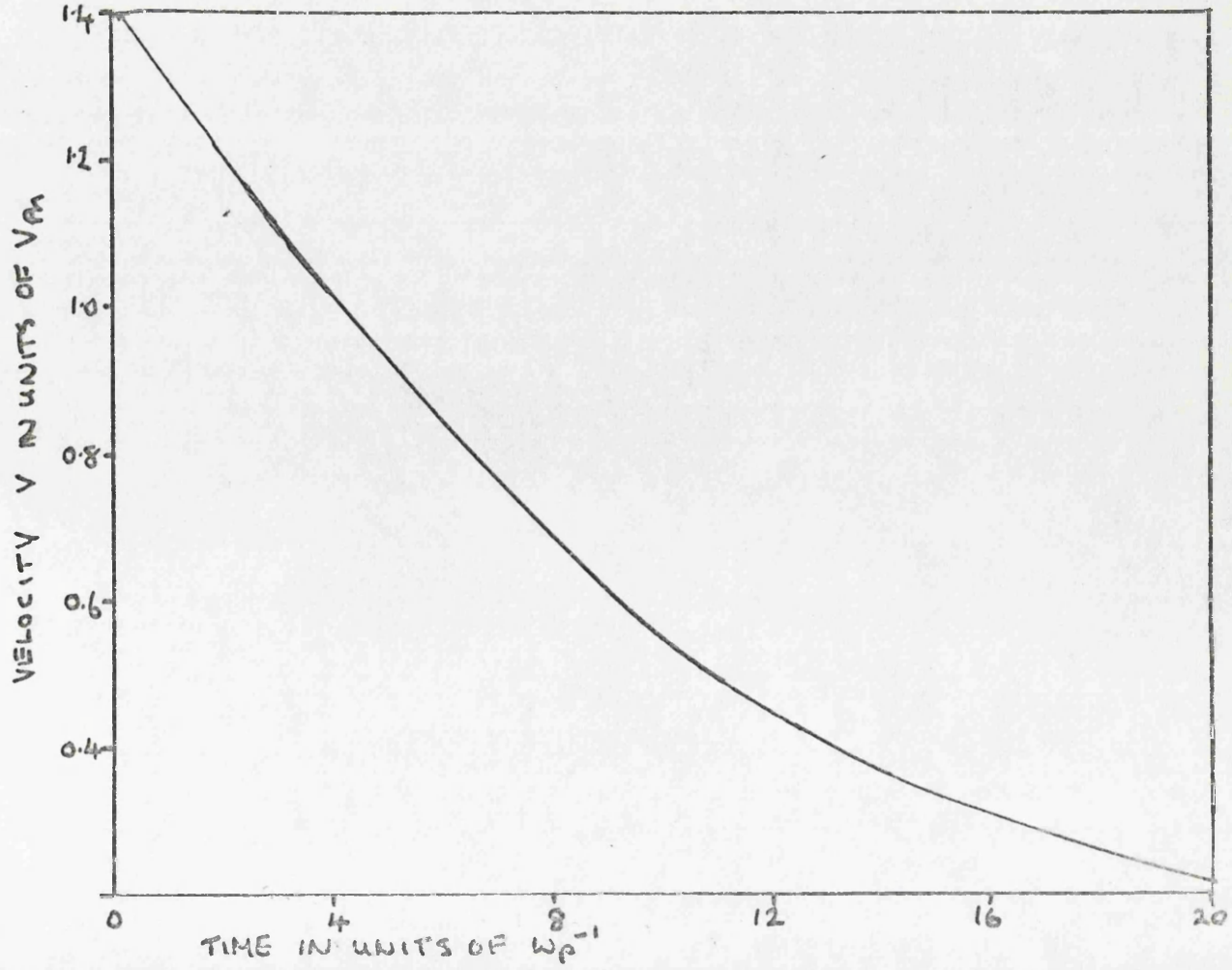

FIG(2.4)

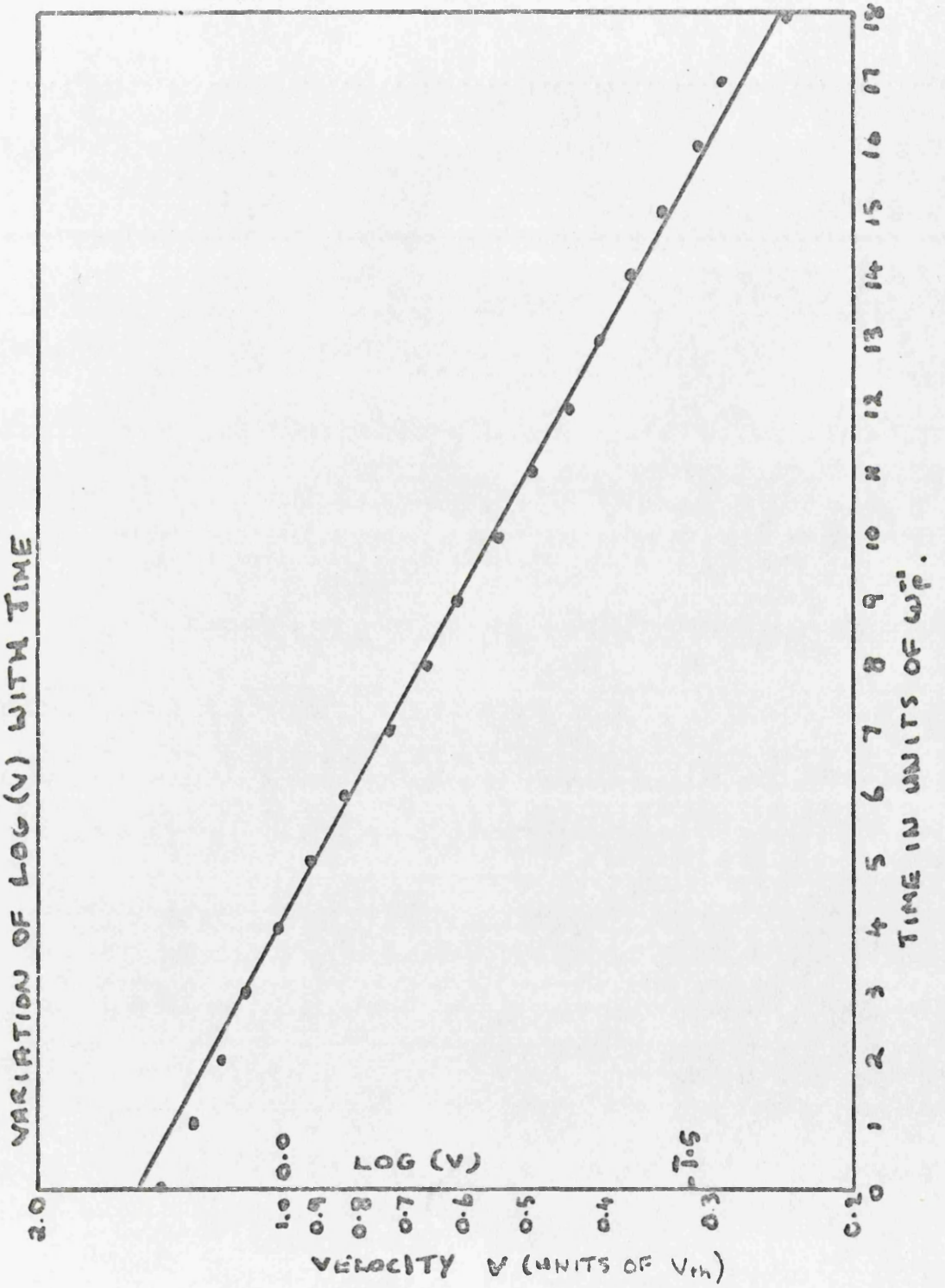
VARIATION OF LOG (V) WITH TIME
LOG (V)
VELOCITY V (UNITS OF Vth)
TIME IN UNITS OF ωp⁻¹.
2.0
1.0
0.9
0.8
0.7
0.6
0.5
0.4
0.3
0.2
0.0
-0.5
0
1
2
3
4
5
6
7
8
9
10
11
12
13
14
15
16
17
18

FIG(25)

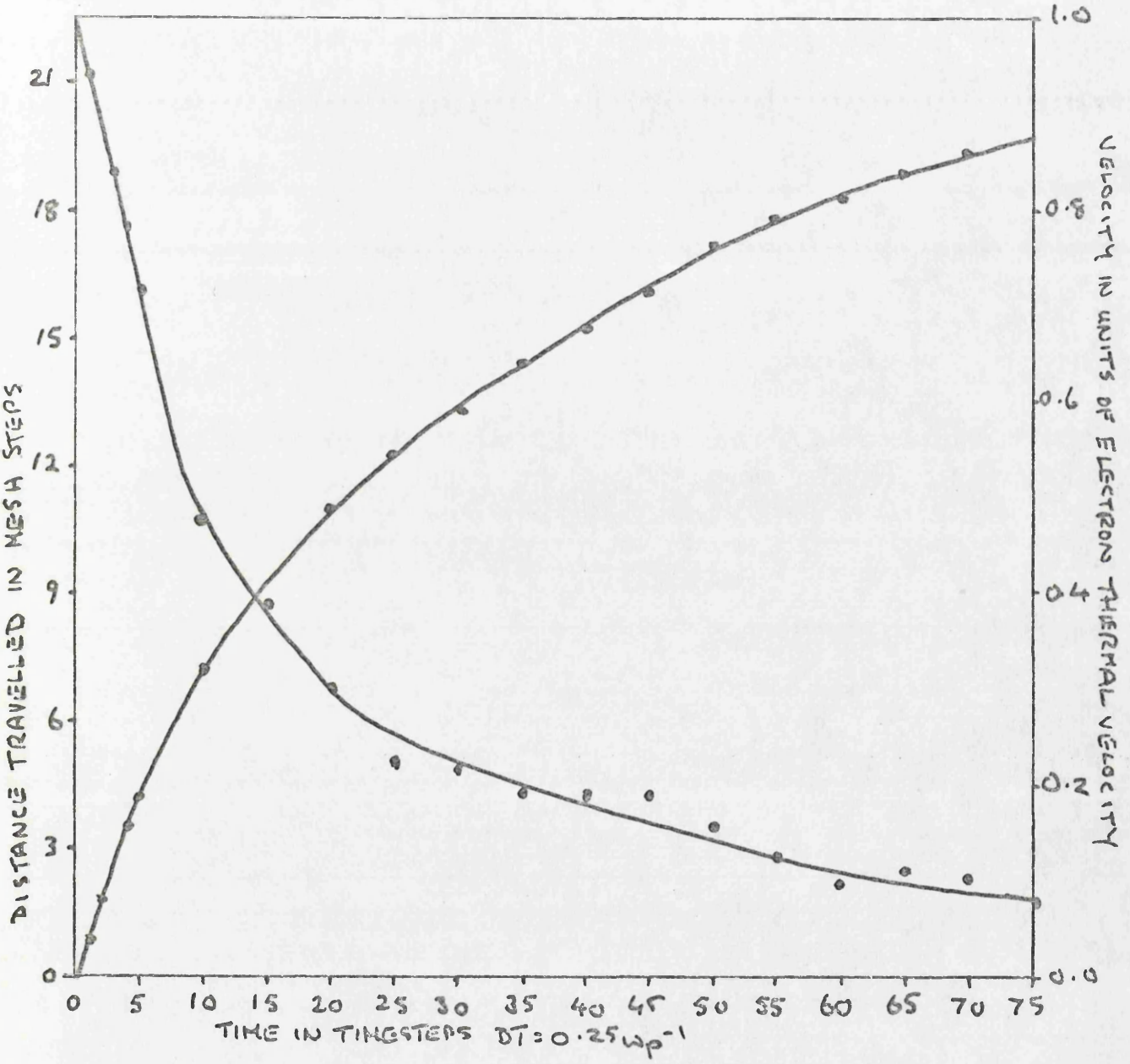

TEST PARTICLE SLOWING : PARTICLE MASS = 200 UNITS = m
CHARGE = 200 UNITS = q

$q^2/mm^* = 1/4$.

1 DEBYE LENGTH = 4 MESH STEPS.
(NOT ALL DATA POINTS ARE INCLUDED)

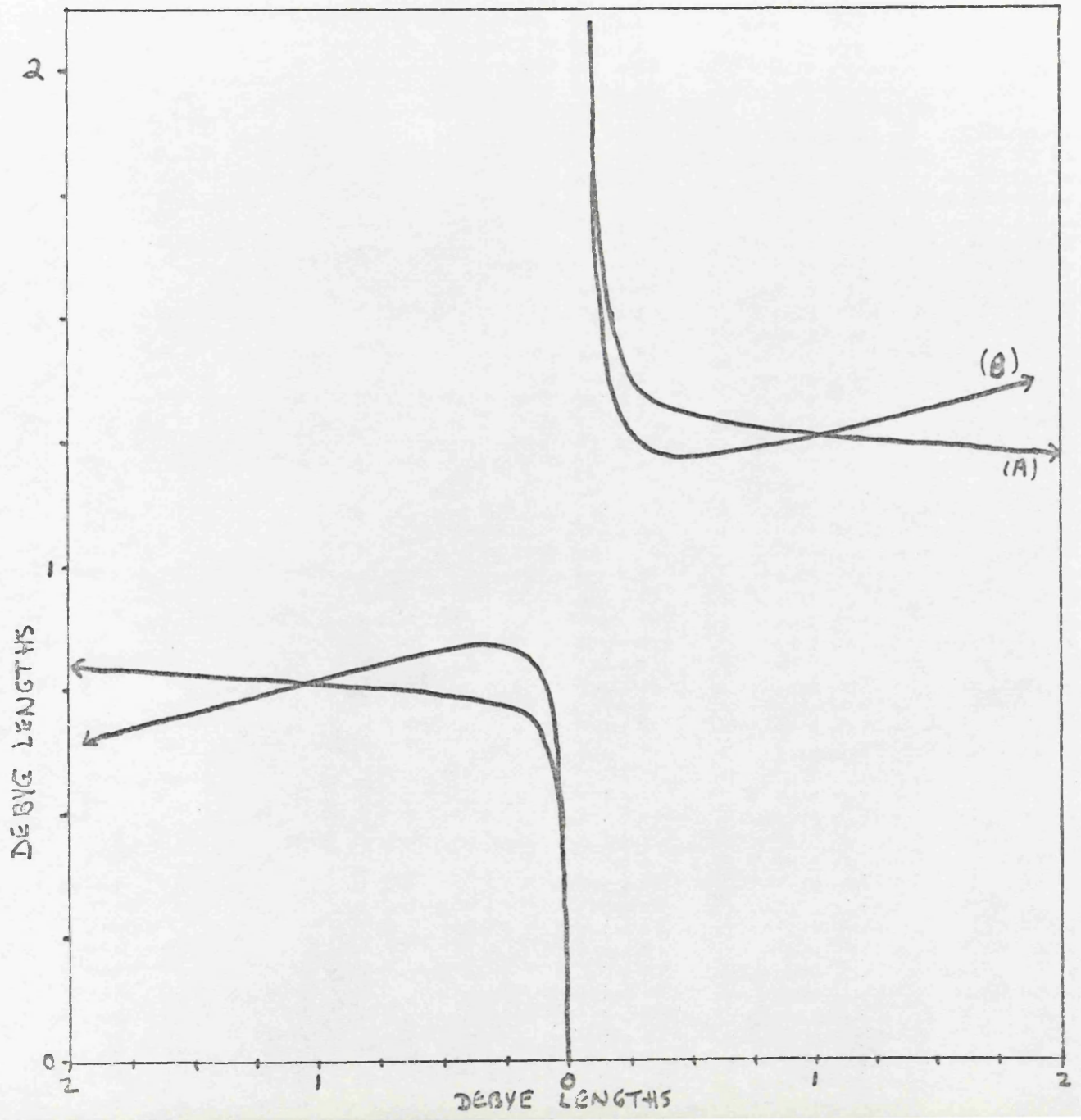

TRAJECTORIES OF 2 PARTICLES IN SYMMETRIC COLLISION

$Q^2/m \div 0.05$

INITIAL RANGE = $2\lambda_D$

INITIAL RELATIVE VELOCITY : $-0.5 v_A$

(A) SIMULATION

(B) THEORY

FIG (25)

FIG(27) PLOT OF $\epsilon(k, i\omega)$ AS A FUNCTION OF ω FOR CONSTANT k

$K = 1, K_D = 1, K_c = 1$

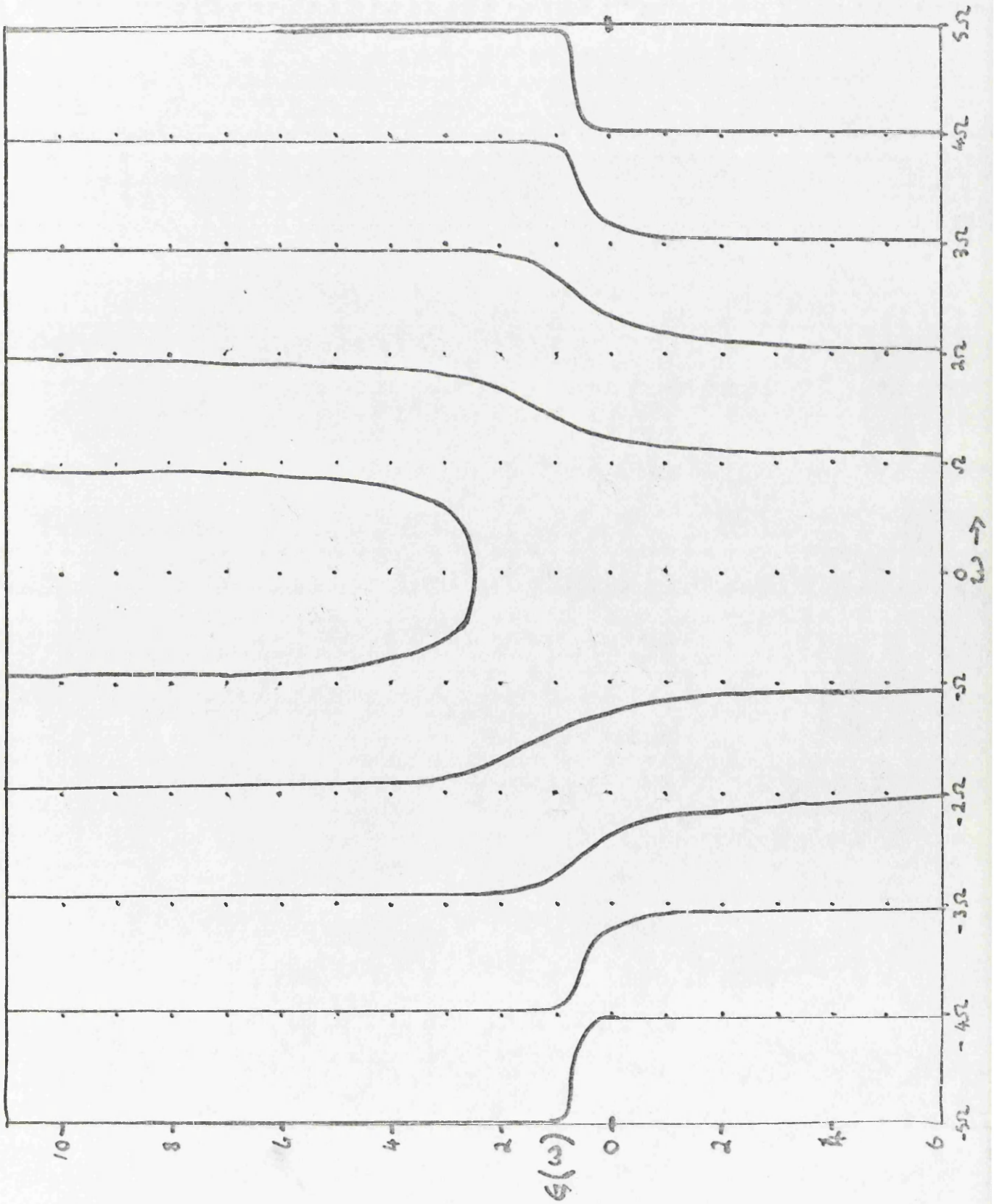

FIG (8?) VARIATION OF SIMULATION PLASMA POTENTIAL ENERGY WITH TIME
TEST PARTICLE IS AT MAXIMUM CHARGE AFTER 26 STEPS
TEST PARTICLE VELOCITY = 0.0
MAGNETISED AND NONMAGNETISED CASES

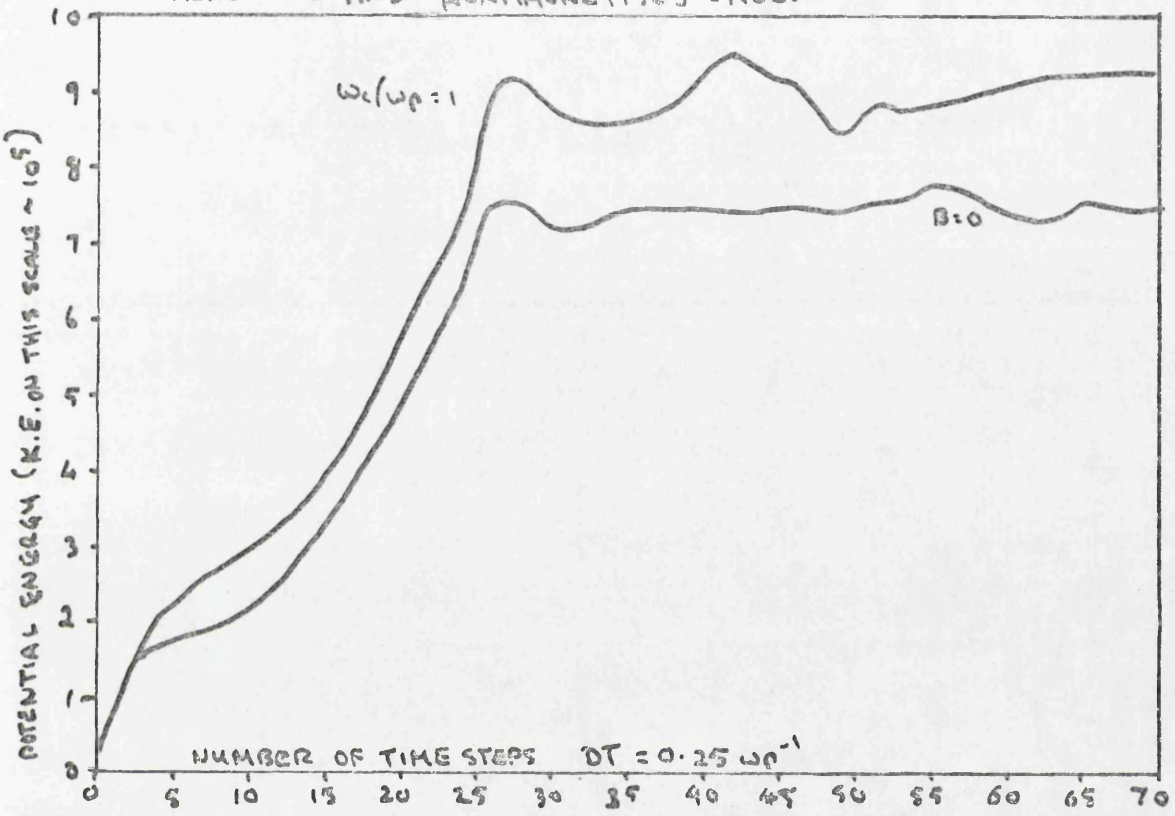

FIG(9?) POTENTIAL AT TEST PARTICLE POSITION, AS A FUNCTION OF TIME
TEST PARTICLE VELOCITY = 0.0

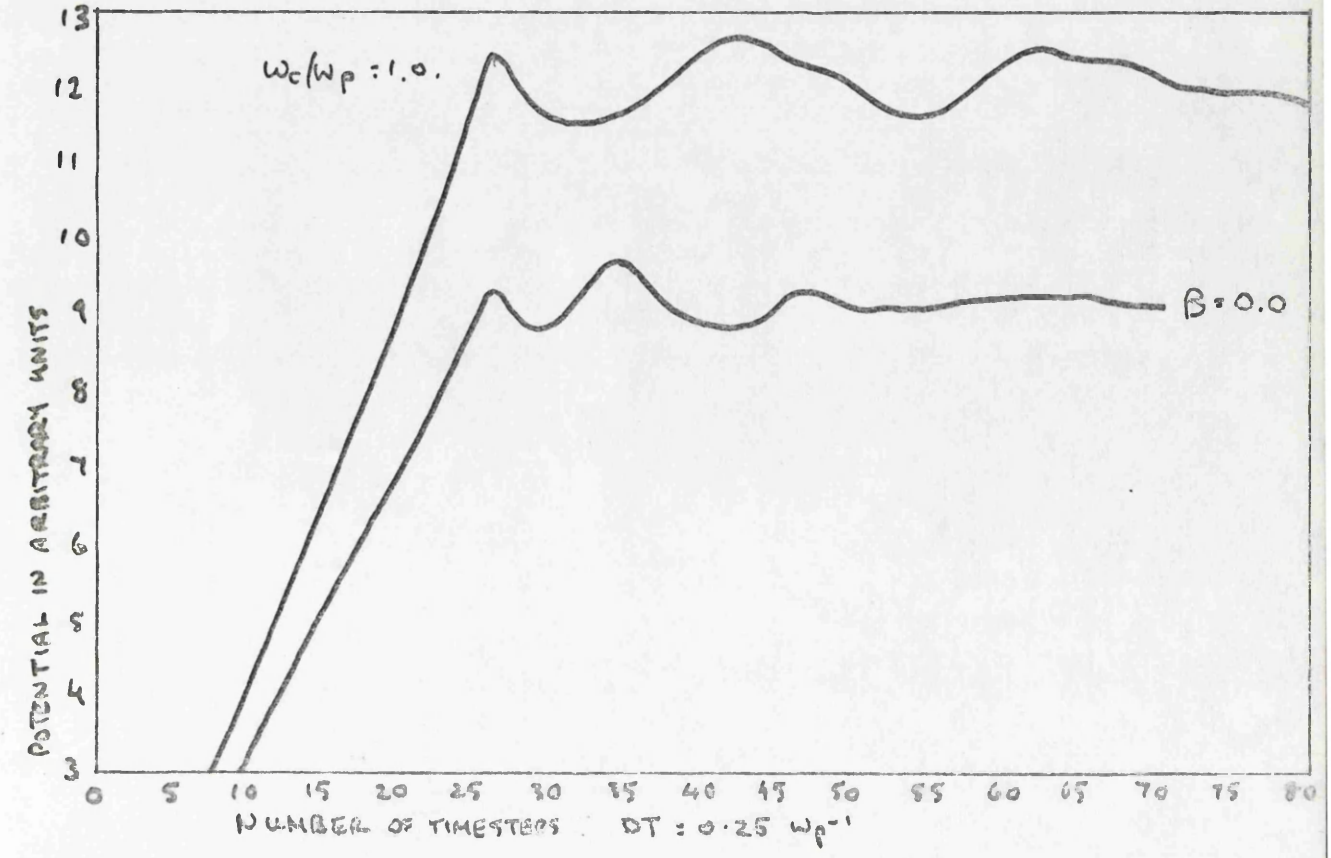

FIG(30)

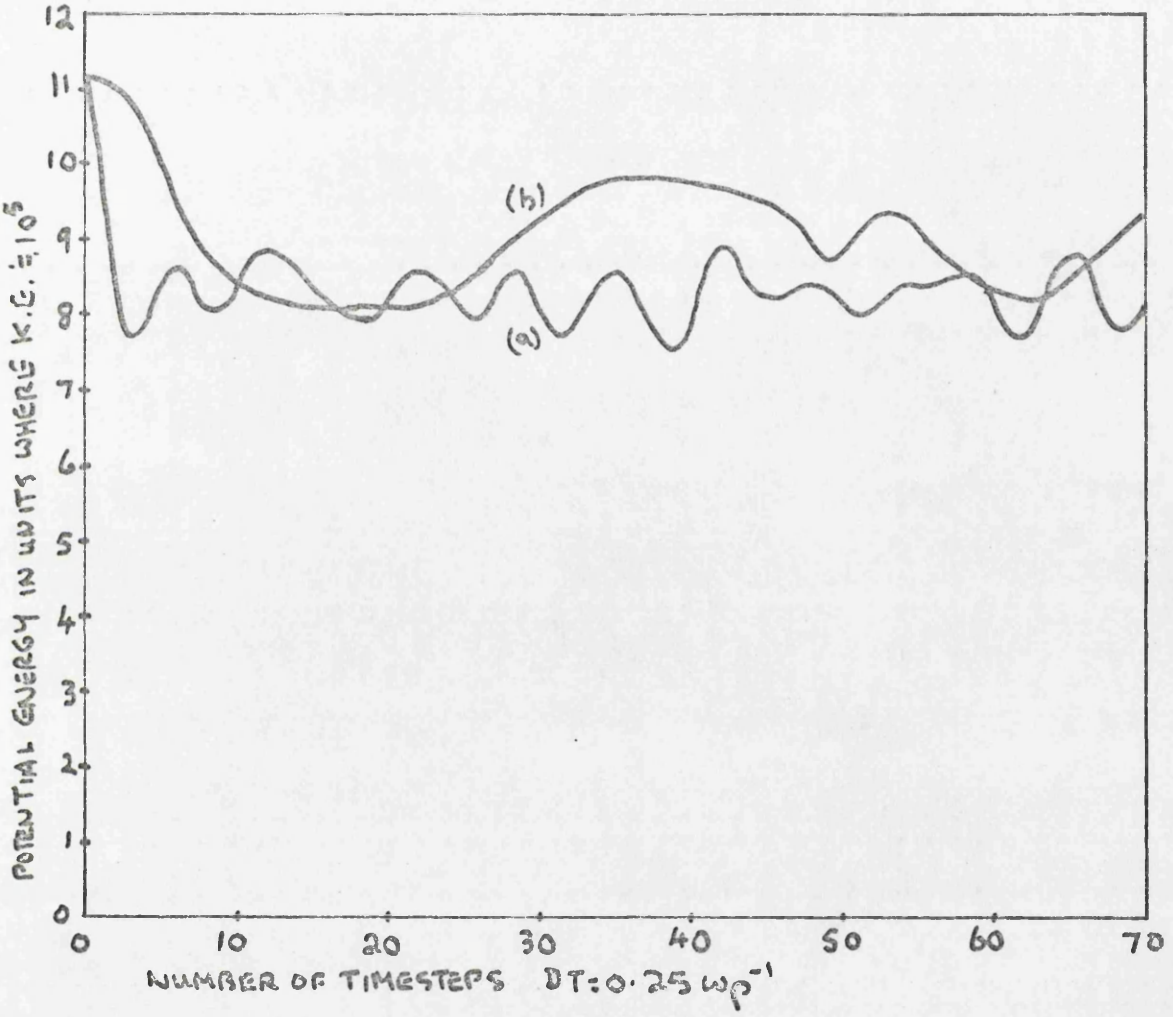

NON-'ADIABATIC' INTRODUCTION OF TEST PARTICLE IN SIMULATION

COMPARISON OF VARIATIONS OF POTENTIAL ENERGY WITH TIME FOR

(a) NON-MAGNETISED PLASMA

(b) MAGNETISED PLASMA, $\omega_c/\omega_p = 1.0$.

FIG(8) STATIONARY TEST PARTICLE : MAGNETIC FIELD PRESENT
$\omega_c/\omega_p = 2.0$
PLOT OF POTENTIAL AGAINST LOG(X) FOR POINTS
X NEAR THE TEST PARTICLE
TIME $T = 8\omega_p^{-1}$

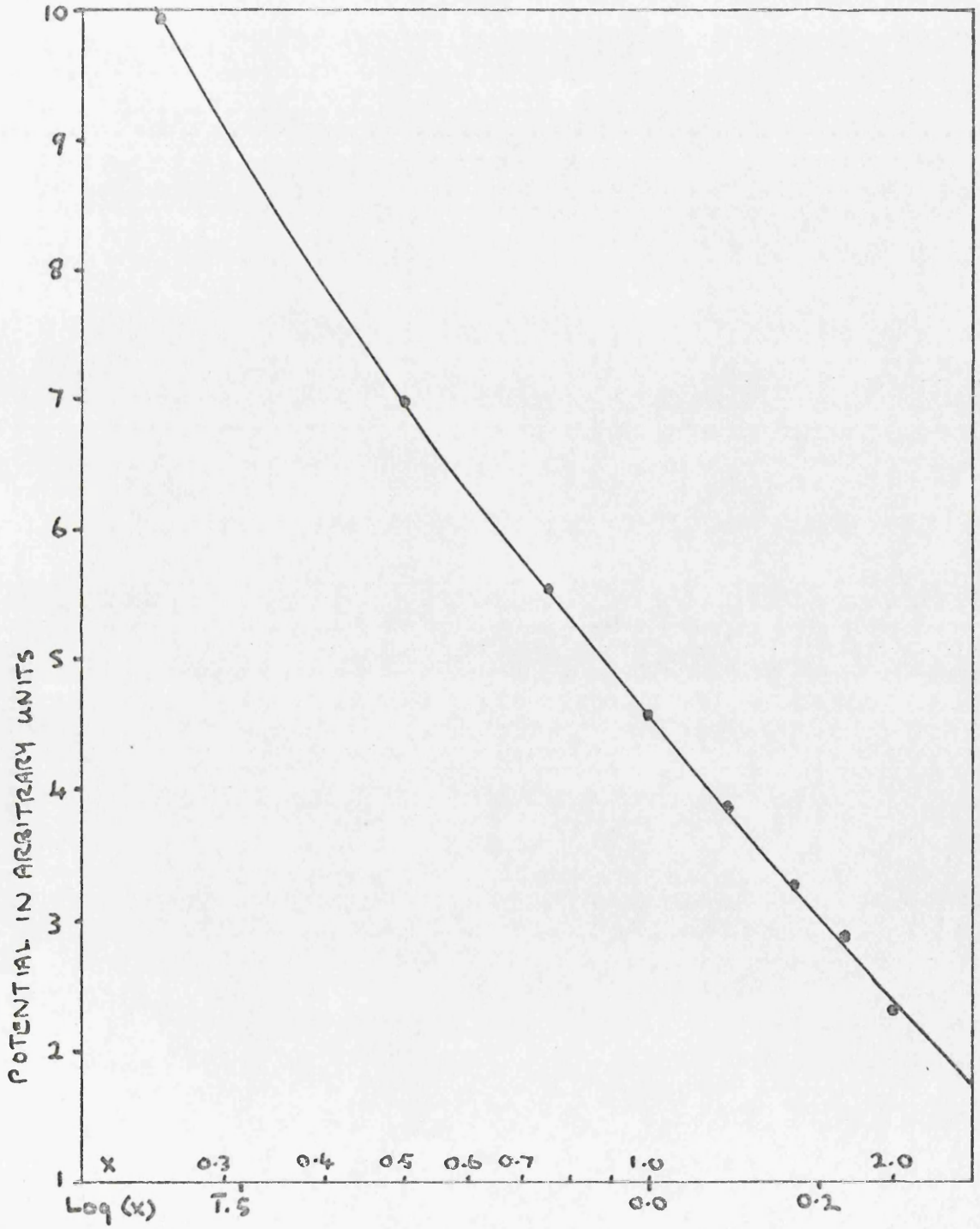

FIG(32)

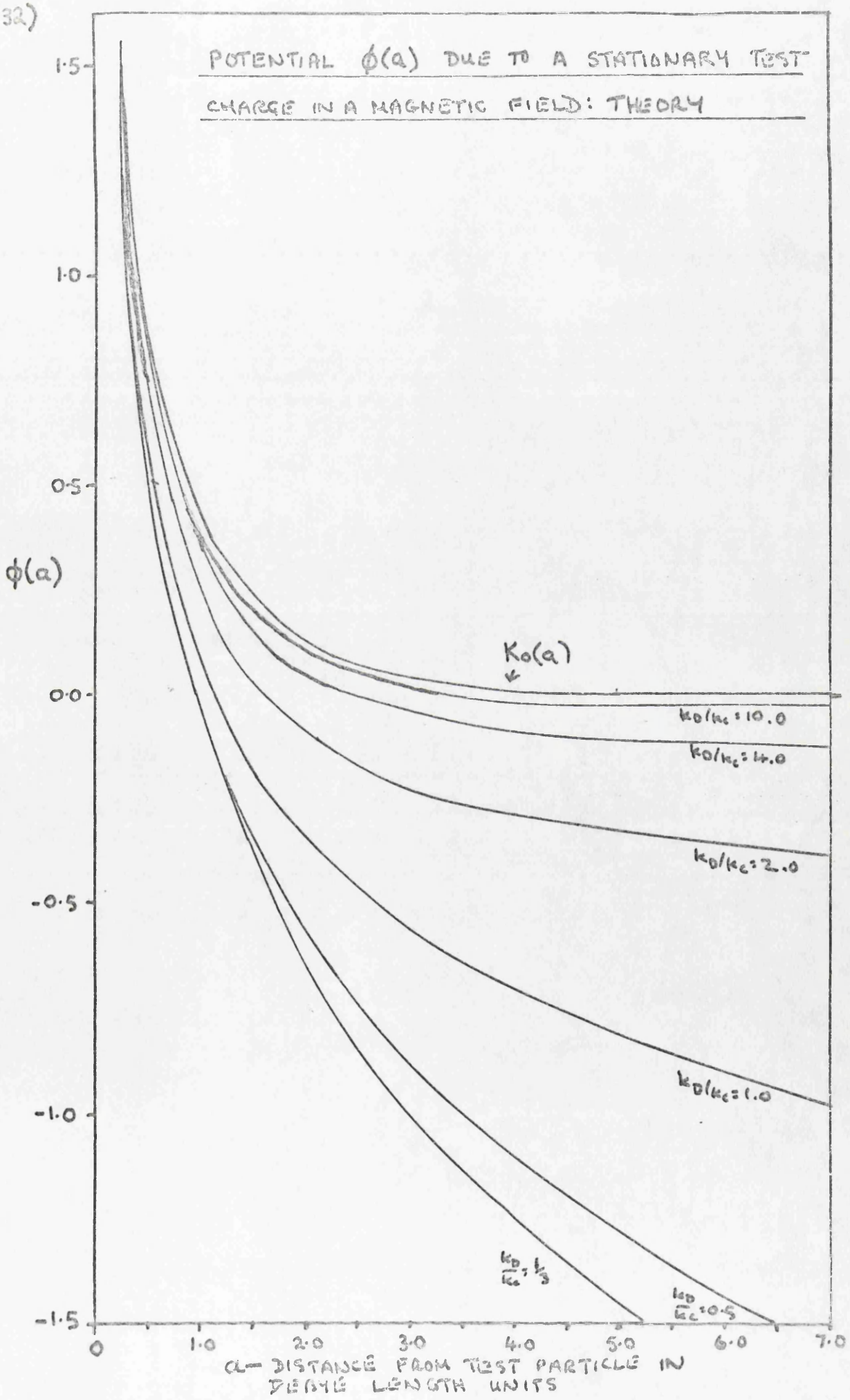
POTENTIAL $\phi(a)$ DUE TO A STATIONARY TEST CHARGE IN A MAGNETIC FIELD: THEORY
1·5
1·0
0·5
0·0
-0·5
-1·0
-1·5
$\phi(a)$
$K_0(a)$
$K_D/K_c = 10.0$
$K_D/K_c = 4.0$
$K_D/K_c = 2.0$
$K_D/K_c = 1.0$
$\frac{K_D}{K_c} = \frac{1}{3}$
$\frac{K_D}{K_c} = 0.5$
0
1·0
2·0
3·0
4·0
5·0
6·0
7·0
a— DISTANCE FROM TEST PARTICLE IN DEBYE LENGTH UNITS

FIG(33) STATIONARY TEST PARTICLE IN MAGNETIC FIELD COMPARISON BETWEEN SIMULATION AND THEORY FOR POINTS WITHIN 2 DEBYE LENGTHS OF PARTICLE

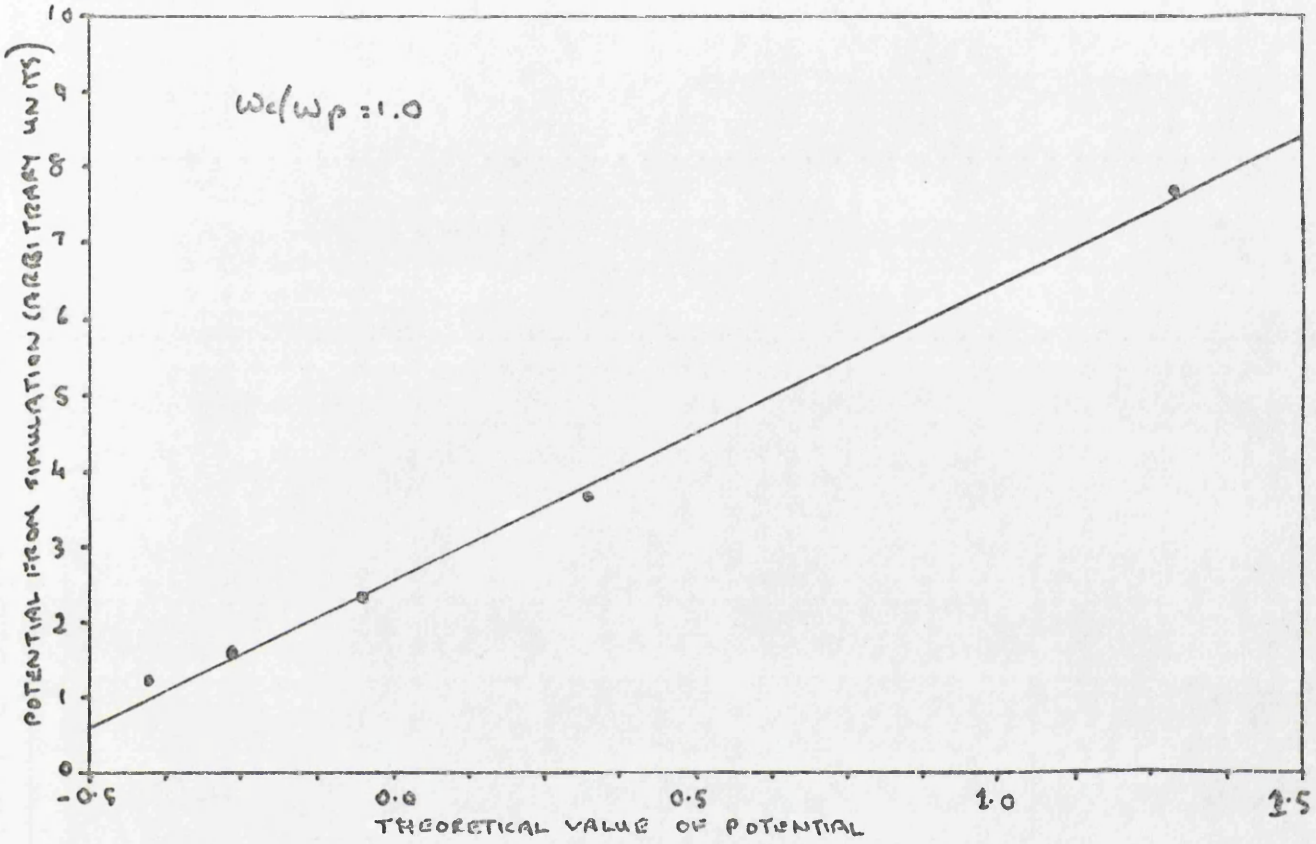

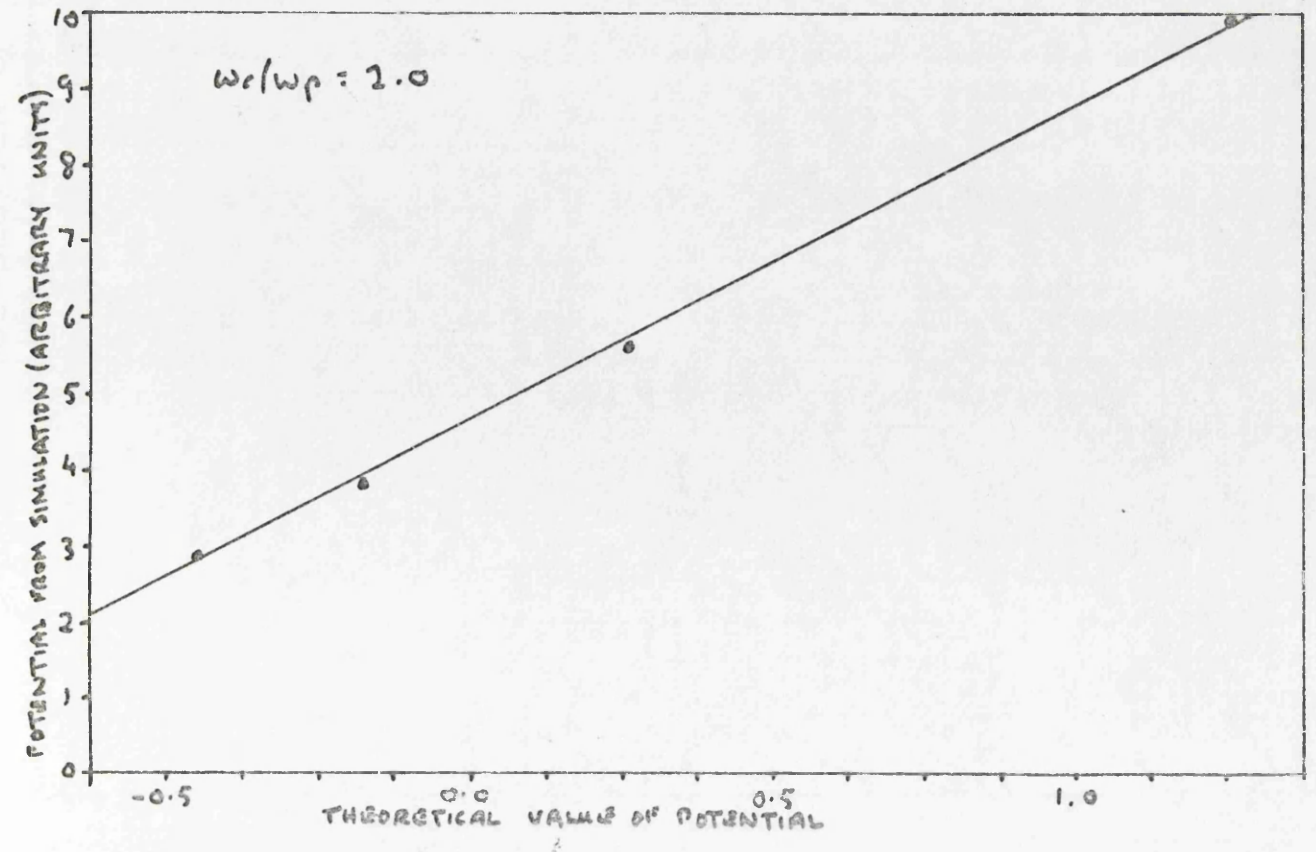

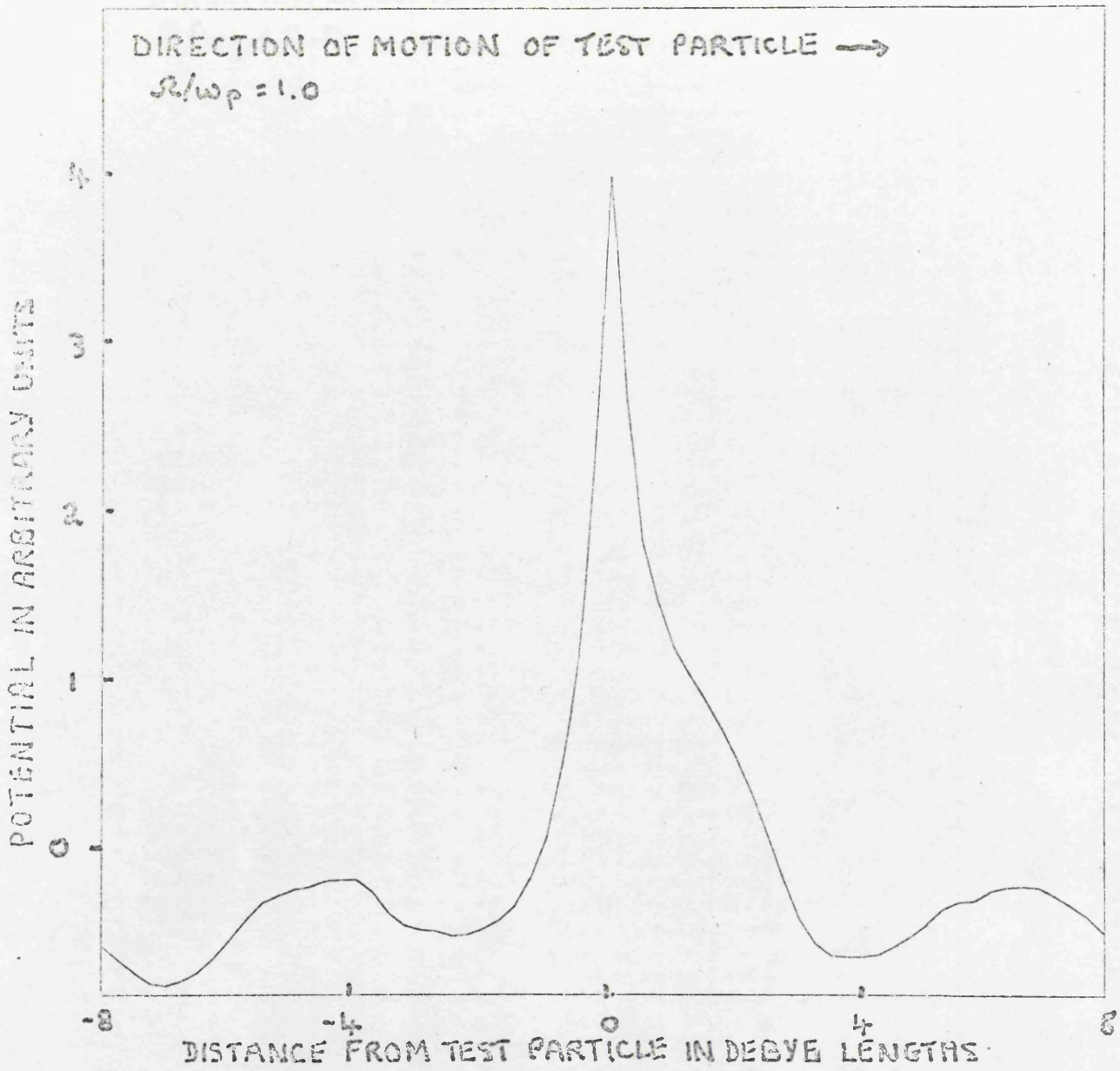
CROSS-SECTION OF POTENTIAL DISTRIBUTION
DIRECTION OF MOTION OF TEST PARTICLE →
$\omega/\omega_p = 1.0$
POTENTIAL IN ARBITRARY UNITS
0
1
2
3
4
-8
-4
0
4
8
DISTANCE FROM TEST PARTICLE IN DEBYE LENGTHS

(134)

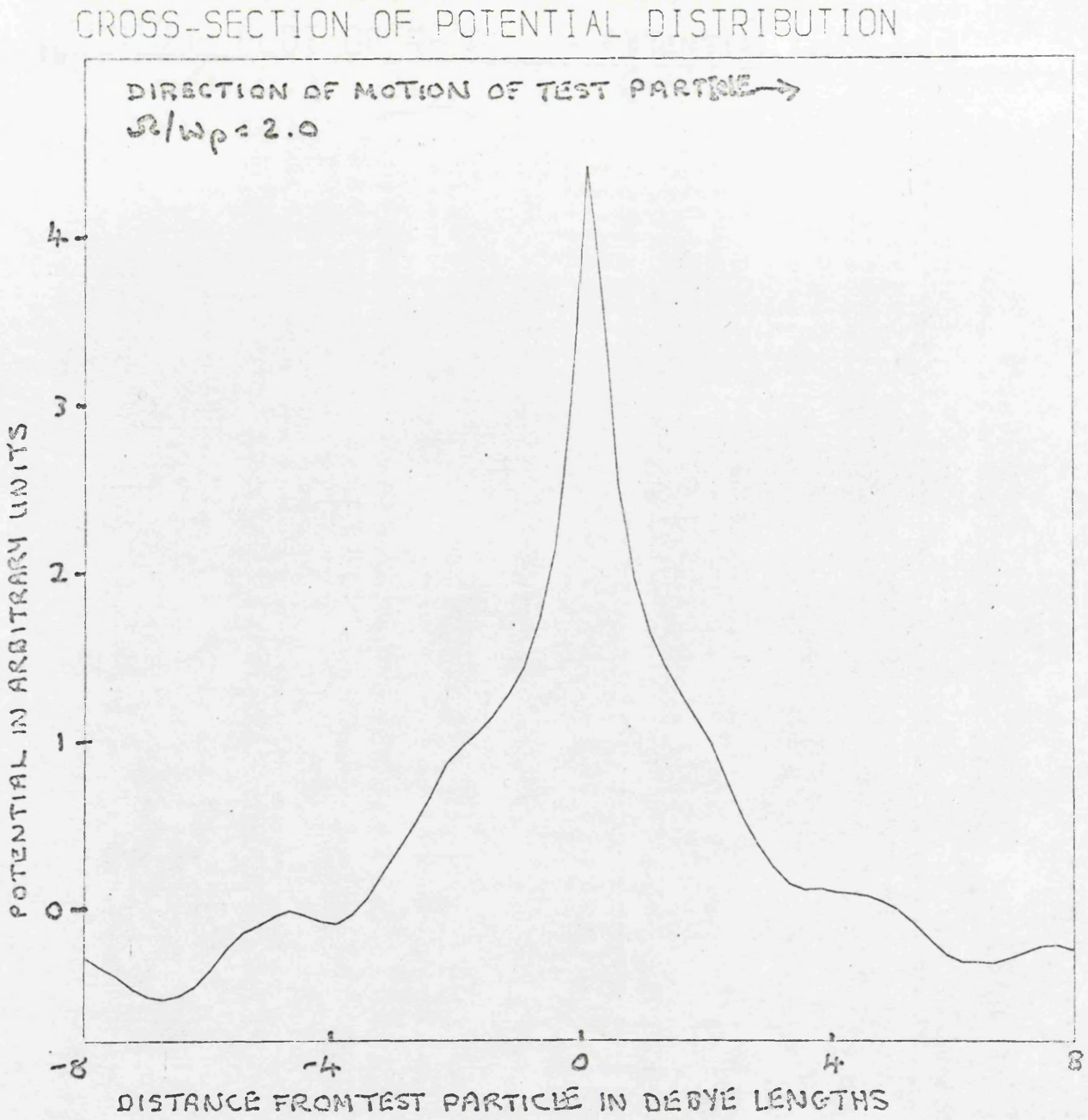
CROSS-SECTION OF POTENTIAL DISTRIBUTION
DIRECTION OF MOTION OF TEST PARTICLE →
Ω/ωp = 2.0
POTENTIAL IN ARBITRARY UNITS
4
3
2
1
0
-8
-4
0
4
8
DISTANCE FROM TEST PARTICLE IN DEBYE LENGTHS

Fig. 3(a)

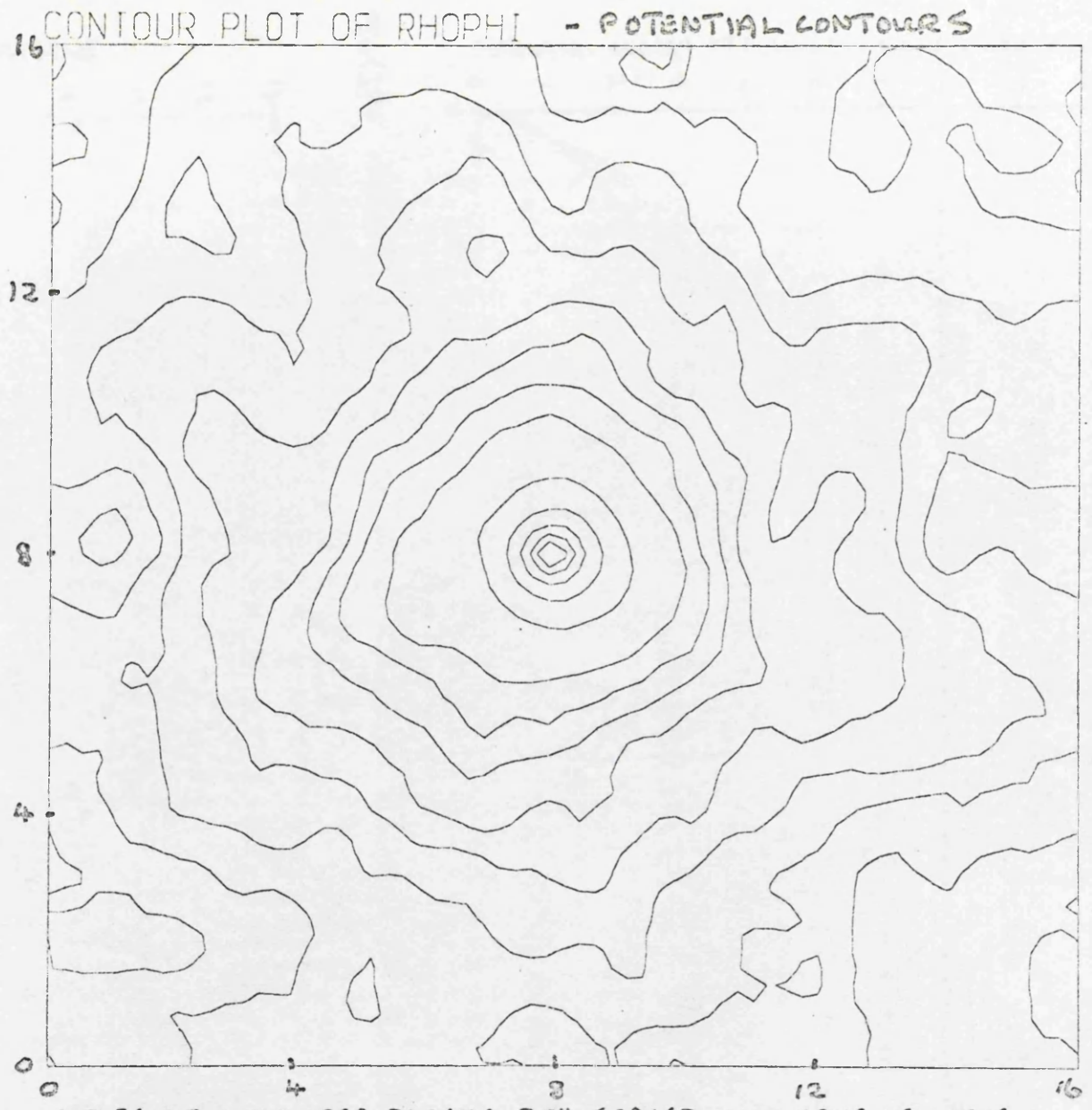
CONTOUR PLOT OF RHOPHI - POTENTIAL CONTOURS
16
12
8
4
0
0
4
8
12
16
SIDES OF COMPUTER PLASMA BOX SCALED IN DEBYE LENGTHS
Ω/ωp = 2.0
TEST PARTICLE IS AT CENTRE OF AREA

FIG(36).

FIG(37) VARIATION OF POTENTIAL ENERGY WITH TIME: MAGNETISED AND UNMAGNETISED CASES; TEST PARTICLE VELOCITY $V_T = V_{th_e}$ ($\frac{1}{2} = \frac{1}{2_E}$)

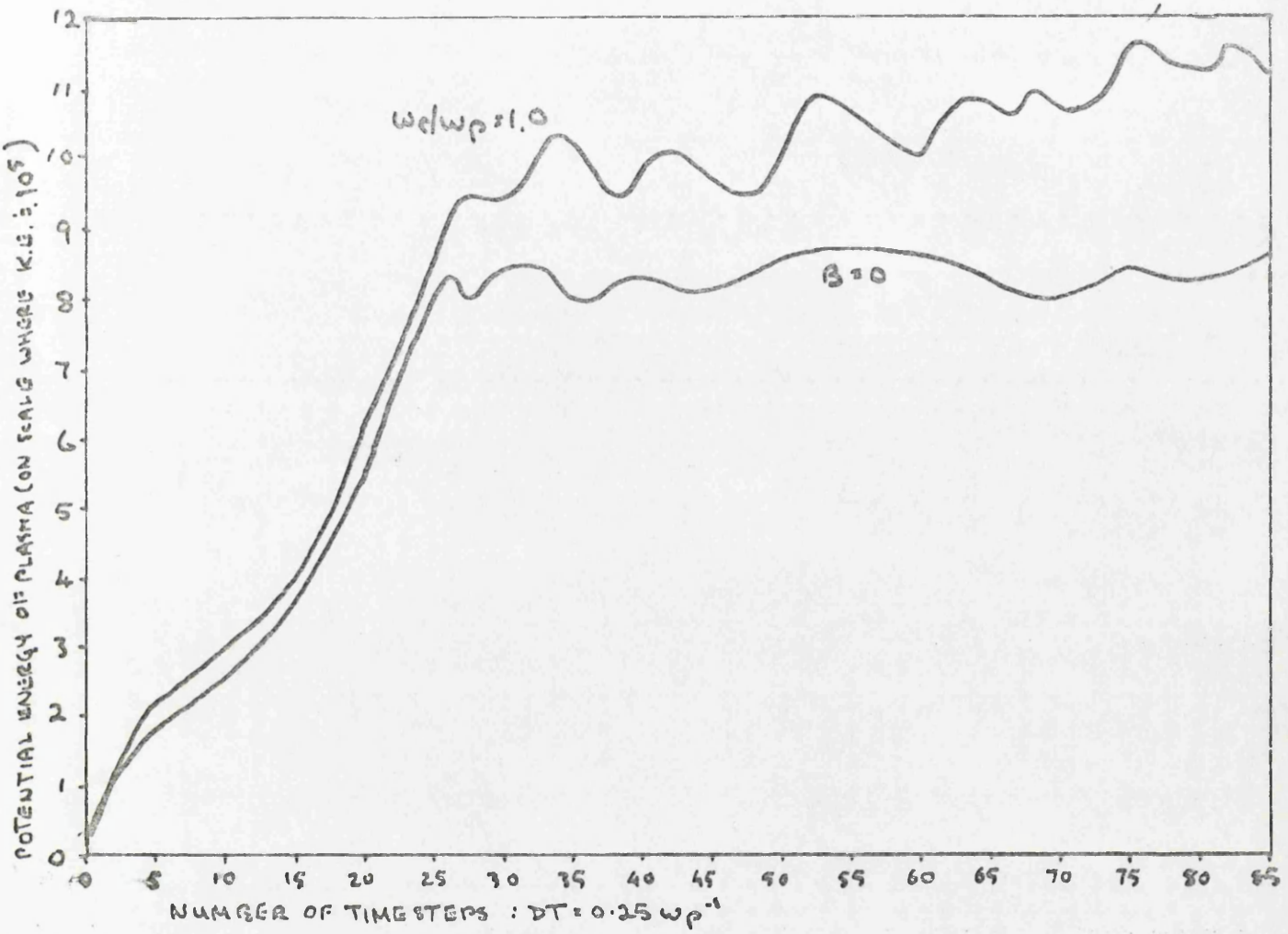

FIG(38) VARIATION OF VALUE OF POTENTIAL AT TEST PARTICLE POSITION, WITH TIME. MAGNETISED AND UNMAGNETISED CASES : TEST PARTICLE VELOCITY = V_{th_e}. POTENTIAL IS IN ARBITRARY UNITS

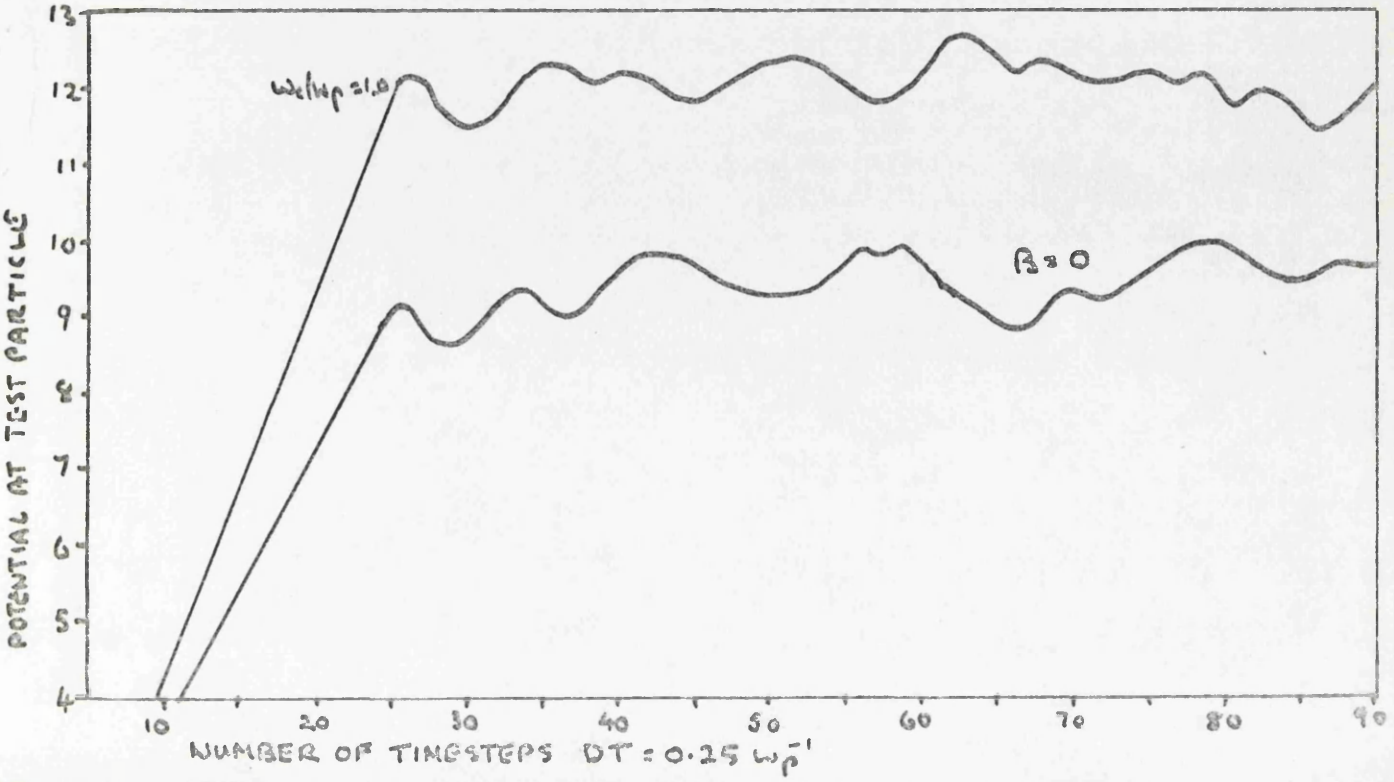

FIG(37) VARIATION WITH TIME OF SINE MODE FOR $K_x = 1, K_y = 0$

..... $\beta = 0$

——— $\omega_c/\omega_p = 1.0$

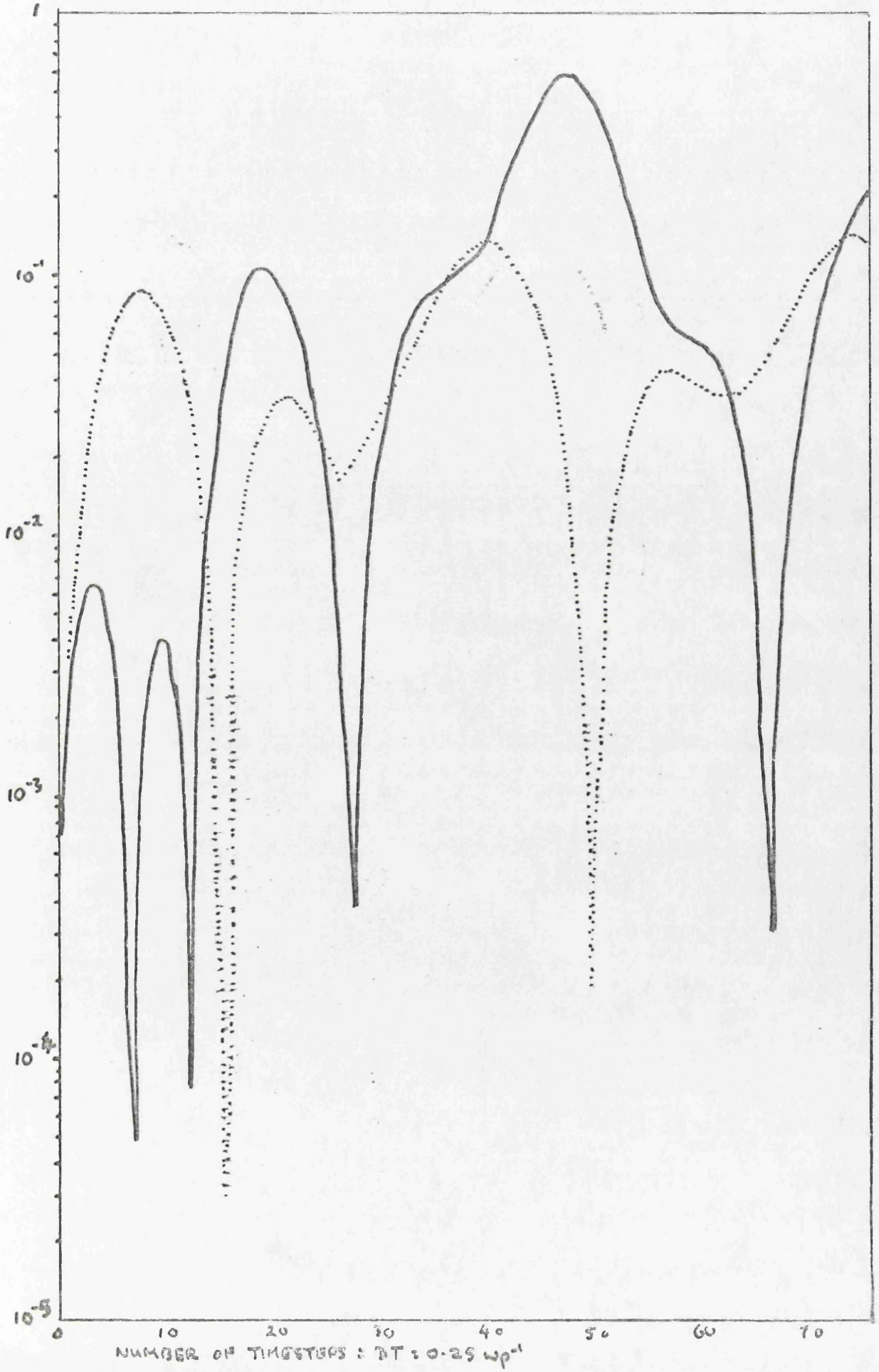

FIG(40)

PLOT OF $D(a)$: $\eta = \omega_c/\omega_p$

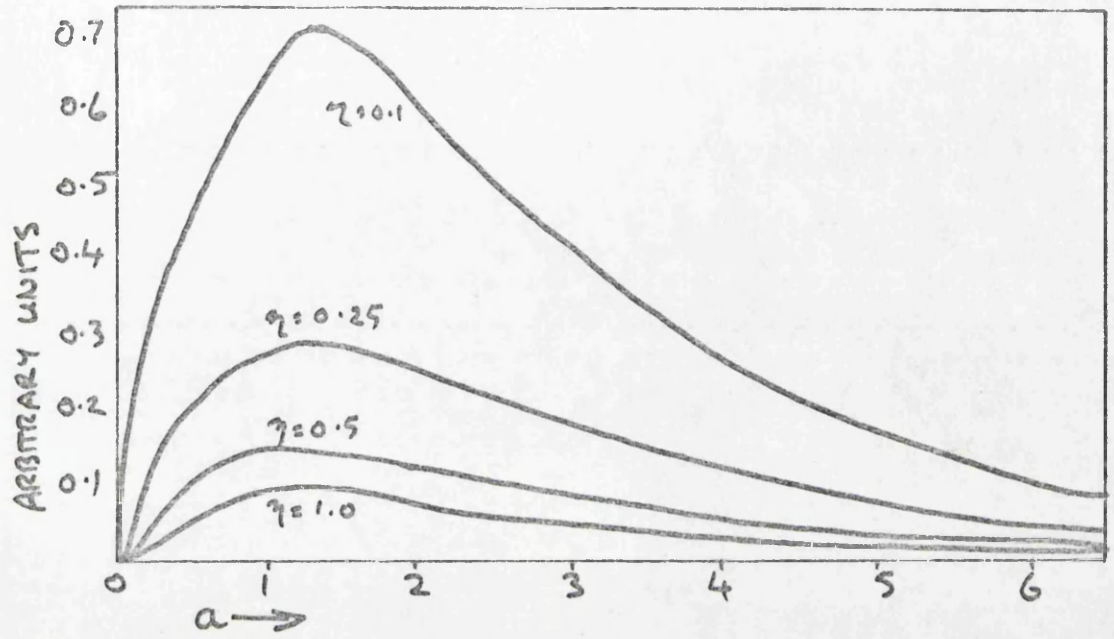

FIG(41)

CROSS SECTION OF POSSIBLE POTENTIAL DISTRIBUTION ALONG LINE OF MOTION OF PARTICLE

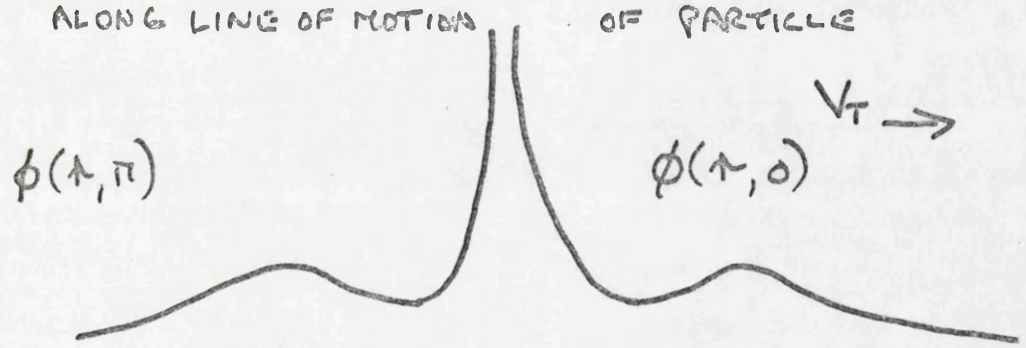

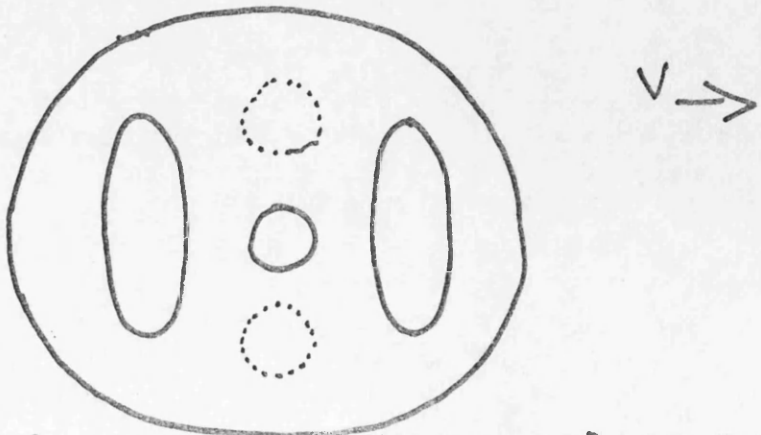

POSSIBLE CONTOUR MAP (SCHEMATIC) OF DISTRIBUTION

generated by a suprathermal test particle in a two-dimens
plasma have been verified within the very noticeable const
of the computer simulation model. Other work has been don
has lent itself better to a good description by simulation
Primarily, in the electrostatic case, the slowing of a tes
particle in a two-dimensional collisionless plasma has bee
adequately quantitatively demonstrated.

In the case of two-dimensional magnetised plasma, e
for the potential due to a test charge have been derived.
shown that the nature of the potential distribution round
particle, and a fortiori, the shielding properties of the
have been radically altered by the inclusion of the magneti
Whatever tractable means were available have been used to
the form of the potential distributions for both stationar
moving test particles.